CEMCAP

Co-funded by the European Union

Grant Agreement Number:
641185

Action acronym:
CEMCAP

Action full title:
CO_2 capture from cement production

Type of action:

H2020-LCE-2014-2015/H2020-LCE-2014-1

Starting date of the action: 2015-05-01
Duration: 42 months

D10.3
Chilled Ammonia Process (CAP) optimization and comparison with pilot plant tests

Due delivery date: 2017-12-31
Actual delivery date: 2018-10-08

Organization name of lead participant for this deliverable:
Swiss Federal Institute of Technology – ETH Zurich

Project co-funded by the European Commission within Horizon2020		
Dissemination Level		
PU	Public	X
CO	Confidential , only for members of the consortium (including the Commission Services)	

Deliverable number:	D10.3
Deliverable title:	Chilled Ammonia Process (CAP) optimization and comparison with pilot plant tests
Work package:	WP 10 Chilled ammonia process (CAP)
Lead participant:	ETHZ

Author(s)		
Name	**Organization**	**E-mail**
José-Francisco Pérez-Calvo*	ETHZ	francisco.perezcalvo@ipe.mavt.ethz.ch
Daniel Sutter	ETHZ	sutter@ipe.mavt.ethz.ch
Matteo Gazzani	UU	m.gazzani@uu.nl
Marco Mazzotti	ETHZ	marco.mazzotti@ipe.mavt.ethz.ch

*Lead author

Keywords

Chilled Ammonia Process, CO_2 capture, Cement, Process optimization, Rate-based model, Pilot plant tests

Abstract

This work reports the results achieved by the optimization of the CAP applied to cement plants for CO_2 capture. A set of operating environments typical for the cement industry in Europe has served as the basis for the CAP optimization. The primary energy consumption per unit of avoided CO_2 emissions has been applied as the objective function. The design of the absorption columns of the CAP has been performed taking into account the results of the pilot plant tests carried out at GE facilities in Växjö (Sweden) for cement plant-like flue gas conditions, and the CAP simulations have been adapted accordingly to implement and reproduce the experimental findings of the pilot tests. The CAP performance is assessed, providing the required input for the integration of the CAP with the cement plant. Mass and heat balances for each optimized case are shown, providing stream tables and the equipment energy consumptions. The sets of operating conditions minimizing the energy consumption of the capture process for each case are in agreement with the differences in the assumed environment. The resulting trends for the optimized energy consumption are in line with the theoretical expectation that higher CO_2 concentrations in the flue gas enable a lower energy penalty for CO_2 capture. Consequently, the results confirm the CAP's potential for highly efficient CO_2 capture from cement plants.

Please cite this report as: *[Pérez-Calvo, José-Francisco], [2018]. [Chilled Ammonia Process (CAP) optimization and comparison with pilot plant tests (D10.3)]*.
Refer to the CEMCAP community in Zenodo.org for citation with DOI.

This project has received funding from the European Union's Horizon2020 Research and Innovation Programme under Grant Agreement No 641185. This work was supported by the Swiss State Secretariat for Education, Research and Innovation (SERI) under contract number 15.0160

TABLE OF CONTENTS

Page

This project has received funding from the European Union's Horizon2020 Research and Innovation Programme under Grant Agreement No 641185. This work was supported by the Swiss State Secretariat for Education, Research and Innovation (SERI) under contract number 15.0160

1 INTRODUCTION

This work reports the results achieved by the optimization of the CAP applied to cement plants for CO_2 capture. The study has been carried out on the grounds of:

(i) The knowledge acquired on the application of the CAP to power plants for CO_2 capture [1,2,3,4].

(ii) The results of the pilot plant tests carried out at the GE facilities in Växjö (Sweden) for different units of the CAP with flue gas compositions typical for cement plants, as part of the CEMCAP project.

The aim of this document is to assess the performance of the CAP when applied to cement plant-like flue gas conditions, considering the cases defined in the CEMCAP common framework [5], and to provide the required information for the integration of the CAP with the cement plant. Process simulations are carried out in Aspen Plus, V8.6. Mass and heat balances for the optimized CAP at different conditions are reported.

This report firstly describes the flowsheet of the CAP proposed for CO_2 capture in cement plants. Secondly, the specifications and constraints that the CAP has to fulfill are discussed, including the description of the conditions of the different cases for which the CAP is simulated and optimized. Next, the simulation framework and optimization approach is described, including a qualitative analysis of the pilot plant test results and the strategy applied for their consideration in the simulation and optimization of the CAP. Subsequently, the results of the optimization of the CAP are shown and discussed, including the optimum set of operating conditions that have been found to minimize the specific energy consumption of the capture process applied to the different operating environments explored in this study. The design and sizing of the CO_2 absorber and the NH_3 absorber is carried out afterwards and the simulations of the CAP are adapted accordingly to implement the experimental findings and reproduce the pilot plant test results. Mass and heat balances for each optimized case are shown in the Annex, providing stream tables and the equipment energy consumptions for each case. Finally, a summary of the findings and conclusions stemming from this work are presented.

This project has received funding from the European Union's Horizon2020 Research and Innovation Programme under Grant Agreement No 641185. This work was supported by the Swiss State Secretariat for Education, Research and Innovation (SERI) under contract number 15.0160

2 THE CAP FOR CEMENT PLANTS

Figure 2.1 shows the flow scheme of the CAP applied to cement plants for CO_2 capture. The main streams of the process have been numbered, and the main pieces of the equipment labelled.

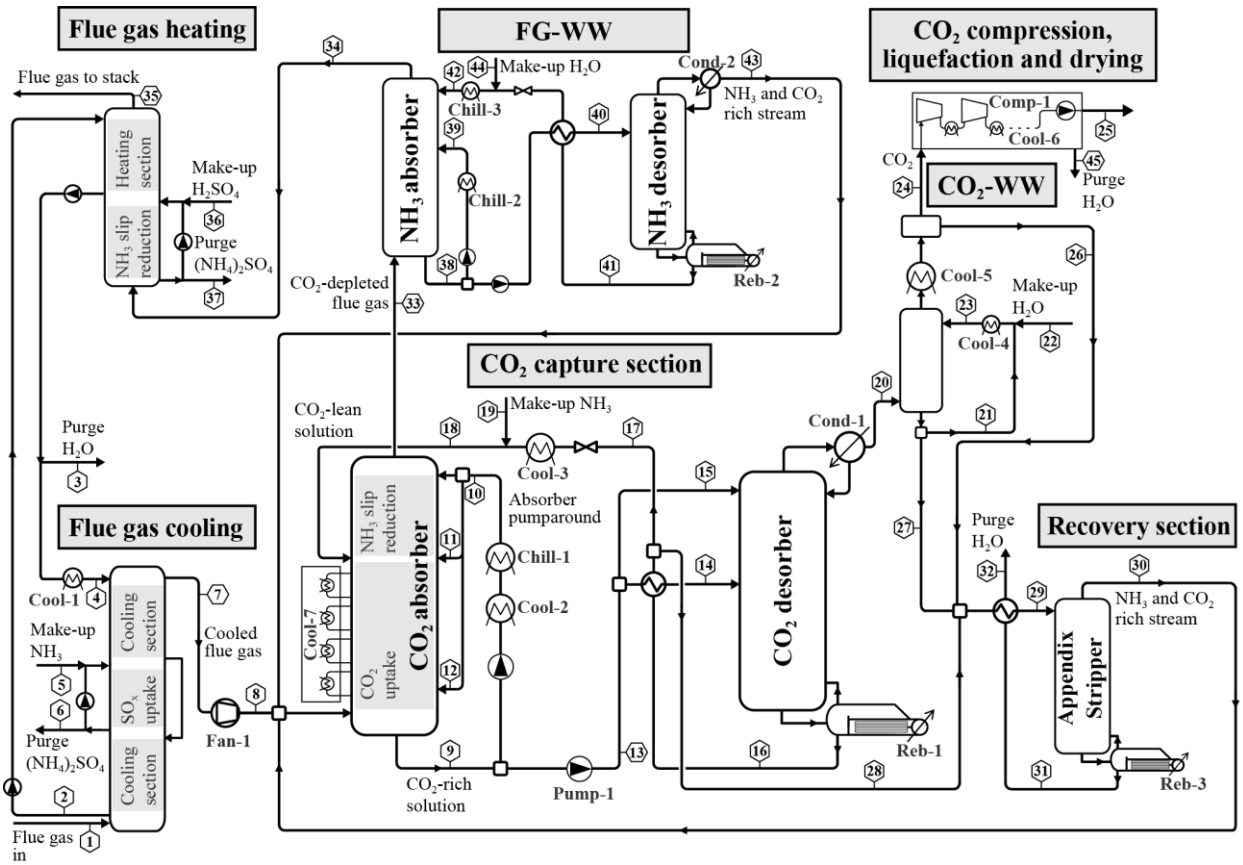

Figure 2.1: Flow scheme of the CAP adopted for CO_2 capture from cement plants.

The proposed CAP for CO_2 capture from cement plants consists of seven main sections, whose goals are described below:

(i) **Flue gas cooling**. The hot flue gas from the power plant enters the DCC (Direct Contact Cooler). A lower and an upper section of the DCC cool down the flue gas to about ambient temperature by means of cooling water flowing in countercurrent. The goal is to remove a significant amount of water contained in the flue gas: The water content in the flue gas entering the CO_2 absorber should approach the water contained in the flue gas leaving the NH_3 absorber in order to minimize the accumulation of water within the CO_2 absorption section, and hence, decreasing the energy consumption in the Appendix Stripper. The lower and the upper section of the DCC consist of packed columns to maximize the heat transfer between the hot flue gas and the cooling water. An intermediate section using diluted aqueous ammonia partially loaded with SO_2 operating at 40°C is used to decrease the SO_2 concentration in the flue gas from 200 mg/Nm^3 to less than 1-2 ppm_v. Otherwise, the SO_2 contained in the flue gas will react with the aqueous ammonia solution in the CO_2 absorber of the CAP, triggering the formation of ammonium sulfate ($(NH_4)_2SO_4$) and, consequently, limiting the CO_2 uptake capacity of the aqueous ammonia solution. The pH of the aqueous ammonia solution containing sulfur species used in the DCC has to be low

This project has received funding from the European Union's Horizon2020 Research and Innovation Programme under Grant Agreement No 641185. This work was supported by the Swiss State Secretariat for Education, Research and Innovation (SERI) under contract number 15.0160

enough to avoid releasing NH_3 from the liquid phase to the gas phase, which would negatively affect the CAP operation downstream, i.e. leading to NH_3 release at the stack. The use of diluted aqueous ammonia as absorbent for the removal of SO_2 leads to the formation $(NH_4)_2SO_4$ as byproduct, that can be commercialized as fertilizer. The intermediate SO_x uptake segment of the flue gas cooling column in Figure 2.1 has been simplified without showing the solid handling equipment that has to be included in the sump of the column section. A flue gas desulfurization (FGD) unit is usually implemented upstream of the CAP when applied to coal-fired power plants for CO_2 capture. The purpose of the FGD unit is to decrease the SO_2 content in the flue gas from approximately 2,000 ppm_v to 50-100 ppm_v. Nevertheless, the SO_2 content in flue gas from the cement plant is 200 mg/Nm^3, according to the CEMCAP common framework [5], which is equivalent to approximately 75 ppm_v. Therefore, the pretreatment of the flue gas in a FGD unit is not required when applying the CAP to cement plants for CO_2 capture. The design and operating conditions of the DCC of the flue gas cooling section of the CAP shown in Figure 2.1, specifically regarding the SO_2 removal from the flue gas, have been supported by pilot plant tests performed within the CEMCAP project, as it will be discussed in Section 4.5.1.

(ii) **CO_2 capture section**. This is the core part of the plant, where CO_2 is removed from the flue gas in an absorber and retrieved in a desorber. The CO_2-lean solution from the CO_2 desorber usually contains 4-10 mol_{NH3}/kg_{water} and 0.25-0.45 mol_{CO2}/mol_{NH3}. The CO_2 contained in the cooled flue gas entering the bottom of the CO_2 absorber is transferred to the liquid flowing down counter-currently. The liquid solution flowing downwards along the CO_2 uptake section of the CO_2 absorber is cooled down using cooling water at several stages of the column, as, overall, it was found to maximize the driving force for CO_2 capture, and hence, to decrease the height of the column. The CO_2-rich solution leaving the bottom of the CO_2 absorber is split into:

a. The so-called absorber pumparound, a stream that is cooled, chilled and sent to the top of the CO_2 absorber in order to minimize the NH_3 slip to the gas. The lower the temperature and the higher the CO_2 loading in the pumparound, the lower the NH_3 concentration in the CO_2-depleted flue gas leaving the CO_2 absorber, as a consequence of the lower NH_3 partial pressure in equilibrium with the liquid. Nevertheless, a minimum temperature exists for each pumparound composition in order to avoid solid formation [3].
b. The so-called cold-rich split solution. A stream that is sent to the top of the CO_2 desorber at the temperature at which it is obtained at the bottom of the CO_2 absorber to control the temperature within the CO_2 desorber and, hence, to limit the NH_3 concentration in the gaseous CO_2 stream leaving the top of the CO_2 desorber, while also removing the need of a condenser.
c. The CO_2-rich solution which is sent to the rich/lean heat exchanger for heat integration before entering the CO_2 desorber at an intermediate stage.

(iii) **CO_2 water-wash (CO_2-WW).** The CO_2 gas recovered in the CO_2 desorber is further purified in a DCC using a liquid water stream flowing in counter-current.

(iv) **CO_2 compression section.** The purified CO_2 gas stream is compressed to meet the specifications required for storage as defined in the CEMCAP common framework [5].

(v) **Flue gas water-wash (FG-WW).** The CO_2 depleted flue gas exiting the absorber contains significant amounts of ammonia, i.e. 2,000 – 15,000 ppm_v; therefore, this stream is further treated in a flue gas water-wash section, which again consists of an

This project has received funding from the European Union's Horizon2020 Research and Innovation Programme under Grant Agreement No 641185. This work was supported by the Swiss State Secretariat for Education, Research and Innovation (SERI) under contract number 15.0160

absorption and a stripping unit. In order to minimize solvent and CO_2 losses, the gas stream leaving the top of the NH_3 desorber, which is rich in CO_2 and NH_3 is recycled to the bottom of the CO_2 absorber. The liquid stream leaving the bottom of the NH_3 desorber is mainly composed of water and is sent, after cooling and chilling, to the top of the NH_3 absorber for a new NH_3 capture process.

(vi) **Recovery section.** In order to avoid water to accumulate within the system, a purge liquid stream is required from the CO_2 absorption-desorption main loop. With the aim of avoiding the loss of ammonia and captured CO_2 with the purge stream, a recovery section composed of an Appendix Stripper is required. Almost pure water is obtained at the bottom of the Appendix Stripper, which is purged to close the water balance within the system. On the other hand, CO_2 and approximately 99.8% of NH_3 is recovered at the top of the column and sent back to the bottom of the CO_2 absorber, minimizing the make-up of fresh ammonia solution. The complete removal of SO_2 from the flue gas before entering the CO_2 capture section reduces the functions of the Appendix Stripper to the control of the water balance within the process and to the recovery of NH_3 and CO_2, such that the Appendix Stripper is not required anymore to control the levels of sulfur components within the CO_2 capture section so as to avoid their accumulation in the absorbent solution.

(vii) **Flue gas heating section.** Finally, the CO_2 and NH_3-depleted flue gas leaving the NH_3 absorber passes through an acid wash column to almost completely remove the ammonia emissions. For that purpose, an aqueous solution of sulfuric acid (H_2SO_4) with a pH of approximately 3 is used. Consequently, $(NH_4)_2SO_4$ is produced, which can be commercialized as by-product. The NH_3 slip reduction section of the column in the flue gas heating section has been simplified without showing the solid handling equipment that has to be included in the sump of the column. In order to increase the temperature of the flue gas at the stack, a direct contact heater (DCH) is needed downstream the acid wash, where the water heated up in the flue gas cooling section is used in counter-current. The heat integration between the flue gas cooling section and the flue gas heating section allows for a lower energy demand for cooling of the water stream entering the top of the DCC and for a decrease of the water purge.

This project has received funding from the European Union's Horizon2020 Research and Innovation Programme under Grant Agreement No 641185. This work was supported by the Swiss State Secretariat for Education, Research and Innovation (SERI) under contract number 15.0160

3 PROCESS SPECIFICATIONS AND CONSTRAINTS

Table 3.1 shows the specifications of the flue gas at the inlet of the CAP as defined in the CEMCAP common framework [5] for two different flowrates of air being drawn into the cement manufacturing process, in following referred to as low and medium "air leak". An increase of the air leak into the cement manufacturing process leads to a higher flue gas flow rate to be treated in the CAP, containing a lower CO_2 content. The rate of air inflow defined for the low air leak case corresponds to that of a Best Available Technology (BAT) reference cement plant, while twice that rate has been assumed for medium air leak conditions [5].

Table 3.1: Specifications of the flue gas entering the CAP as a function of the flowrate of air leak into the cement manufacturing process [5].

Variable	Unit	Value	
		Medium air leak	Low air leak
Air leak in mill, flowrate	kg/h	139,806	69,903
Total flow rate	kg/h	388,098	318,192
Temperature	°C	110	130
Gas phase composition, wet basis			
CO_2	vol%	18	22
Air	vol%	73	67
H_2O	vol%	9	11
Impurity concentration			
SO_2	mg/Nm^3	200	200

As shown in Table 3.1, we include SO_2 as a flue gas impurity, representing the most important and likely most challenging impurity to be handled. As aforementioned, SO_2 is removed from the flue gas in the DCC to negligible concentrations around 1-2 ppm_v. Otherwise, SO_2 interacts with the aqueous ammonia solution in the CO_2 absorber. Contrary to amine-based CO_2 capture processes, the aqueous ammonia solvent remains chemically stable despite the presence of the common flue gas impurities SO_x and NO_x. Nonetheless, the uptake of these acidic compounds partially neutralizes the basic solution and reduces the CO_2 uptake capacity accordingly. As a consequence, the accumulation of these impurities in the CAP should be prevented. Nitrous oxides (NO_x) leaving the cement plant after the SNCR system will mainly contain NO, which will slowly transform into NO_2 when decreasing the temperature. It is expected that the flue gas will pass through the CAP in less than a minute, i.e. from the outlet of the cement process to the stack, considering: (i) the expected length of the units of the CAP that the flue gas has to go through before reaching the stack, i.e. the DCC, the CO_2 absorber and the NH_3 absorber, and (ii) the velocity of the flue gas throughout the CAP will be 1-2 m/s. As a consequence, it can be assumed that the transformation of NO into NO_2 will be negligible. NO has a very low solubility in water and does not react with aqueous ammonia solutions. Therefore, it will pass through the CAP units reaching the stack without interacting with the aqueous ammonia solution, as shown in the literature [6] for multi-pollutant control pilot tests performed with power plant-like flue gas compositions. Consequently, NO_x, in the form of NO, will be assumed to behave as an inert within the CAP and it will not be taken into account in the process simulation and will be neglected in the material and energy balances. Other flue gas impurities specified in the CEMCAP common framework [5], i.e. carbon monoxide, organic compounds, gaseous inorganic chlorine compounds, gaseous inorganic fluorine compounds, dioxins, furans and dust, will be neglected in the CAP simulations and will not be included in the material and energy

This project has received funding from the European Union's Horizon2020 Research and Innovation Programme under Grant Agreement No 641185. This work was supported by the Swiss State Secretariat for Education, Research and Innovation (SERI) under contract number 15.0160

balances, assuming that these species behave as inert compounds with respect to the liquid absorbent and do not influence the CO_2 capture process. If needed, these can be removed with state-of-the-art technologies, that are currently employed in power generation from coal and wastes.

The CAP is designed to avoid the formation of solids in the process. Avoidance of solid formation within the packings or within other sections of the process that are not specifically designed for solid handling prevents blockages and the associated operational issues. The applied thermodynamic model is capable of indicating potential solid formation for the various intermediate solid compounds known for the CO_2-NH_3-H_2O system.

Concerning the specifications of common process units, those defined in the CEMCAP common framework [5] were used for the CAP simulations presented in this work. The exception is the pinch point temperature in heat exchangers using cooling water as cooling medium. Here, the minimization of chilling requirements in the CAP represents significant motivation to invest in advanced heat exchangers. Therefore, the pinch point temperature in these heat exchangers was fixed to 3°C, and hence, the outlet temperature of the process stream has been set to 21.2°C.

The CO_2 concentration in the CO_2 product stream which is sent to the compression section must be above 99%vol in order to fulfil the final CO_2 purity requirements for pipeline transport.

Regarding the NH_3 concentration in the outlet gas streams of the CAP:

- Due to the limitations of the simulation model used in Aspen Plus for the CO_2 compression process, NH_3 is not accounted for in the model of the gas phase in this specific process section. Therefore, the NH_3 concentration in the CO_2 stream sent for compression is limited to a threshold of 50 ppm_v. However, further NH_3 removal from the CO_2 gas stream is expected during the compression process, especially in the intercooling steps, where a significant share of the NH_3 contained in the gas will leave within the aqueous condensate. Consequently, limiting the NH_3 concentration in the CO_2 product is a conservative approach that will ensure 50 ppm_v in the CO_2 pipeline, as specified in the CEMCAP common framework [5].
- The NH_3 concentration in the CO_2-depleted flue gas leaving the NH_3 absorber is limited to a maximum value of 200 ppm_v in order to allow for the complete depletion of NH_3 in the acid wash of the flue gas heating section. In the acid wash, the NH_3 concentration in the flue gas is decreased to values below 10 ppm_v in order to meet common environmental limitations.

The CAP has been simulated and optimized for the cases summarized in Table 3.2, as defined in the CEMCAP common framework [5]. In total, four different cases have been considered. Besides the different assumptions concerning the rate of air leakage into the cement plant describe above, different assumptions on CO_2 capture rate and steam availability are made for the different cases. In all of them, the CO_2 stream obtained as a result of the capture process has to meet the specifications to be transported by pipeline, i.e. 110 bar and temperature below 30°C [5]. A “Ship transport” case, i.e. a variation of the “Base case” in which the CO_2 captured is delivered for ship transport instead of being delivered for pipeline transport, is defined additionally in the CEMCAP common framework [5]. Nevertheless, the modification of the CO_2 specifications for transport will not affect the simulation and optimization of the CAP with respect to the “Base case”, except for the CO_2 compression and liquefaction section, which will

This project has received funding from the European Union's Horizon2020 Research and Innovation Programme under Grant Agreement No 641185. This work was supported by the Swiss State Secretariat for Education, Research and Innovation (SERI) under contract number 15.0160

be simulated specifically in the CEMCAP deliverable D4.6 of CEMCAP for the comparison of technologies. Consequently, the "Ship transport" case has not been included in this report. Except for the "Constant low air leak" case, the rest of the cases have been defined considering increasing rates of air leakage into the cement manufacturing process over the year: Maintenance of the cement facility allows to decrease the air leak into the process to the low level, i.e. the one defined for the BAT reference cement plant [5]; afterwards, the air leak into the cement plant will gradually increase over time, leading to the increase of the flowrate and to the decrease of the CO_2 concentration in the generated flue gas, as shown in Table 3.1. Maintenance operations in cement plants usually take place once a year. With the aim of mimicking the variation of the flowrate and composition of the flue gas from the cement plant over the year, the CAP is simulated at low air leak during the first half of the year and at medium air leak during the second half of the year in those cases considering increasing air leak: The design of the plant, namely the sizing of the CO_2 absorber, is carried out considering the flue gas conditions for medium air leak into the cement process. Then, the CAP with the same CO_2 absorber design and size has to be simulated at the flue gas conditions obtained when low air leak into the cement manufacturing process is considered, i.e. the flue gas flowrate decreases, and hence, the CO_2 concentration increases. When a case shown in Table 3.2 is run at the same flue gas conditions used for the design of the CAP, the case will be referred to as "Design case" hereinafter, while if it is run at different flue gas conditions to those used for the design of the process, the case will be referred to as "Non-design case". This categorization is also included in Table 3.2. Additionally, an "Optional extent of capture" has been defined, in which the CO_2 capture rate (CCR) of the CAP is not specified at 90%, but is only limited to a value above 85%. Finally, the heat required in the reboilers of the CAP can be obtained: (i) by steam produced in a natural gas boiler (NG boiler) built on-site with the sole purpose of supplying steam for the CAP, or (ii) by steam imported from an external coal CHP plant located in the neighborhood of the cement plant. Additionally, some heat can be recovered from the cement manufacturing process to produce steam for the CAP, as specified in the CEMCAP common framework [5].

Table 3.2: Overview of cases studied in CEMCAP, for which the CAP has been simulated and optimized.

Case					CO_2 in the FG	CCR	Steam scenario
Name	**Air leak**	**Designed for**	**Run at**	**Type**			
Base case	Increasing	Medium air leak	Low air leak	Non-design case	22%vol	90%	NG boiler and recovered heat from the cement plant
			Medium air leak	Design case	18%vol		
Constant low air leak	Constant low	Low air leak	Low air leak	Design case	22%vol	90%	NG boiler and recovered heat from the cement plant
Optional extent of capture	Increasing	Medium air leak	Low air leak	Non-design case	22%vol	Optional (>85%)	NG boiler and recovered heat from the cement plant
			Medium air leak	Design case	18%vol		
Steam import	Increasing	Medium air leak	Low air leak	Non-design case	22%vol	90%	Steam import and recovered heat from the cement plant
			Medium air leak	Design case	18%vol		

This project has received funding from the European Union's Horizon2020 Research and Innovation Programme under Grant Agreement No 641185. This work was supported by the Swiss State Secretariat for Education, Research and Innovation (SERI) under contract number 15.0160

4 SIMULATION AND OPTIMIZATION APPROACH

As a first effort, the conventional CAP system had to be adapted to cement plant-like flue gas conditions. This activity was focused on the CO_2 absorber, which represents the core of the CAP plant. Secondly, a rate-based model obtained from the literature was used to simulate the absorber of the CAP for cement plant-like flue gas. As a result, Murphree efficiency values for the individual stages of the CO_2 absorber could be calculated. Next, overall CAP simulations were performed combining equilibrium-based simulations with the updated values of the Murphree efficiencies for the absorber stages. This combination limits the computational costs compared to a fully rate-based CAP simulation. Eventually, the CAP process simulations were modified and adapted making use of the results obtained during the pilot plant tests of the DCC, the CO_2 absorber and the NH_3 absorber, carried out within the CEMCAP project. The CAP simulations are carried out in Aspen Plus, Version 8.6.

4.1 Adaptation of the CAP to cement plant-like flue gas conditions

As a point of departure, the set of operating conditions of the CAP applied to coal-fired power plants found by Sutter et al. [4] that minimized the energy consumption of the process were used. Subsequently, a comprehensive simulation approach was defined to predict meaningful operating conditions for the CAP application to cement plants. The absorption column was simulated considering the cement-like flue gas compositions provided in the CEMCAP common framework [5] in order to investigate multiple combinations of: (i) NH_3 content in the lean solution, (ii) CO_2-lean loading, (iii) CO_2-lean to flue gas flowrate ratio (L/G), (iv) pumparound split fraction, and (v) pumparound temperature. The resulting internal absorber profiles of temperature, pressure, as well as composition and flowrate of the vapor and liquid streams were compared to the power plant case [7]. At this stage, the simulation of the CO_2 absorber was carried out by means of equilibrium-based simulations making use of the thermodynamic model developed by Kaj Thomsen's group at DTU (referred to as Thomsen model hereinafter) for the CO_2-NH_3-H_2O system [8,9]. The Thomsen model has been proven to properly reproduce the experimental VLE results as well as the solid formation data, a feature that is not fulfilled by other thermodynamic models available in the literature for the CO_2-NH_3-H_2O system [3]. Mass transfer limitations were initially considered in the model by means of Murphree efficiencies suitable for power plant-like flue gas compositions, as defined by Sutter et al. [4]. In order to meet the specifications and constraints of the process, still with reasonable temperature and composition profiles within the CO_2 absorber, the operating conditions of the CAP were adapted for the cement plant case as indicated in Table 4.1.

This project has received funding from the European Union's Horizon2020 Research and Innovation Programme under Grant Agreement No 641185. This work was supported by the Swiss State Secretariat for Education, Research and Innovation (SERI) under contract number 15.0160

Table 4.1: Set of operating conditions for: (i) the CAP applied to coal-fired power plants with 14%vol CO_2 in the inlet flue gas, as proposed by Sutter et al. [4], that minimizes the energy consumption of the process; and (ii) the adaptation of the CAP to cement plant-like flue gas compositions, i.e. 18 and 22%vol CO_2, as defined in the CEMCAP common framework [5] for medium air leak and low air leak conditions, respectively. See Table 3.1 for the properties of the inlet flue gas to the CAP in each case.

Variable			Power plant case [4]	Air leak into the cement process	
				Medium air leak	Low air leak
CO_2-lean NH_3 concentration	$C^{in}_{NH_3}$	mol_{NH3}/kg_{water}	8.9	8.0	8.0
CO_2-lean CO_2 loading	$l^{in}_{CO_2}$	mol_{CO2}/mol_{NH3}	0.354	0.334	0.336
CO_2-lean to inlet flue gas flowrate ratio	L^{in}/G^{in}	kg/kg	4.1	5.0	6.0
Pumparound split fraction	f_s	-	0.28	0.25	0.18
Pumparound temperature	T_{pa}	°C	10	5	5

4.2 Preliminary rate-based model

The CO_2 absorber with the adapted operating conditions for the cement plant case was simulated using the more computationally intensive, yet more comprehensive, rate-based model. First, a literature research on rate-based models implemented in Aspen Plus for the simulation of CO_2 capture processes with aqueous ammonia solutions was carried out. Special attention was paid to the selected transport property models, mass transfer correlations and kinetic models for chemical reactions. Sensitivity analyses on the Aspen Plus input parameters for the rate-based model such as the film and the column length discretization, and the hydrodynamic model were then performed. Based on the acquired knowledge, a preliminary custom-made rate-based model for the CAP was implemented in Aspen Plus.

The preliminary rate-based model implemented in Aspen Plus for CEMCAP using the information available in literature (hereinafter referred to as "Literature model") considers [7]:

- Thermodynamic model: Thomsen model [9].
- Flow model: VPlug with discretizations of the column length up to 0.1 m.
- Film discretization: Geometrical discretization in the liquid film with 7 segments increasing in length (ratio 1.5) from the gas-liquid interface to the liquid bulk.
- Activity-based kinetics of bicarbonate and carbamate ion formation obtained from Pinsent et al. (1956) [11,12].
- Mass transfer coefficients and interfacial areas computed with the correlations of Bravo and Fair (1992) [13].
- Transport property models validated elsewhere [10]:
    - Viscosity: Andrade and DIPPR (Design Institute for Physical Properties) models plus electrolyte correction using the Jones-Dole model.
    - Surface tension: Hakim-Steinberg-Stiel and DIPPR models, corrected with the Onsager-Samaras model.
    - Thermal conductivity: Sato-Riedel and DIPPR models and the Vredeveld mixing rule and adjusted using the Riedel model.

This project has received funding from the European Union's Horizon2020 Research and Innovation Programme under Grant Agreement No 641185. This work was supported by the Swiss State Secretariat for Education, Research and Innovation (SERI) under contract number 15.0160

- Diffusivity: Wilke-Chang model for molecular species and Nernst-Hartley model for ions.

Subsequently, a preliminary validation of the Literature model was carried out using the data available in the literature for coal-fired power plant-like flue gas compositions, performed by CSIRO at the Munmorah pilot plant [6,10]. The validation of the Literature model is given by the parity plots shown by Pérez-Calvo et al. [7]. In general, experimental values are predicted by the rate-based model with a deviation smaller than 20%.

4.3 Reduced order CO_2 absorber model with Murphree efficiencies

Eventually, the Murphree efficiencies obtained from the rate-based simulation of the CO_2 absorber using the Literature model for cement plant-like flue gas conditions were used hereinafter for full CAP simulations. A structured packing of the type Mellapak 350X has been considered for the rate-based simulations of the CO_2 absorber. Average values of the obtained Murphree efficiencies are shown in Table 4.2.

Table 4.2: Murphree efficiencies obtained from the preliminary rate-based simulations of the CO_2 absorber for 5 and 15 stages of the NH_3 removal section and the CO_2 capture section, respectively, considering the inlet flue gas specifications defined in the CEMCAP common framework [5] for the medium and low air leak case, i.e.18 and 22%vol CO_2, respectively.

Section and compound	Average Murphree efficiencies	
	Medium air leak	Low air leak
NH_3 removal section		
CO_2	0.085	0.063
NH_3	0.861	0.792
CO_2 capture section		
CO_2	0.861	0.134
NH_3	1	1

A reduced order model is also implemented in the NH_3 absorber for full simulations of the CAP, using equilibrium-based simulations with Murphree efficiencies whose values were taken from Sutter et al. [4]. The use of Murphree efficiencies allows to account for the mass transfer limitations between the vapor and the liquid phase, while minimizing the convergence issues and the computational costs of the full CAP simulations.

The CO_2 compression is simulated in Aspen Plus, Version 8.6, using a PC-SAFT-based thermodynamic model and neglecting components in the gas stream other than CO_2 and H_2O.

4.4 Process optimization

The CAP performance depends on several variables (e.g. solution composition, temperature levels, flowrates), therefore an optimization framework is needed to investigate the different possibilities. The optimization strategy consists of the following steps:

- Stage 1. Simulations that fulfills all specifications and constraints are established for each flue gas conditions defined in Table 3.1.
- Stage 2. Single variable sensitivity analyses are carried out in order to study the influence of some operating variables on the energetic performance of the CAP applied to cement plants. As a result, the studied variables are classified in two different categories: (i) variables that

This project has received funding from the European Union's Horizon2020 Research and Innovation Programme under Grant Agreement No 641185. This work was supported by the Swiss State Secretariat for Education, Research and Innovation (SERI) under contract number 15.0160

will be fixed in the next stages of the process optimization at the value that minimizes the energetic consumption of the CAP, and (ii) variables that will be included in a more extensive multi-variable sensitivity analysis, i.e. in Stage 3.

- Stage 3. A nested multi-variable heuristic optimization of the CAP applied to cement plants for CO_2 capture is performed. The CAP is optimized for each Design case specified in Table 3.2. In order to maximize the number of converged simulations, still accounting for the main energy consumers of the CAP, the heuristic optimization of the process was applied to a simplified flow scheme of the CAP, shown in Figure 4.1. For example, it was found out that including the Appendix Stripper considerably decreases the chances for the full CAP simulation to converge and, consequently, it limits the amount of available results and hinders the automated heuristic optimization of the process. In the simplified flow scheme of the CAP used for the heuristic optimization, the water purge from the CO_2-WW is sent to the CO_2 desorber, whose reboiler duty will account for the reboiler duties of the CO_2 desorber and the Appendix Stripper of the actual CAP flow scheme shown in Figure 2.1. The heuristic optimization methodology has the following steps:
  - Stage 3.1. The operating conditions of the CO_2 absorber are screened through an extensive, automated sensitivity analysis. Here, five variables are investigated: (i) the ammonia concentration of the lean stream, $c^{\text{in}}_{\text{NH}_3}$, (ii) the CO_2-loading of the lean stream $l^{\text{in}}_{\text{CO}_2}$, defined as $\text{mol}_{\text{CO2}}/\text{mol}_{\text{NH3}}$, (iii) the liquid-to-gas flowrate ratio, defined as the ratio between the mass flowrate of the CO_2-lean stream and the mass flowrate of the flue gas stream entering the CO_2 absorber, $L^{\text{in}}/G^{\text{in}}$, (iv) the pumparound split fraction, f_{s}, and (v) the temperature of the pumparound chilling, T_{pa}.
  - Stage 3.2. Then, those sets of operating conditions that lead to successful simulations of the CO_2 absorber in terms of convergence and fulfillment of the specifications and constraints are used to run the CO_2 capture section, including the absolute reboiler duty of the CO_2 desorber, $Q_{\text{reb,CO}_2}$, in the sensitivity analysis.
  - Stage 3.3. Subsequently, the simulations of the CO_2 capture section that are successful provide data for the FG-WW section. Here a rigorous optimization based on successive quadratic programming is carried out. In particular, the specific reboiler duty of the NH_3 desorber is minimized by changing the pumparound split fraction, $f_{\text{s,FG-WW}}$, and the liquid-to-gas flowrate ratio of the NH_3 absorber, $L^{\text{in}}_{\text{FG-WW}}/G^{\text{in}}_{\text{FG-WW}}$, and the absolute reboiler duty of the NH_3 desorber, $Q_{\text{reb,NH}_3}$.
  - Stage 3.4. Finally, those set of operating conditions showing the most promising results in terms of energy performance are considered for a further sensitivity analysis in which the pressure of the CO_2 desorber, $P_{\text{CO}_2\text{des}}$, and the cold-rich split fraction, f_{cr}, are included. Although the latter variables were initially considered for their inclusion in the automated sensitivity analysis described in Stage 3.3, they were eventually excluded in order to minimize convergence issues of the automatized full CAP simulations. The CAP flow scheme shown in Figure 2.1.
- Stage 4. In order to integrate the results of this three-step optimization with the cement plant and obtain the optimal set of operating conditions of the CAP for each case defined in Table 3.2, the SPECCA (Specific Primary Energy Consumption for CO_2 Avoided) index, as defined in the CEMCAP common framework [5], is computed. Cooling and chilling demands are converted to electricity as defined in the CEMCAP common framework [5], and added to the electricity demanded by the auxiliary pumps, the compressor and the fans of the CAP, as well as by the CO_2 compression section. The total primary energy required to produce electricity is computed considering the conversion efficiency defined in the

This project has received funding from the European Union's Horizon2020 Research and Innovation Programme under Grant Agreement No 641185. This work was supported by the Swiss State Secretariat for Education, Research and Innovation (SERI) under contract number 15.0160

CEMCAP common framework [5]. The climate impact associated with the electricity requirements are computed by means of a CO_2 emission factor for electricity generation whose value is defined in the CEMCAP common framework [5], too. On the other hand, the heat requirements are provided by steam with two different qualities depending on the reboiler temperature: (i) steam at around 140-160°C in the reboiler of the CO_2 desorber, and (ii) steam at around 110-120°C in the reboilers of the NH_3 desorber and the Appendix Stripper. According to the CEMCAP common framework [5], steam can be acquired in two different ways: (i) the steam is produced in a natural gas boiler built specifically on-site to supply steam for the CAP; available heat in the cement manufacturing process can be recovered to produce steam, decreasing both the fuel requirements and the associated CO_2 emissions; the heat recovered from the cement plant is first integrated in the NG boiler producing steam at 110-120°C and, if still available, in the NG boiler producing steam at 140-160°C, or (ii) the steam is imported from an external coal CHP plant located in the neighborhood of the cement plant; the heat recovered from the cement plant is used in this case to produce steam at 140-160°C to be used in the reboiler of the CO_2 desorber. The climate impact and the primary energy consumption associated with the steam requirements are defined in the CEMCAP common framework [5] for both alternatives, as well as the heat that can be recovered from the cement plant as a function of the steam temperature.

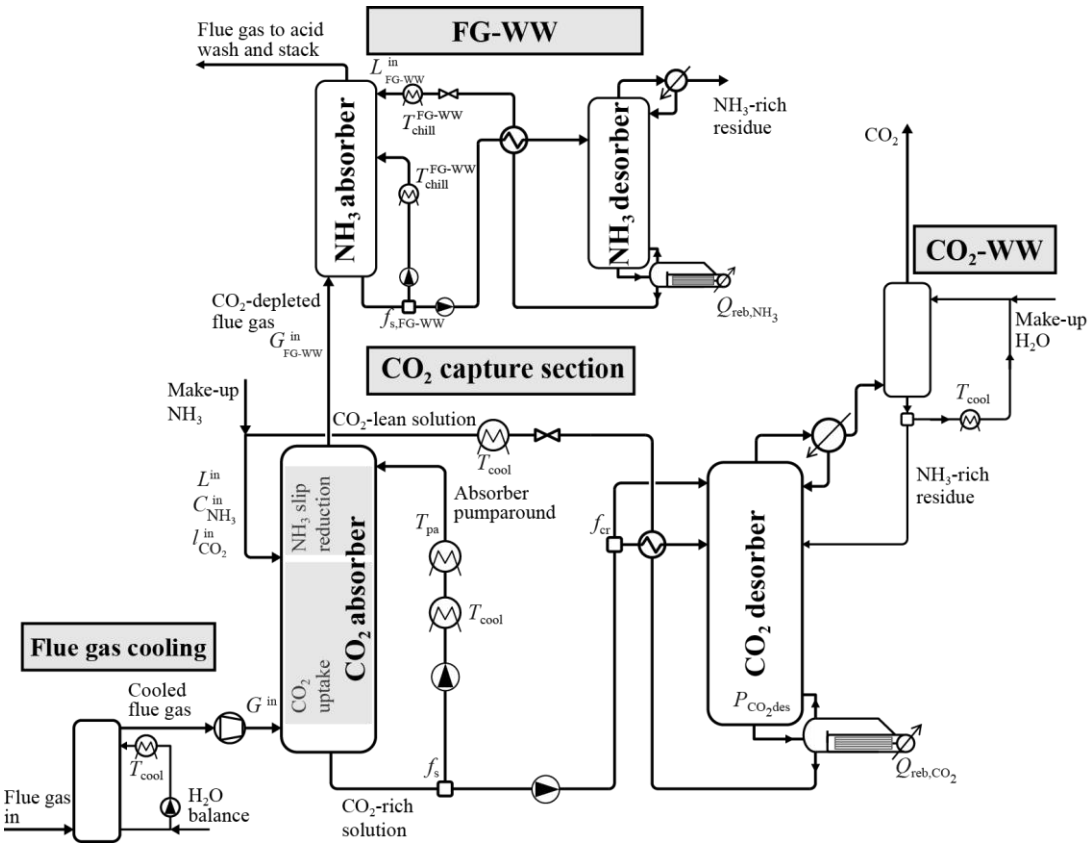

Figure 4.1: Simplified flow scheme of the CAP used during the heuristic optimization of the process.

This project has received funding from the European Union's Horizon2020 Research and Innovation Programme under Grant Agreement No 641185. This work was supported by the Swiss State Secretariat for Education, Research and Innovation (SERI) under contract number 15.0160

4.5 Consideration of pilot plant test results and adaptation of process simulations

The simulations of the CAP using the optimum set of operating conditions found in the optimization of the process for each case specified in Table 3.2 were revised, if needed, taking into account the results obtained in the pilot plant tests performed within the CEMCAP project at the GE facilities in Växjö (Sweden). These pilot plant tests were performed at cement plant-like flue gas conditions for those units of the CAP (see Figure 2.1 for reference) whose operation can be affected with respect to the power plant case by the higher CO_2 concentration in the flue gas and/or by the different level of impurities, i.e. SO_2, in the flue gas: (i) the SO_x uptake section of the DCC column in the flue gas cooling section; (ii) the CO_2 absorber of the CO_2 capture section; and (iii) the NH_3 absorber of the FG-WW section.

4.5.1 DCC tests

The pilot plant tests of the DCC have demonstrated that the use of a diluted aqueous ammonia solution allows decreasing the SO_2 concentration in the flue gas to values below 1-2 ppm_v departing from SO_2 concentrations in the inlet flue gas of up to 100 ppm_v. A square column containing a structured packing material Mellapak Plastic 125X with 4.2 meter-height was used, operating with a sulfur-loaded aqueous ammonia solution with pH 5 and temperature 40°C, a flue gas superficial gas velocity of 1-2 m/s and a liquid-to-gas flowrate rate of 5. This process configuration allows for a rapid oxidation of sulfites to sulfates within the liquid, maximizing the SO_2 uptake; its integration within the DCC of the flue gas cooling section, as shown in Figure 2.1, allows to decrease the concentration of SO_2 in the flue gas entering the CO_2 absorber from 200 mg/Nm^3 (equivalent to 62-84 ppm_v), as specified in the CEMCAP common framework [5] for the flue gas produced in the cement plant, to negligible levels, i.e. below 1-2 ppm_v. Consequently, this configuration allows to decouple the SO_2 uptake from the CO_2 capture in the CO_2 absorber while using an aqueous ammonia solution as absorbent in both cases.

Therefore, the results of the pilot plant tests of the DCC led to the following considerations for the simulation of the CAP: (i) the configuration of the flue gas cooling section shown in Figure 2.1 has been proposed for the CAP applied to cement plants for CO_2 capture; and (ii) sulfur species are not included in the Aspen Plus simulations. Instead, the specifications of streams containing sulfur species in the flue gas cooling section and in the flue gas heating section are computed by means of material balances considering apparent compositions of molecular species.

4.5.2 CO_2 absorber tests

The detailed design of the CO_2 absorber, i.e. configuration, height and diameter, requires the use of rate-based process simulations. The preliminary rate-based model presented in Section 4.2, i.e. the Literature model, was initially validated [7] with pilot plant CO_2 absorption tests performed with flue gases containing only up to 12 %vol CO_2 [6,10]. Nevertheless, the application of the CAP to cement plants, where the CO_2 concentration can be as high as 35 %vol, is expected to affect the CO_2 absorption unit, which will have to face higher partial pressure of CO_2 in the inlet stream. Consequently, CO_2 absorption tests have been performed in a pilot plant in order to test the system at cement plant-like flue gas compositions and fine-tune the rate-based model before designing and sizing the CO_2 absorber.

This project has received funding from the European Union's Horizon2020 Research and Innovation Programme under Grant Agreement No 641185. This work was supported by the Swiss State Secretariat for Education, Research and Innovation (SERI) under contract number 15.0160

A schematic of the test rig used during the experimental campaigns of the CO_2 absorber is shown in Figure 4.2. The packing of the absorption column is 3 m high, with a diameter of 450 mm. The packing used was Koch Glitsch Flexipac M 350X. Online measurements of the CO_2 and NH_3 concentration in the liquid streams were performed using Fourier Transform Near-Infrared spectroscopy (FT-NIR), while OPSIS gas analyzers were used in the gas streams. A mass-balance tool was used to predict the necessary additions (lean solution, rich solution, ammonia solution, water and drain) to keep the concentration in the tank – and consequently in the liquid at the top of the absorber – invariant over time. Sampling of the absorber inlet and outlet liquid streams was carried out for offline liquid composition determination by titration. For each experiment, average values of the measured variables were computed while the system was at steady state.

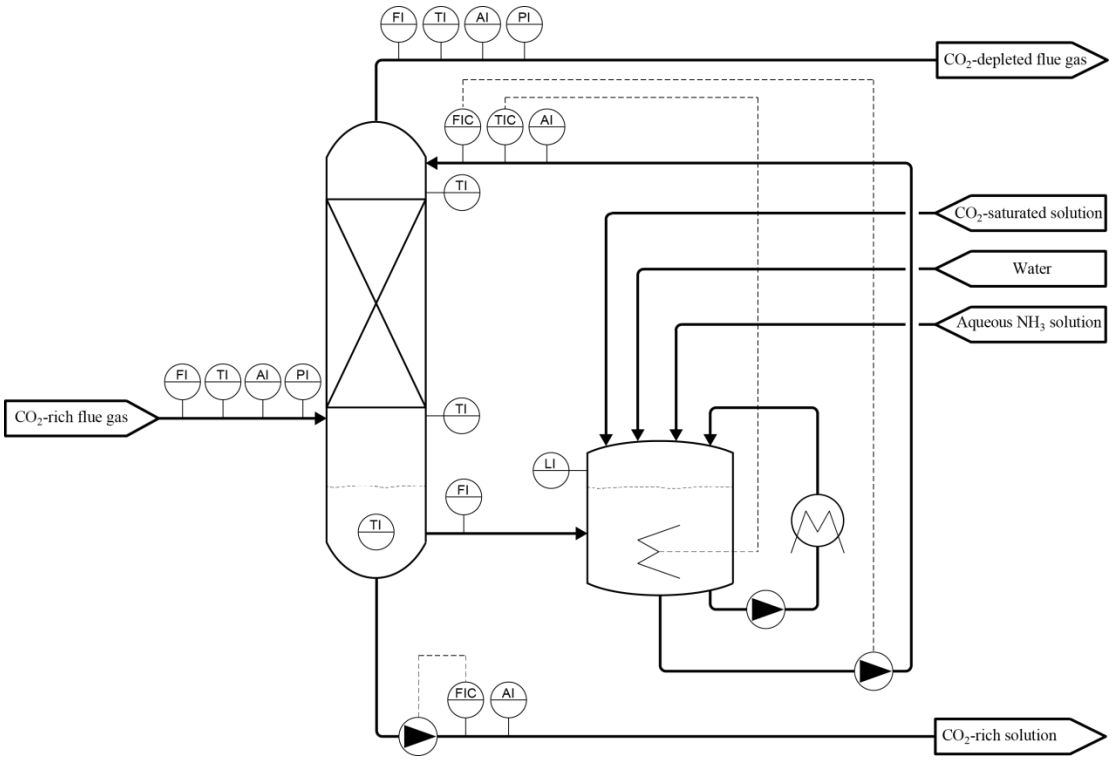

Figure 4.2: Schematic of the pilot plant used during the CO_2 absorption tests.

Table 4.3 shows the boundary conditions of the operating variables selected for the pilot plant tests. Experiments were divided into 3 different types of tests representing the different sections of a real column [3] assuming 90% of CO_2 capture rate (CCR): (i) tests simulating the bottom part of the industrial absorber where the CO_2 concentration is at its maximum (up to 35 %vol in the case of flue gases from cement plants) and the aqueous ammonia solution has been enriched in CO_2 (Campaign 1); (ii) tests mimicking the middle section of the industrial absorber, right below the feed position of the CO_2-lean stream, where the flue gas has already been partially depleted in CO_2 (Campaign 2); and (iii) experiments reproducing the conditions found at the top of the industrial absorber, where a split stream of the CO_2-rich liquid stream is cooled down and sent to the top of the absorber (often referred to as "pumparound") to limit the NH_3 slip in the CO_2-depleted flue gas leaving the column (Campaign 3). In comparison with the pilot plant experiments available in the literature [6], not only the CO_2 concentration in the inlet flue gas has been increased up to 35 %vol in order to simulate cement plant-like flue gas conditions, but

This project has received funding from the European Union's Horizon2020 Research and Innovation Programme under Grant Agreement No 641185. This work was supported by the Swiss State Secretariat for Education, Research and Innovation (SERI) under contract number 15.0160

also the experimental range of the liquid NH_3 concentration has been increased from 0-4 to 4-10 mol_{NH_3}/kg_{water} in order to test typical operating conditions of the absorber [3]. Avoidance of solid formation for all tests was preliminary checked making use of the Thomsen model and confirmed experimentally afterwards. The design of experiments can be seen in Figure 4.3, where each colored sphere corresponds to one single experiment performed at certain combination of CO_2 partial pressure in the inlet gas stream, and CO_2 loading, NH_3 concentration and temperature in the inlet liquid stream to the column. The experimental space studied for those tests belonging to Campaigns 1 and 2 is shown in Figure 4.3A), while the tests performed during Campaign 3 are shown in Figure 4.3B). In addition, reproducibility experiments were carried out.

Table 4.3: Summary of experimental conditions for the pilot plant tests of the CO_2 absorber.

Stream	Variable		Unit	Campaign 1	Campaign 2	Campaign 3
Inlet liquid	NH_3 concentration	$C^{in}_{NH_3}$	mol_{NH3}/kg_{water}	3.9 – 10.2	4.1 – 10.2	4.1 – 9.6
	CO_2 loading	$l^{in}_{CO_2}$	mol_{CO2}/mol_{NH3}	0.43 – 0.70	0.24 – 0.52	0.46 – 0.61
	Temperature	T^{in}_{L}	°C	5 – 45	5 – 25	0 - 25
Inlet gas	CO_2 partial pressure	$p^{in}_{CO_2,G}$	kPa	20 – 35	8 – 20	2 – 7
	NH_3 partial pressure	$p^{in}_{NH_3,G}$	kPa	0 – 3	0 – 8	4 – 7
	Superficial velocity	$v^{in}_{S,G}$	m/s	0.7 – 0.9	0.7 – 1.1	0.8 – 0.9
	Temperature	T^{in}_{G}	°C	10 – 15	10 – 15	10 – 15
Inlet liquid and gas	Liquid-to-gas flowrate ratio	L^{in}/G^{in}	kg/kg	7.5 – 12.0	7.5 – 12.5	2.0 – 3.0

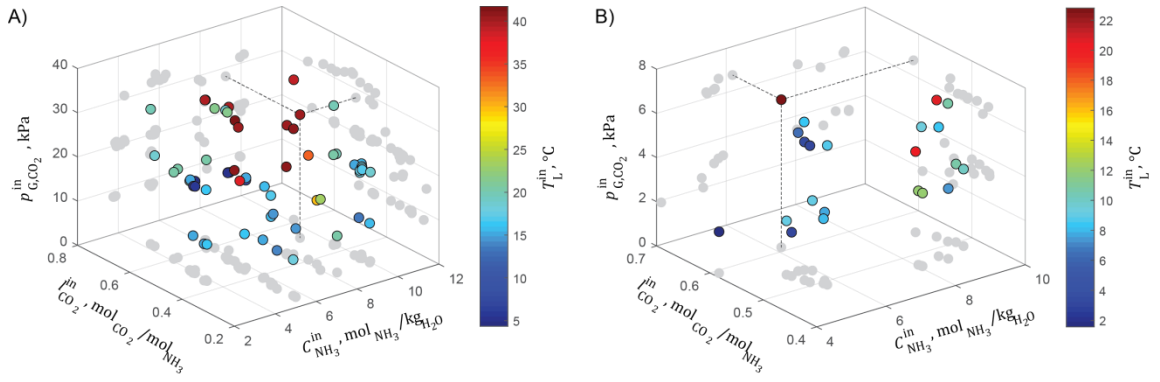

Figure 4.3: Experimental space studied during the pilot plant tests of the CO_2 absorber: A) Tests of Campaigns 1 and 2; and B) Tests of Campaign 3. The projections of each sphere (experimental point) upon each plane are shown in grey.

In total, 82 experimental points have been obtained from the pilot plant CO_2 absorption tests simulating cement plant-like flue gas conditions, in all cases closing the component and overall mass balances within 10% of accuracy. Solids have not been formed in any case. Net CO_2 transfer from the gas to the liquid was obtained experimentally in all tests. Experimentally, it has been observed that higher NH_3 concentration and lower CO_2-loading in the inlet liquid stream

This project has received funding from the European Union's Horizon2020 Research and Innovation Programme under Grant Agreement No 641185. This work was supported by the Swiss State Secretariat for Education, Research and Innovation (SERI) under contract number 15.0160

lead to a desirable increase of the CO_2 capture efficiency, but increase the NH_3 slip. Consequently, it was confirmed experimentally that the optimization of the operating conditions of the industrial CO_2 absorber requires the consideration of these opposing effects.

The validation of the Literature model introduced in Section 4.2 by means of the CO_2 absorber pilot plant tests performed within the CEMCAP project is shown in Figure 4.4 for the CO_2 absorption rate and the NH_3 absorption rate (Figure 4.4A and Figure 4.4B, respectively). In general, the CO_2 absorption rate values obtained experimentally are not well predicted by the Literature model: Deviations greater than 20% are found for a considerable amount of tests. As aforementioned, the Literature model was initially validated with the CO_2 absorption pilot tests available in the literature [6,10], performed with flue gases containing only up to 12 %vol CO_2 and using solutions with NH_3 concentration from 0-4 mol_{NH_3}/kg_{water}. The higher partial pressure of CO_2 in the inlet flue gas and the higher NH_3 concentration in the inlet aqueous ammonia solution considerably affect the CO_2 absorption unit, leading to different temperature and concentration profiles along the column [7] that might be outside the validity range of the Literature model.

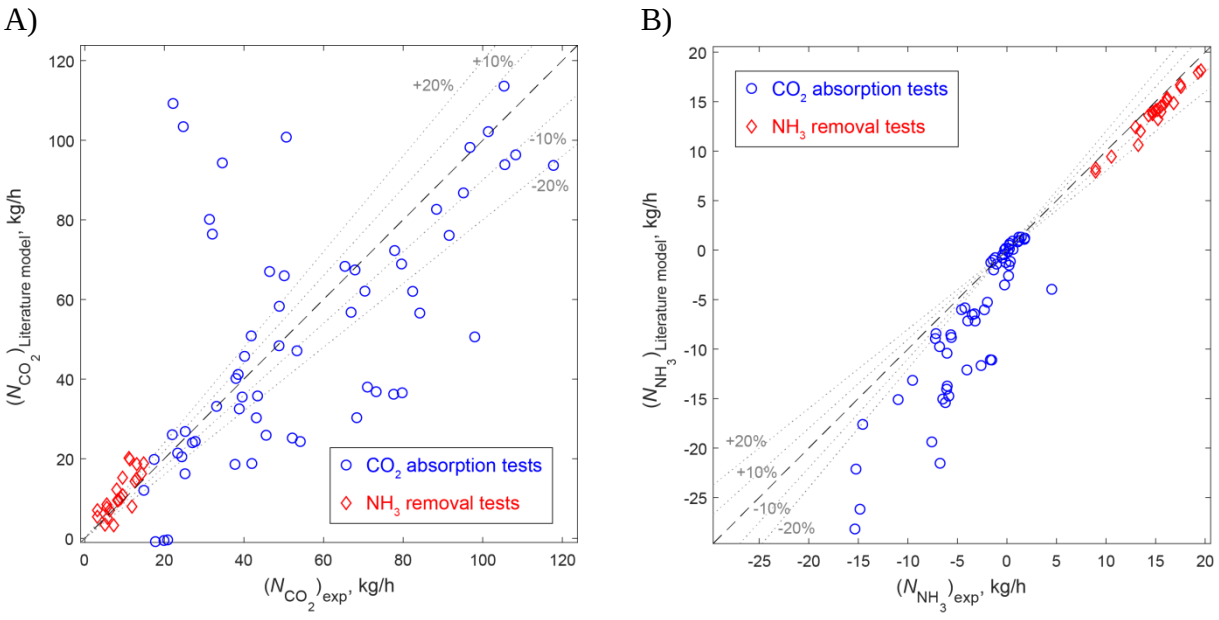

Figure 4.4: Parity plots showing the prediction of the preliminary rate-based model described in Section 4.2 (Literature model) vs. the experimental values for: (A) the CO_2 absorption rate; and (B) the NH_3 absorption rate. Experimental results have been obtained during the pilot plant tests of the CO_2 absorber performed at the GE facilities in Växjö (Sweden) , while the predicted values have been calculated using the preliminary rate-based model taken from the literature and described in Section 4.2 (Literature model). CO_2 absorption tests are represented by blue circles and were obtained during Campaign 1 and Campaign 2, while NH_3 removal tests are shown by red diamonds and the experimental results were obtained during Campaign 3. The experimental conditions tested during the three pilot test campaigns of the CO_2 absorber are shown in Table 4.3. The dashed line indicates parity between the experimental results and the prediction of the model, while the dotted lines indicate 10 and 20% of deviation.

Therefore, the preliminary rate-based model, i.e. the Literature model, has been updated as described by Pérez-Calvo et al. [14] making use of the CO_2 absorber pilot plant tests performed

This project has received funding from the European Union's Horizon2020 Research and Innovation Programme under Grant Agreement No 641185. This work was supported by the Swiss State Secretariat for Education, Research and Innovation (SERI) under contract number 15.0160

within the CEMCAP project. Namely, the correlations to compute the liquid-vapor mass transfer coefficients and the liquid-vapor interfacial area have been modified and the kinetic parameters of the reaction between CO_2 and NH_3 have been updated. The validation of the updated rate-based model (hereinafter referred to as "CEMCAP model") by means of the CO_2 absorber pilot plant tests performed within the CEMCAP project is shown in Figure 4.5 for the CO_2 absorption rate and the NH_3 absorption rate (Figure 4.5A and Figure 4.5B, respectively).

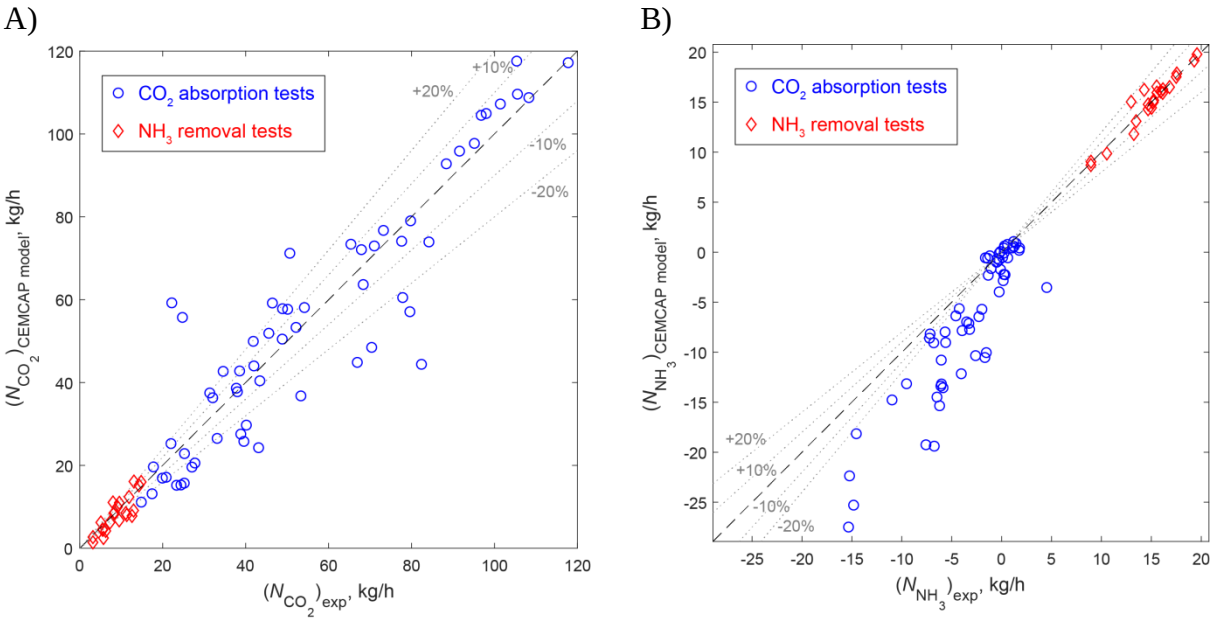

Figure 4.5: Parity plots showing the prediction of the updated rate-based model using CEMCAP pilot plant tests (CEMCAP model) vs. the experimental values for: (A) the CO_2 absorption rate; and (B) the NH_3 absorption rate. Experimental results have been obtained during the pilot plant tests of the CO_2 absorber performed at the GE facilities in Växjö (Sweden), while the predicted values have been obtained using the rate-based model updated with the aforementioned pilot plant tests performed in CEMCAP (CEMCAP model). CO_2 absorption tests are represented by blue circles and were obtained during Campaign 1 and Campaign 2, while NH_3 removal tests are shown by red diamonds and the experimental results were obtained during Campaign 3. The experimental conditions tested during the 3 pilot test campaigns of the CO_2 absorber are shown in Table 4.3. The dashed line indicates parity between the experimental results and the prediction of the model, while the dotted lines indicate 10 and 20% of deviation.

The CEMCAP model considerably improves the performance of the Literature model when predicting the CO_2 absorption rate (Figure 4.4A and Figure 4.5A, respectively). In general, experimental values of the CO_2 absorption rate (see Figure 4.5A) are predicted with a deviation smaller than 20% by the CEMCAP model, with the following exceptions: (i) the CO_2 absorption rate is overestimated by the model by more than 20% in a couple of experiments with an inlet liquid temperature as low as 5°C, which is outside the operating range of the CO_2 uptake section of the CO_2 absorber; and (ii) the CO_2 absorption rate is underestimated by the CEMCAP model by more than 20% in approximately 10% of the tests. Nevertheless, a lower CO_2 absorption rate predicted by the model with respect to the actual experimental value will lead to a conservative sizing of the CO_2 absorber, i.e. the height of the CO_2 absorber estimated by the CEMCAP model might lead to a greater CO_2 capture efficiency when scaled-up. As far as the NH_3 absorption rate is concerned, the experimental values of the NH_3 absorption rate (see Figure 4.5B) are predicted

This project has received funding from the European Union's Horizon2020 Research and Innovation Programme under Grant Agreement No 641185. This work was supported by the Swiss State Secretariat for Education, Research and Innovation (SERI) under contract number 15.0160

with a deviation smaller than 20% in all NH_3 removal tests, i.e. those tests belonging to Campaign 3 mimicking the conditions in the NH_3 uptake section of the industrial CO_2 absorber (see Table 4.3). Regarding the CO_2 absorption tests, the NH_3 desorption rate might be overestimated by the model, i.e. when release of NH_3 from the liquid to the gas is expected ($\left(N_{NH_3}\right)_{exp} < 0$): The model predicts a higher NH_3 slip to the gas than the value obtained experimentally. Consequently, the CEMCAP model might be conservative in the prediction of the NH_3 concentration leaving the top of the CO_2 absorber, so that no higher values than those predicted in the simulations are expected in reality. Overall, the CEMCAP model can be used with engineering purposes for the approximate design and sizing of the CO_2 absorber of the CAP applied to cement plants for CO_2 capture: Any deviation when scaling up the CO_2 absorber is expected to be conservative, i.e. a shorter column might be needed and a lower NH_3 concentration in the exiting gas stream might be obtained in reality. The development of a more mechanistic rate-based model based on the pilot plant tests performed in CEMCAP will be the subject of a future publication in a peer reviewed scientific journal.

In the pilot plant tests of the CO_2 absorber described above, CO_2 capture efficiencies as high as 65% were achieved with only 3 m of packing at NH_3 concentrations in the liquid of 10 mol_{NH3}/mol_{water}. Decreasing the NH_3 concentration in the liquid down to 4 mol_{NH3}/mol_{water} allowed to reach CO_2 capture efficiencies up to 30% within the 3 m high packing. Despite this remarkable uptake, the CO_2 capture efficiency targeted in CEMCAP for the CAP applied to cement plants, i.e. around 90%, would require a higher CO_2 absorber than the one available in the pilot plant. Consequently, the updated rate-based model, i.e. the CEMCAP model, was used to design and size the industrial CO_2 absorber of the CAP for each Design case defined in Table 3.2. The operating conditions of the CO_2 absorber in each case were taken from the case-wise optimized full CAP simulations obtained previously.

4.5.3 NH_3 absorber tests

A schematic of the configuration of the NH_3 absorber used when applying the CAP to coal-fired power plants for CO_2 capture is shown in Figure 4.6. The CO_2-depleted flue gas leaving the top of the CO_2 desorber and containing approximately 12,500 ppm_v of NH_3 enters the bottom of the NH_3 absorber. The NH_3 absorber is divided into 2 sections: (i) a lower section whose goal is the removal of the bulk amount of NH_3 contained in the entering flue gas, i.e. down to approximately 5,000 ppm_v, and (ii) an upper section in which the NH_3 concentration in the flue gas is further decreased to values below 200 ppm_v, before sending the CO_2 and NH_3-depleted flue gas to the flue gas heating section for further removal of NH_3 and flue gas heating before reaching the stack. The NH_3-lean solution regenerated in the NH_3 desorber is chilled before entering the top of the NH_3 absorber. While flowing down along the column, the aqueous ammonia solution captures NH_3 and CO_2 from the flue gas flowing upwards in counter-current, increasing both its NH_3 and its CO_2 concentration. The NH_3-rich stream loaded with CO_2 obtained at the bottom of the NH_3 absorber is sent back to the NH_3 desorber, where NH_3 and CO_2 are stripped off from the liquid solution, regenerating the NH_3-lean stream to be used again in the NH_3 absorber. A fraction of the NH_3-rich solution leaving the bottom of the NH_3 desorber is recycled to an intermediate stage of the NH_3 absorber after being chilled. The goals of this recycled stream are: (i) to approach the NH_3 concentration in the flue gas leaving the lower section of the NH_3 absorber to the NH_3 partial pressure in equilibrium with the recycled liquid stream using a high enough liquid-to-gas flowrate ratio, and (ii) to maximize the NH_3 removal in the lower section of the NH_3 absorber by decreasing the temperature of the liquid solution.

This project has received funding from the European Union's Horizon2020 Research and Innovation Programme under Grant Agreement No 641185. This work was supported by the Swiss State Secretariat for Education, Research and Innovation (SERI) under contract number 15.0160

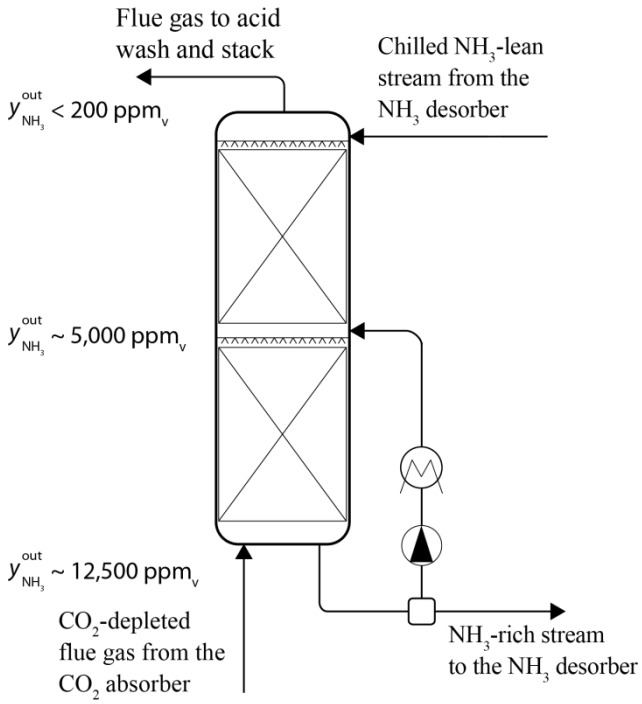

Figure 4.6: NH_3 absorber configuration used in the application of the CAP to power plants for CO_2 capture.

Nevertheless, assuming that the CO_2 capture rate in the CO_2 absorber is kept constant with respect to the power plant case (targeting a 90% capture rate overall), the remaining CO_2 concentration in the flue gas entering the NH_3 absorber will increase when applying the CAP to cement plants. Therefore, pilot plant tests of the NH_3 absorber of the CAP at flue gas conditions typical from cement plants have been performed as part of the CEMCAP project, pursuing the following goals:

- Understand how the increase of the CO_2 concentration in the flue gas entering the NH_3 absorber will affect the NH_3 capture with respect to the operation at power plant-like flue gas conditions.
- Determine qualitatively the influence of the operating parameters on the NH_3 capture in the NH_3 absorber at cement plant-like flue gas conditions, and determine the set of operating conditions that, still achieving the levels of NH_3 in the flue gas specified in Figure 4.6, are expected to minimize the energy consumption of the capture process.
- Adapt the in-silico design and simulation of the NH_3 absorber of the CAP applied to cement plants, obtaining full CAP simulation that reproduces the results of the pilot plant tests.

Table 4.4 shows the boundary conditions of the operating variables selected for the pilot plant tests. Experiments were divided into 2 different types of tests representing the different sections of the foreseen industrial NH_3 absorber shown in Figure 4.6: (i) tests simulating the bottom part of the industrial NH_3 absorber (Campaign 1), and (ii) tests reproducing the expected conditions at the top of the industrial NH_3 absorber (Campaign 2). In addition, the reproducibility of the experiments was tested. The pilot tests of the NH_3 absorber were performed following a similar procedure as described for the CO_2 capture pilot tests, as well as the same test rig shown in Figure 4.2. The packing of the column is 3 m high, with a diameter of 450 mm. The packing used was Koch Glitsch Flexipac M 350X.

This project has received funding from the European Union's Horizon2020 Research and Innovation Programme under Grant Agreement No 641185. This work was supported by the Swiss State Secretariat for Education, Research and Innovation (SERI) under contract number 15.0160

Table 4.4: Summary of experimental conditions for the pilot plant tests of the NH_3 absorber.

Stream	Variable		Unit	Campaign 1	Campaign 2
Inlet liquid	NH_3 concentration	$C_{NH_3}^{in}$	$kmol_{NH3}/m^3$	0.5-2.5	0-0.1
	CO_2 loading	$l_{CO_2}^{in}$	mol_{CO2}/mol_{NH3}	0.28-0.58	0
	Temperature	T_L^{in}	°C	3-13	5-30
Inlet gas	CO_2 concentration	$y_{CO_2}^{in}$	%vol	0-10	1-5
	NH_3 concentration	$y_{NH_3}^{in}$	ppm_v	12,500	5,000
	Superficial velocity	$v_{S,G}^{in}$	m/s	1.3-1.5	1.3-1.5
	Temperature	T_G^{in}	°C	10-15	10-15
	Pressure	P_G^{in}	kPa	~100	~100
Inlet liquid and gas	Liquid-to-gas flowrate ratio	L^{in}/G^{in}	kg/kg	1.0-6.0	0.1-0.3

The results of the pilot plant tests of the NH_3 absorber performed at the flue gas conditions typical for cement plants have led to the following conclusions:

- The NH_3 capture is enhanced by the higher CO_2 concentration in the flue gas leaving the CO_2 absorber of the CAP, with respect to the power plant case.
- The levels of NH_3 specified in Figure 4.6 can be achieved using a lower and an upper section with a packing Koch Glitsch Flexipac M 350X of 3 m high each.
- Considering that the flue gas entering the NH_3 absorber of the industrial CAP applied to cement plants will contain approximately 3%vol CO_2, the operating conditions that experimentally achieved the specified NH_3 concentration (see Figure 4.6) with the lowest expected energy consumption, were:
    - Upper section. Inlet liquid stream with a temperature of 15°C and a NH_3 concentration of 0.05 $kmol/m^3$, and a liquid-to-gas flowrate ratio of 0.2 kg/kg.
    - Lower section. Inlet liquid stream with a temperature of 10°C, NH_3 concentration of 1.5-2.5 $kmol/m^3$ and CO_2 loading around 0.55-0.6 mol_{CO_2}/mol_{NH_3}, and liquid-to-gas flowrate ratio of 1 kg/kg. The actual values of the NH_3 concentration and CO_2 loading of the recycle liquid stream of the lower section will depend on the fulfillment of the material and energy balance around the NH_3 absorber.

A more quantitative analysis of the NH_3 absorber tests performed in the CEMCAP project will be the subject of a future publication in a peer reviewed scientific journal. Nevertheless, the qualitative analysis presented above has been enough to determine the adaptations that the NH_3 absorber of the CAP applied to cement plants requires with respect to the power plant case, and to obtain simulation results that reproduce the pilot plant experimental results.

This project has received funding from the European Union's Horizon2020 Research and Innovation Programme under Grant Agreement No 641185. This work was supported by the Swiss State Secretariat for Education, Research and Innovation (SERI) under contract number 15.0160

5 RESULTS AND DISCUSSION

5.1 Single variable sensitivity analyses

Single variable sensitivity analyses were performed at two different sets of operating conditions in the CO_2 absorber of the CAP, i.e. OC1 and OC2, as specified in Table 5.1. In all cases, the conditions of the flue gas were those corresponding to medium air leak into the cement plant, that can be found in Table 3.1, i.e. containing 18%vol CO_2. In each single variable sensitivity analysis, one parameter was varied at a time, fixing the others to the value of OC1/OC2. The influence of each variable on the performance of the CAP was assessed analyzing the impact on the energy consumers and on the specifications and constraints of the process.

Table 5.1: Set of operating conditions of the CO_2 absorber used in the single variable sensitivity analyses. All simulations of the CAP performed at this stage were carried out considering flue gas conditions associated with the medium air leak into the cement plant, i.e. flue gas containing 18%vol CO_2 as specified in Table 3.1.

Variable		Unit	Operating conditions of the CO_2 absorber	
			OC1	OC2
CO_2-lean NH_3 concentration	$C_{NH_3}^{in}$	mol_{NH3}/kg_{water}	6.0	8.0
CO_2-lean CO_2 loading	$l_{CO_2}^{in}$	mol_{CO2}/mol_{NH3}	0.375	0.330
CO_2-lean to inlet flue gas flowrate ratio	L^{in}/G^{in}	kg/kg	5.6	5.0
Pumparound split fraction	f_s	-	0.18	0.25
Pumparound temperature	T_{pa}	°C	15	5

As a result of the single variable sensitivity analyses, seven parameters were included in the heuristic optimization of the CAP applied to cement plants: (i) the ammonia concentration of the lean stream, $C_{NH_3}^{in}$, (ii) the CO_2-loading of the lean stream $l_{CO_2}^{in}$, defined as mol_{CO2}/mol_{NH3}, (iii) the liquid-to-gas flowrate ratio, defined as the ratio between the mass flowrate of the CO_2-lean stream and the mass flowrate of the flue gas stream entering the CO_2 absorber, L^{in}/G^{in}, (iv) the pumparound split fraction, f_s, (v) the temperature of the pumparound chilling, T_{pa}, (vi) the pressure of the CO_2 desorber, $P_{CO_2 des}$, and (vii) the cold-rich split fraction, f_{cr}. On the other hand, the operating pressure of the Appendix Stripper, the operating pressure of the NH_3 desorber, the temperature of the liquid entering the top of the DCC and the liquid-to-gas flowrate ratio in the DCC of the CO_2-WW were fixed in the heuristic optimization of the CAP. The reasoning to fix the value of the latter variables is described in the following sub-sections.

5.1.1 Operating pressure of the Appendix Stripper

The pressure of the Appendix Stripper has been varied between 1.15 and 4 bar. As shown in Figure 5.1, the reboiler duty and the reboiler temperature of the Appendix Stripper increase with the operating pressure of the column, for the two different sets of operating conditions of the CO_2 absorber studied. The effect of the operating pressure of the Appendix Stripper on the temperature of the reboiler of the column is similar for both sets of operating conditions. The increase of the temperature is justified by the increase of the bubble point of the liquid at increasing pressure. On the other hand, the greater liquid flowrate entering the Appendix Stripper in the case of OC1 operating conditions, makes the reboiler duty of the Appendix

This project has received funding from the European Union's Horizon2020 Research and Innovation Programme under Grant Agreement No 641185. This work was supported by the Swiss State Secretariat for Education, Research and Innovation (SERI) under contract number 15.0160

Stripper more sensitive to changes in the pressure than in the case of running the CAP at OC2 operating conditions of the CO_2 absorber.

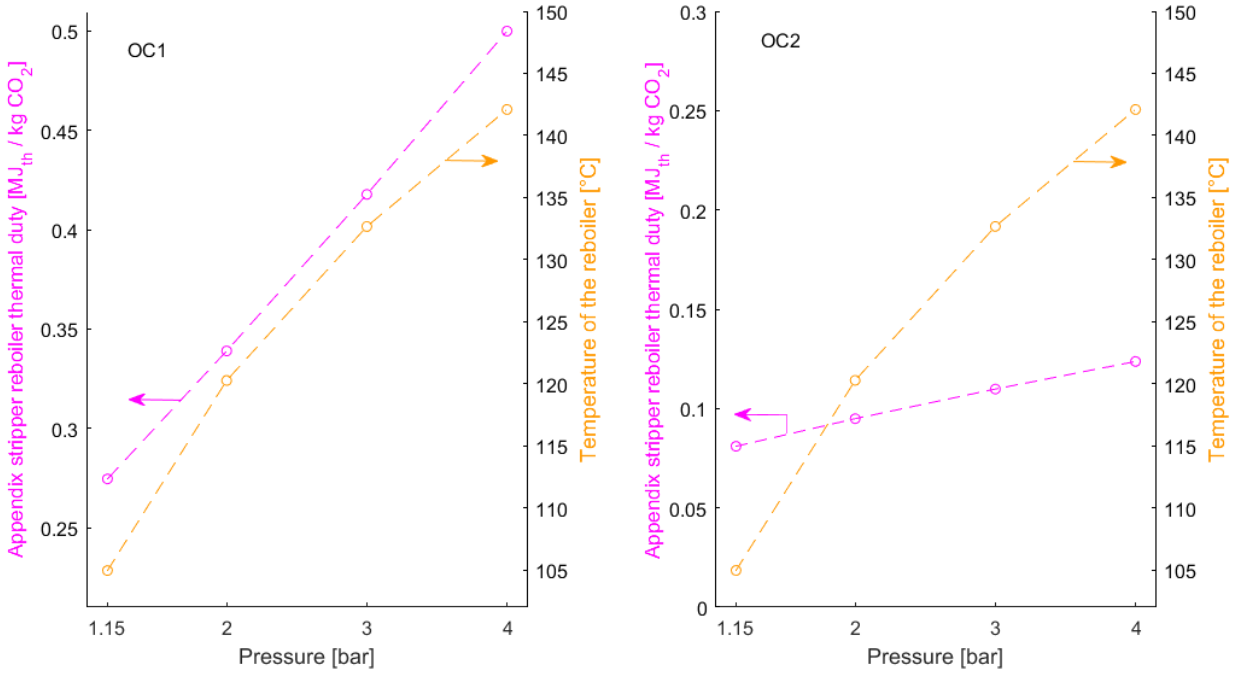

Figure 5.1: Reboiler specific thermal duty and temperature of the reboiler of the Appendix Stripper vs the operating pressure of the Appendix Stripper, for OC1 (left) and OC2 (right) operating conditions. The specific values of the energy consumers are computed per kg of CO_2 captured.

Higher reboiler duty and temperature of the reboiler will increase the value of the SPECCA index associated with the steam required in the reboiler of the Appendix Stripper. Therefore, the pressure of the Appendix Stripper has been fixed to atmospheric pressure.

5.1.2 Operating pressure of the NH_3 desorber

A similar analysis to that presented in Section 5.1.1 for the Appendix Stripper has been performed for the NH_3 desorber. Figure 5.2 shows the influence of the pressure of the NH_3 desorber on the reboiler duty and the reboiler temperature of the column. Similar effects, trends and conclusions to those obtained for the pressure of the Appendix Stripper can be drawn in this case. Consequently, the pressure of the NH_3 desorber has been fixed to the atmospheric pressure.

This project has received funding from the European Union's Horizon2020 Research and Innovation Programme under Grant Agreement No 641185. This work was supported by the Swiss State Secretariat for Education, Research and Innovation (SERI) under contract number 15.0160

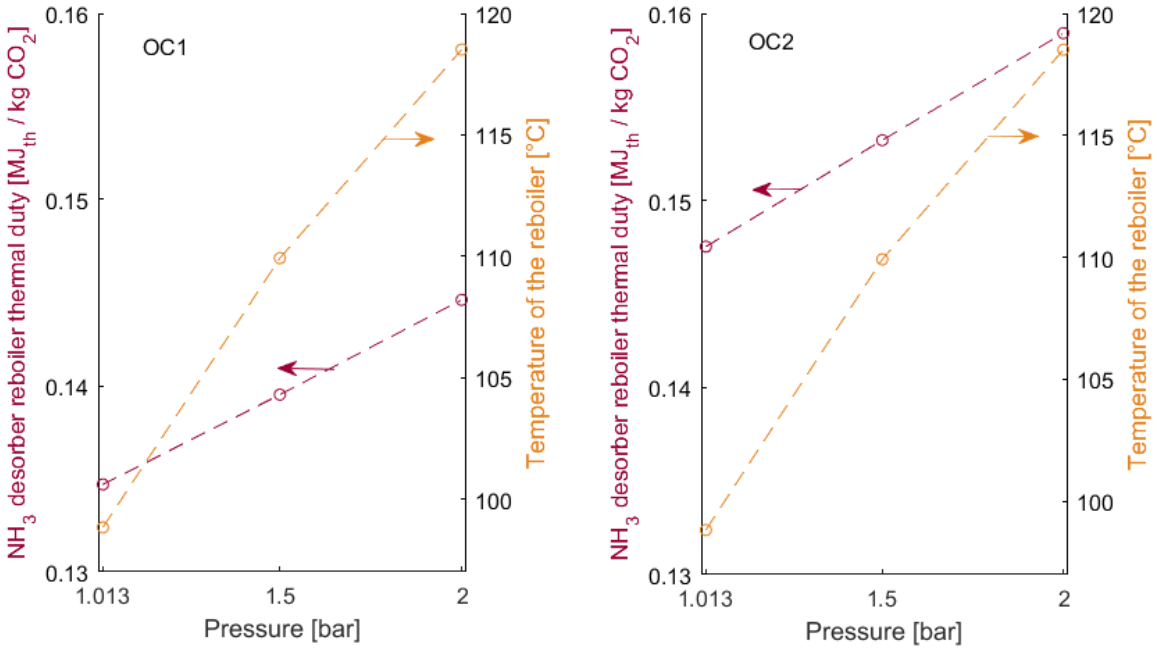

Figure 5.2: Thermal reboiler duty and reboiler temperature in the NH_3 desorber vs the operating pressure of the NH_3 desorber, for OC1 (left) and OC2 (right) operating conditions. The specific values of the energy consumers are computed per kg of CO_2 captured.

5.1.3 Temperature of the liquid entering the top of the DCC

One of the two goals of the DCC (column in the flue gas cooling section of the CAP shown in Figure 2.1) is to remove a significant amount of water contained in the flue gas, as earlier introduced in Section 2. The water content in the flue gas entering the CO_2 absorber should approach the water contained in the flue gas leaving the NH_3 absorber in order to minimize the accumulation of water within the capture process. As a consequence, the flowrate of the purge required to close the water balance within the CO_2 capture section decreases, and so does the reboiler duty of the Appendix Stripper. In general, a lower temperature of the liquid water stream entering the top of the DCC decreases the water content in the flue gas entering the CO_2 absorber, and hence, the reboiler duty of the Appendix Stripper, at the cost of increasing the chilling demand in the DCC. Figure 5.3 shows these effects quantitatively. A decrease of the temperature of the water entering the DCC increases the chilling demand by a factor of three with respect to the decrease achieved for the reboiler duty of the Appendix Stripper (for OC1 operating conditions). This ratio increases to six in the case of the OC2 operating conditions. Therefore, the temperature of the liquid stream entering the DCC has been set to the minimum value achievable using cooling water, i.e. 21.2°C, with the aim of minimizing the reboiler duty of the Appendix Stripper without increasing the chilling duty of the CAP. Notably, the temperature value is very much dependent on ambient conditions: generally speaking CAP applied to cold environment will benefit of lower electricity demand for chilling, but also lower reboiler duty thanks to more affordable chilling.

This project has received funding from the European Union's Horizon2020 Research and Innovation Programme under Grant Agreement No 641185. This work was supported by the Swiss State Secretariat for Education, Research and Innovation (SERI) under contract number 15.0160

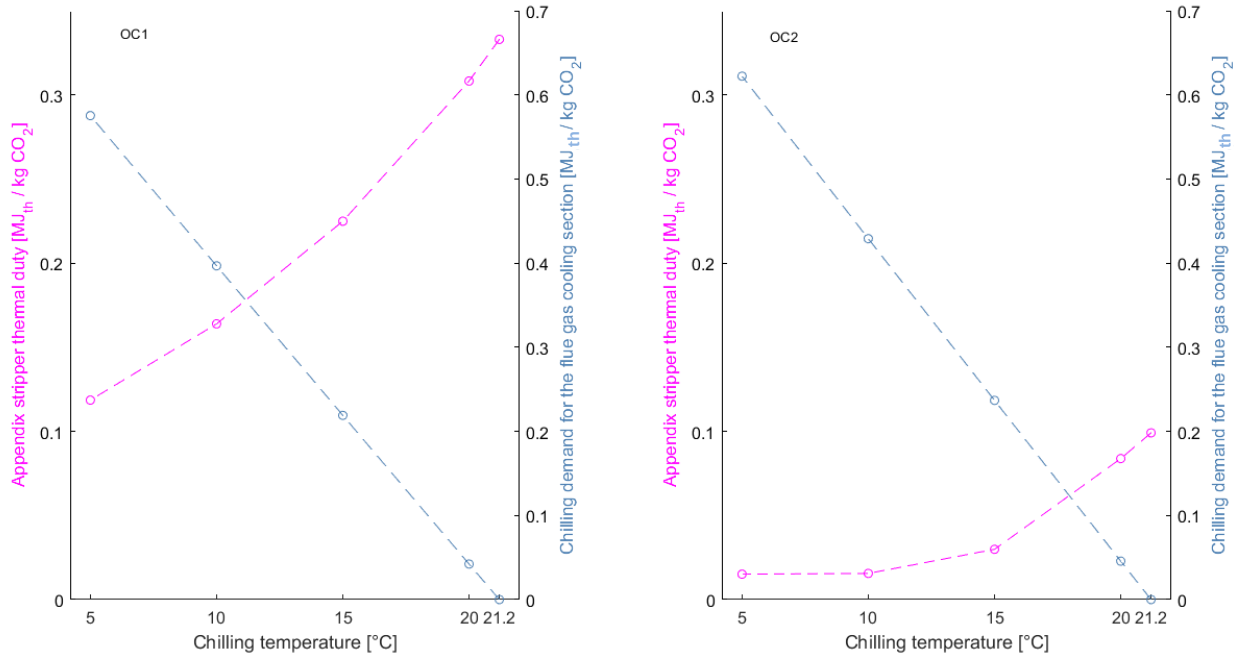

Figure 5.3: Thermal reboiler duty of the Appendix Stripper (magenta) and chilling demand required for the flue gas cooling section (blue) vs the temperature of the liquid stream entering the top of the DCC for operating conditions OC1 (left) and OC2 (right). The specific values of the energy consumers are computed per kg of CO_2 captured.

5.1.4 Liquid-to-gas flowrate ratio in the CO_2-WW column

The CO_2-WW serves the purpose of further purifying the CO_2 gas recovered in the CO_2 desorber, specifically by removing NH_3. A liquid water stream enters the top of a packed column where it flows down in counter-current with the CO_2 gas stream. The water takes up NH_3 (and a very small amount of CO_2) from the CO_2 gas stream. In order to avoid excessive NH_3 accumulation within the CO_2-WW loop, a purge stream is required, that is sent to the Appendix Stripper to recover NH_3 (and CO_2). Consequently, a fresh water make-up is needed to maintain the liquid-to-gas flowrate ratio in the packed column of the CO_2-WW. Hence, the operation in the CO_2-WW affects the energy consumption of the Appendix Stripper. Figure 5.4 shows the impact of the liquid-to-gas flowrate ratio in the packed column of the CO_2-WW on the reboiler duty of the Appendix Stripper, for two different sets of operating conditions of the CO_2 absorber, i.e. OC1 and OC2, and for two different pressures in the CO_2 desorber, i.e. 10 and 20 bar. In addition, the evolution of the water make-up flowrate required in the CO_2-WW and of the total flowrate of purged streams entering the Appendix Stripper are shown. The decrease of the liquid-to-gas flowrate ratio in the packed column of the CO_2-WW decreases the reboiler duty of the Appendix Stripper in all cases, due to the reduction of the water make-up flowrate required in the CO_2-WW, and hence, to the decrease of the flowrate of the purged stream sent to the Appendix Stripper.

This project has received funding from the European Union's Horizon2020 Research and Innovation Programme under Grant Agreement No 641185. This work was supported by the Swiss State Secretariat for Education, Research and Innovation (SERI) under contract number 15.0160

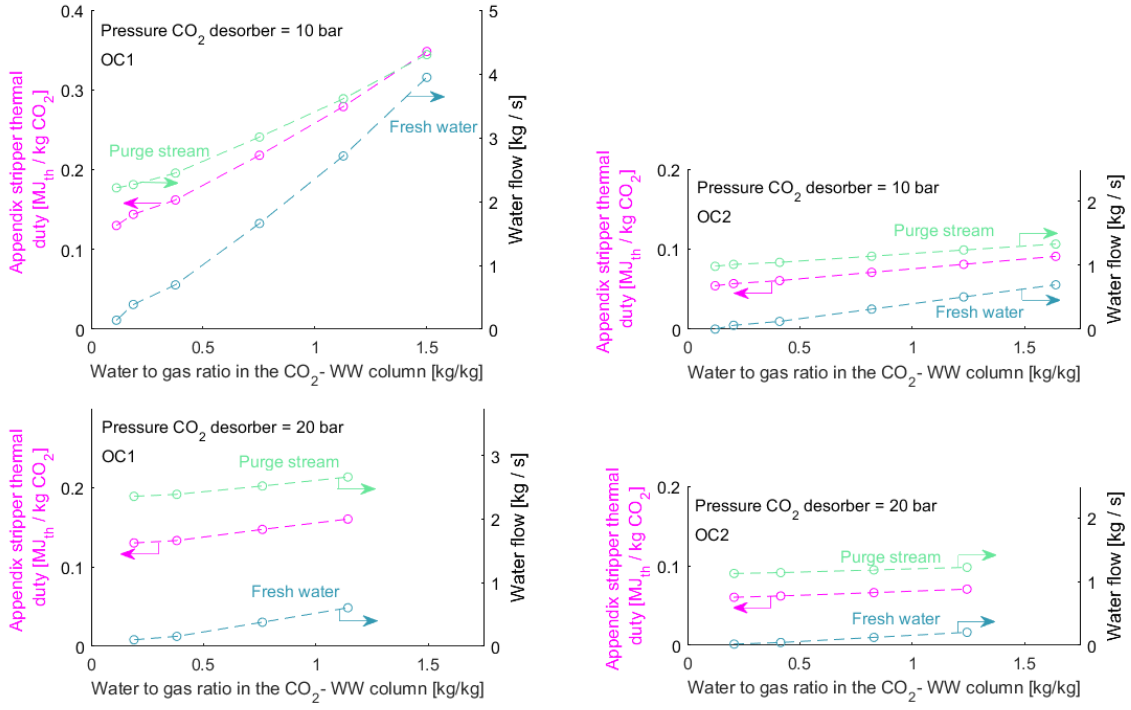

Figure 5.4: Reboiler specific thermal duty of the Appendix Stripper (magenta), flowrate of the water make-up introduced in the CO_2-WW section (blue) and water flowrate (apparent) of the stream purged from the CO_2 capture section (green) vs the liquid-to-gas flowrate ratio in the CO_2-WW for operating conditions OC1 (left) and OC2 (right) with the CO_2 desorber operating at 10 bar (top) or 20 bar (bottom). The specific values of the energy consumers are computed per kg of CO_2 captured.

On the other hand, the NH_3 concentration in the CO_2 stream sent for compression is limited to max. 50 ppm_v (representing a strict and thus conservative limitation, as discussed in Section 3). Figure 5.5 shows the effect of varying the liquid-to-gas flowrate ratio in the CO_2-WW on the NH_3 concentration in the CO_2 gas stream sent to the CO_2 compression section. The NH_3 concentration in the CO_2 gas stream increases if the liquid-to-gas flowrate ratio in the CO_2-WW is decreased. Additionally, the NH_3 content in the CO_2 gas stream sent for compression does not seem to depend on the set of operating conditions selected for the CO_2 absorber. On the contrary, it increases if the pressure of the CO_2 desorber is lowered. The NH_3 concentration in the CO_2 gas stream sent for compression is always below the NH_3 concentration threshold (shown by the black dotted line in Figure 5.5) for all the cases considered here. However, operating the CO_2 desorber at 10 bar with a liquid-to-gas flowrate ratio in the CO_2-WW below 0.2 kg/kg leads to the formation of solids in the condensate generated out of the cooler placed after the packed column of the CO_2-WW.

This project has received funding from the European Union's Horizon2020 Research and Innovation Programme under Grant Agreement No 641185. This work was supported by the Swiss State Secretariat for Education, Research and Innovation (SERI) under contract number 15.0160

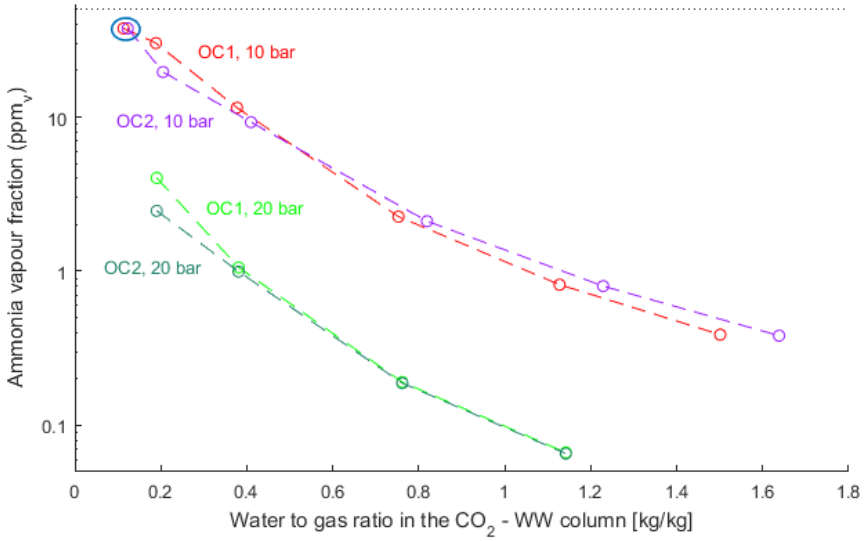

Figure 5.5: Ammonia concentration in the CO_2 stream sent for compression vs the liquid-to-gas flowrate ratio in the CO_2-WW column for operating conditions OC1 and OC2, both with CO_2 desorber operating pressures of 10 and 20 bar. The upper black dotted line represents the NH_3 concentration limit in the CO_2 to be stored. The blue circle indicates solid formation in the condensate produced in the cooler placed downstream the packed column of the CO_2-WW section.

Therefore, a liquid-to-gas flowrate ratio of 0.3 kg/kg in the packed column of the CO_2-WW is selected as a trade-off between minimizing the reboiler duty of the Appendix Stripper and avoiding the formation of solids downstream for a broad range of pressures of the CO_2 desorber.

5.2 Heuristic optimization

The results of the heuristic optimization of the CAP applied to cement plant-like flue gas conditions are shown in Figure 5.6, for the four Design Cases defined in Table 3.2. In total, an average of 35,000 simulations were performed for the optimization of each case, with different combinations of the operating conditions in the CO_2 absorber, namely: (i) the ammonia concentration of the lean stream, $c^{\text{in}}_{\text{NH}_3}$, (ii) the CO_2-loading of the lean stream $l^{\text{in}}_{\text{CO}_2}$, defined as $\text{mol}_{\text{CO2}}/\text{mol}_{\text{NH3}}$, (iii) the liquid-to-gas flowrate ratio, defined as the ratio between the mass flowrate of the CO_2-lean stream and the mass flowrate of the flue gas stream entering the CO_2 absorber, $L^{\text{in}}/G^{\text{in}}$, (iv) the pumparound split fraction, f_{s}, and (v) the temperature of the pumparound chilling, T_{pa}. Each symbol in Figure 5.6 represents one full simulation that has converged and fulfills the specifications and constraints defined in Section 3 for each case. Points are colored according to the value of the SPECCA index. The two coordinates represent the variables with the strongest effect on the variation of the total SPECCA. (i.e. contribution to the SPECCA by the chillers and contribution to the SPECCA by the reboilers). In addition, chilling demand and steam demand minimization are opposing objectives. Consequently, the minimum SPECCA is found on the frontier of the ensemble of points closest to the origin. It is also worth noting that the total SPECCA is a strong function of the total reboiler duties and only weakly affected by the chilling duty.

This project has received funding from the European Union's Horizon2020 Research and Innovation Programme under Grant Agreement No 641185. This work was supported by the Swiss State Secretariat for Education, Research and Innovation (SERI) under contract number 15.0160

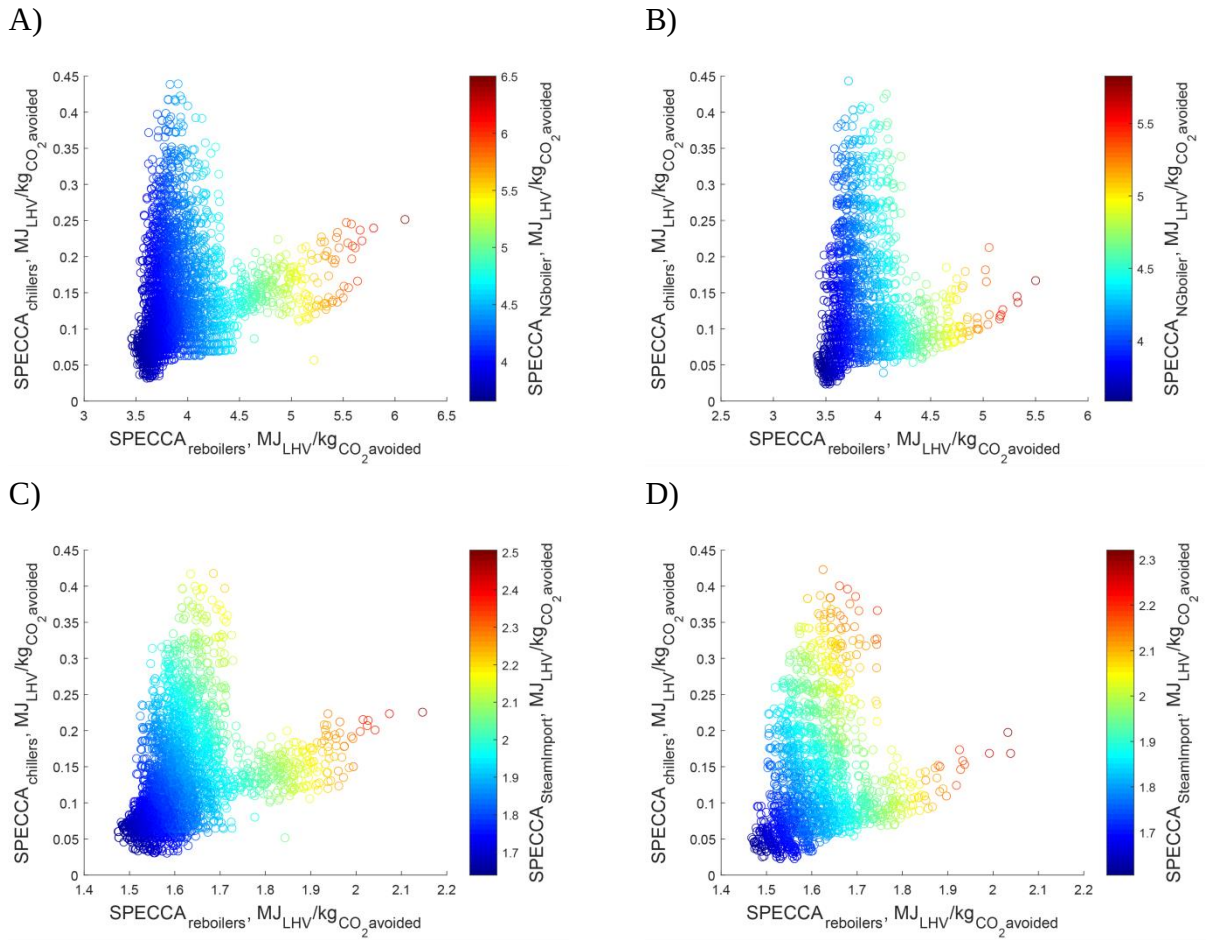

Figure 5.6: Resulting SPECCA value of all CAP simulations plotted in a chilling contribution to the SPECCA vs. reboiler contribution to the SPECCA plane when: (A) the flue gas is produced in a cement plant with medium air leak into the mill and contains 18%vol CO_2, and the steam required in the reboilers of the CAP is generated in a NG boiler built on-site; (B) the flue gas is produced in a cement plant with low air leak into the mill and contains 22%vol CO_2, and the steam required in the reboilers of the CAP is generated in a NG boiler built on-site; (C) the flue gas is produced in a cement plant with medium air leak into the mill and contains 18%vol CO_2, and the steam required in the reboilers of the CAP is imported from a CHP plant located in the neighborhood of the cement plant; and (D) the flue gas is produced in a cement plant with low air leak into the mill and contains 22%vol CO_2, and the steam required in the reboilers of the CAP is imported from a CHP plant located in the neighborhood of the cement plant. The SPECCA values shown in these plots are computed considering the steam demand and the chilling demand in the CO_2 capture section and the FG-WW section, as well as the electricity demand required in the auxiliaries. The simplified flow scheme of the CAP shown in Figure 4.1 has been used for the simulations.

Figure 5.7 shows the SPECCA values for the CAP simulations included in Figure 5.6 as a function of the CO_2 capture efficiency of the CAP, i.e. percentage of CO_2 flowrate captured by the CAP and sent for transport with respect to total flowrate of CO_2 entering the CAP within the flue gas produced in the cement plant. Each cloud of points shown in Figure 5.7 has been obtained from the same ensemble of CAP simulations performed to obtain each plot in Figure 5.6. In general, Figure 5.7 shows that the minimum SPECCA value increases with the targeted

This project has received funding from the European Union's Horizon2020 Research and Innovation Programme under Grant Agreement No 641185. This work was supported by the Swiss State Secretariat for Education, Research and Innovation (SERI) under contract number 15.0160

CO_2 capture efficiency. Additionally, lower SPECCA values are obtained when increasing the CO_2 concentration in the entering flue gas to the CAP.

A)

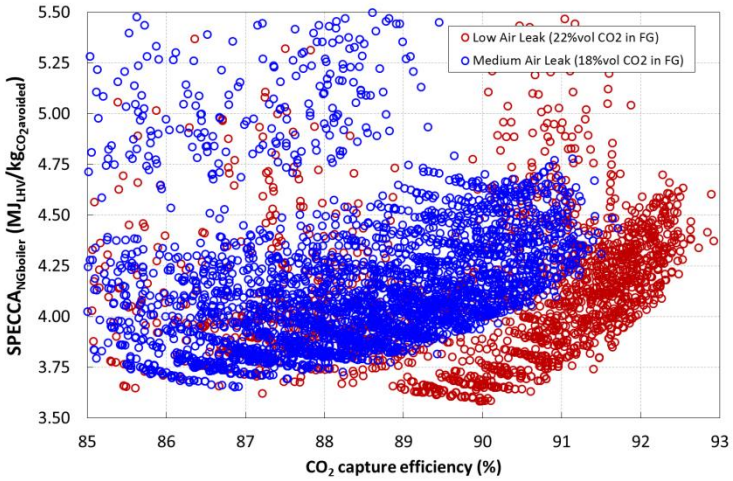

B)

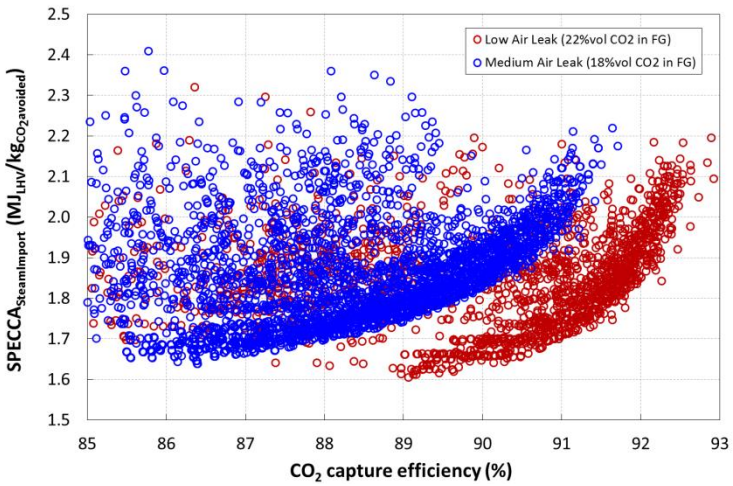

Figure 5.7: SPECCA values as a function of the CO_2 capture efficiency (CCR) of the CAP applied to a flue gas containing 22 and 18%vol CO_2. The SPECCA has been computed considering that the steam required in the reboiler of the desorbers is: (A) Produced in a NG boiler built on-site, or (B) Imported from a CHP plant located in the neighborhood of the cement plant, as defined in the CEMCAP common framework [5]. The SPECCA values shown in this plot consider the steam demand and the chilling demand in the CO_2 capture section and the FG-WW section, as well as the electricity demand required in the auxiliaries. The simulations have been performed using the simplified flow scheme of the CAP shown in Figure 4.1.

The heuristic optimization performed for each case shown in Figure 5.6 was extended by analyzing the effect of the pressure of the CO_2 desorber, $P_{CO_2 des}$, and of the cold-rich split fraction, f_{cr}, for the most promising set of operating conditions of the CO_2 absorber in terms of SPECCA index. The results are shown in Figure 5.8, where the SPECCA computed assuming that the steam is imported from a CHP plant is plotted versus the SPECCA index calculated considering that the steam is produced in a NG boiler built on-site. Each circle represents one full simulation that has converged and fulfills the specifications and constraints defined in

This project has received funding from the European Union's Horizon2020 Research and Innovation Programme under Grant Agreement No 641185. This work was supported by the Swiss State Secretariat for Education, Research and Innovation (SERI) under contract number 15.0160

Section 3 for each case. Points are colored according to the value of the pressure of the CO_2 desorber. The pressure of the CO_2 desorber shows opposing effects on the value of the SPECCA index depending on the origin of the steam used in the reboilers of the CAP: While operating the CO_2 desorber at higher pressure decreases the SPECCA when the steam is generated in an on-site NG boiler, it increases the SPECCA when the steam is imported from a CHP plant. Increasing pressure in the CO_2 desorber, up to 20-25 bar, decreases the specific reboiler duty of the CO_2 desorber, although it leads to a higher reboiler temperature, and hence, to a higher temperature of the required steam. On the one hand, the specific energy consumed in the NG boiler, and hence the amount of natural gas burnt, does not depend on the temperature of the steam required, which makes the associated SPECCA independent of the reboiler temperature. On the other hand, when the steam is provided by a CHP plant, the amount of electricity lost in the CHP plant increases with the higher temperature of the withdrawn steam, which in turn increases the associated SPECCA value in this scenario.

A) B)

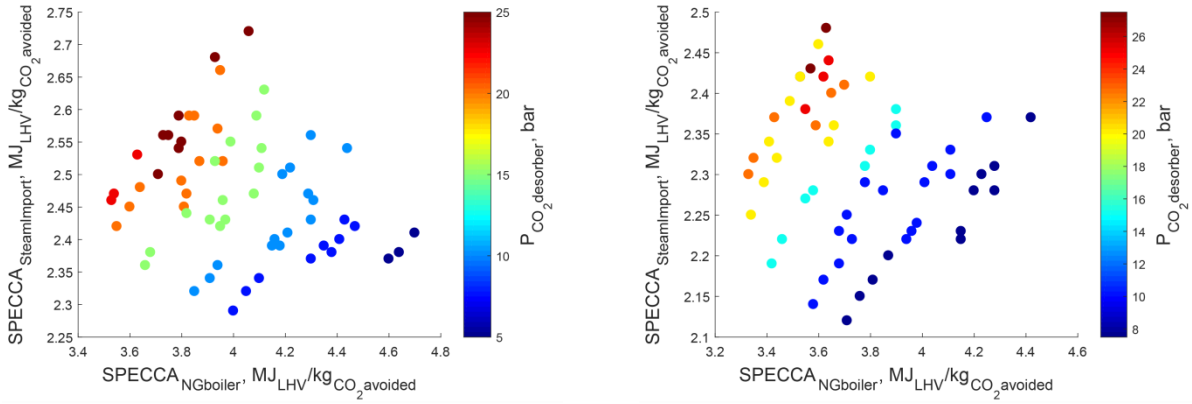

Figure 5.8: SPECCA importing the steam for the reboilers of the CAP from a CHP plant vs. SPECCA producing the steam for the reboilers of the CAP in an on-site NG boiler, for the most promising CAP simulations shown in Figure 5.6, when: (A) the flue gas is produced in a cement plant with medium air leak into the mill and contains 18%vol CO_2; and, (B) the flue gas is produced in a cement plant with low air leak into the mill and contains 22%vol CO_2. The SPECCA values shown in these plots are computed considering the steam demand, the chilling demand, the cooling demand, and the energy demand for CO_2 compression and in the auxiliaries, as well as the heat recovered from the cement plant to produce steam for the reboilers of the CAP. The flow scheme of the CAP shown in Figure 2.1 has been used for the simulations.

Therefore, high pressures of the CO_2 desorber are preferred if the steam of the CAP is produced in an on-site NG boiler. In this case, an optimum value of 20-25 bar has been found. Higher pressure levels do not decrease the specific reboiler duty of the CO_2 desorber significantly and increases the reboiler temperature above 150°C. The experience acquired on the application of the CAP to power plants for CO_2 capture, as for example the CAP demo plant built at Mountaineer [15], has shown that aqueous ammonia solutions at temperatures above 150°C may pose corrosion issues for the most common materials used in the construction of equipment at industrial scale, i.e. stainless steel or carbon steel.

This project has received funding from the European Union's Horizon2020 Research and Innovation Programme under Grant Agreement No 641185. This work was supported by the Swiss State Secretariat for Education, Research and Innovation (SERI) under contract number 15.0160

On the contrary, low pressure levels in the CO_2 desorber are preferred if the steam required in the reboilers of the CAP is imported from a CHP plant located in the neighborhood of the cement plant. An optimum value of 10 bar has been found in this case. Although further decreasing the pressure of the CO_2 desorber to 7.5 bar would still decrease the SPECCA index slightly, the NH_3 concentration in the CO_2 gas stream produced in the CO_2 desorber increases exponentially. At such conditions, the CO_2-WW would not be able to decrease the NH_3 concentration in the CO_2 gas stream to values below 50 ppm_v, as defined in the specifications and constraints of the process.

As a result, the optimum set of operating conditions that minimizes the SPECCA index for each Design case defined in Table 3.2 were obtained and are shown in Table 5.2. The range of the input parameters that has been tested in the heuristic optimization of the CAP is also shown in Table 5.2, as well as the CO_2 concentration in the inlet flue gas and the CO_2 capture rate of the process (CCR), as defined above.

Table 5.2: Optimum sets of operating conditions that minimize the SPECCA index for each Design case defined in Table 3.2. The range of input parameters that has been used in the heuristic optimization of the CAP are shown too, as well as the CO_2 capture rate (CCR) achieved and the CO_2 concentration in the flue gas considered in each case.

Variable		Unit	Range for optimization		Best set of operating conditions of the CAP per case [5] run at the same flue gas conditions of the Design case (see Table 3.2)			
					Base case	Constant low air leak	Optional extent of capture	Steam import
			Min	Max	18%vol CO_2 90% CCR	22%vol CO_2 90% CCR	18%vol CO_2 86% CCR	18%vol CO_2 90% CCR
CO_2-lean NH_3 concentration	$C_{NH_3}^{in}$	mol_{NH3}/kg_{water}	3.5	10.0	6.0	4.0	5.0	6.0
CO_2-lean CO_2 loading	$l_{CO_2}^{in}$	mol_{CO2}/mol_{NH3}	0.25	0.45	0.387	0.340	0.346	0.387
CO_2-lean to inlet flue gas flowrate ratio	L^{in}/G^{in}	kg/kg	3.5	10.0	6.5	7.0	5.0	6.5
Pumparound split fraction	f_s	-	0.05	0.45	0.18	0.15	0.21	0.18
Pumparound temperature	T_{pa}	°C	5	19	9	12	12	9
CO_2 desorber pressure	$P_{CO_2 des}$	bar	5.0	27.5	25.0	20.0	20.0	10.0
Cold-rich split fraction	f_{cr}	-	0.01	0.20	0.035	0.04	0.04	0.05

5.3 CO_2 absorber design

5.3.1 Design cases applied with design conditions

The CEMCAP model is used to design and size the CO_2 absorber of the CAP for each Design case given in Table 3.2. A CO_2 absorption column with intercooling stages has been proposed, as shown in Figure 5.9A): The liquid solution is cooled using cooling water at different levels of the absorption column. This configuration is well understood and commonly applied in industry and by researches for such processes [16]. The absorption of CO_2 (and NH_3) is an exothermic

This project has received funding from the European Union's Horizon2020 Research and Innovation Programme under Grant Agreement No 641185. This work was supported by the Swiss State Secretariat for Education, Research and Innovation (SERI) under contract number 15.0160

process. Therefore, the temperature of the liquid solution increases as it takes up CO_2 from the flue gas when flowing down along the column. The intercooling of the liquid solution allows for a shift of the thermodynamic vapor-liquid equilibrium, increasing the CO_2 driving force from the vapor phase to the liquid phase, and hence, decreasing the column height required to achieve certain CO_2 capture efficiency. The composition and temperature of the flue gas along the CO_2 absorption column is shown in Figure 5.9B) for the Base case designed with the flue gas conditions obtained considering medium air leak into the cement manufacturing process and run at the same flue gas condition, i.e. containing 18%vol CO_2 as specified in Table 3.1.

A) B)

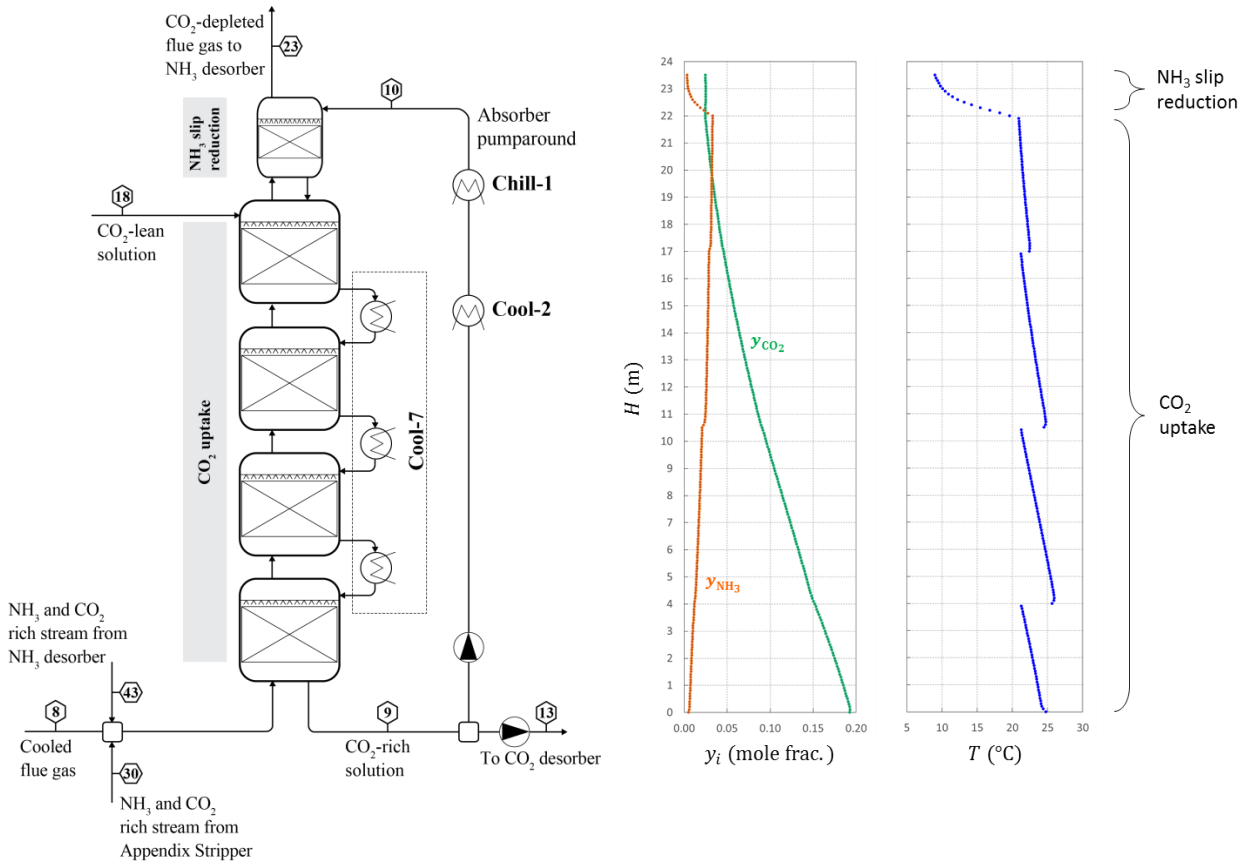

Figure 5.9: (A) Schematic of the CO_2 absorption column of the CAP applied to cement plants using intercooling stages. The stream numbering corresponds to the identification given in the flow scheme of the full CAP shown in Figure 2.1. (B) Flue gas composition and temperature profiles along the column for the Base case designed and run at medium air leak flue gas conditions using the optimum set of operating conditions specified in Table 5.2.

As shown by Figure 5.9B), the CO_2 concentration in the flue gas linearly decreases along the CO_2 uptake section of the column, from the bottom to the top, while the NH_3 concentration increases. Subsequently, the NH_3 concentration in the flue gas is decreased in the upper section of the column, i.e. in the NH_3 slip reduction section, by a chilled CO_2-rich solution, i.e. the absorber pumparound, as detailed in Section 2.

The size, i.e. height and diameter, of the CO_2 absorber and the number of required intercooling stages for each Design case, running with the optimum set of operating conditions shown in Table 5.2, are given in Table 5.3. The packing heights proposed for each case considered in the

This project has received funding from the European Union's Horizon2020 Research and Innovation Programme under Grant Agreement No 641185. This work was supported by the Swiss State Secretariat for Education, Research and Innovation (SERI) under contract number 15.0160

CEMCAP project are within the same range of the packing height of the CO_2 absorbers implemented when applying the CAP to power plants, e.g. 20-29 m at TCM [17], or to the height of the CO_2 absorber at the amine-based CO_2 capture process at Boundary-Dam, i.e. 54 m [18]. The column heights specified in Table 5.3 have been obtained considering the same structured packing used during the pilot plant tests of the CO_2 absorber performed within the CEMCAP project, i.e. Koch Glitsch Flexipac M 350X. Similarly, the column diameters of the CO_2 uptake section proposed in Table 5.3 have been obtained considering a gas superficial velocity similar to the value used during the pilot plant tests, i.e. around 1 m/s. A smaller diameter is proposed for the NH_3 slip reduction section in all cases, since a higher superficial gas velocity has no impact on the NH_3 absorption rate, as shown experimentally in Campaign 1 of the NH_3 absorber for similar operating conditions. Nevertheless, the NH_3 slip reduction section could have the diameter of the CO_2 uptake section, leading to minor changes on the NH_3 concentration in the flue gas leaving the top of the CO_2 absorber.

Table 5.3: Summary of the CO_2 absorber design for the cases proposed in the CEMCAP common framework [5] and specified in Table 3.2 as Design cases. The design and size of the CO_2 absorber allow for CO_2 capture rates of 90% in all cases, except for the design that corresponds to the "Optional extent of capture" case, where 86% was obtained. The optimum set of operating conditions found for each case and given in Table 5.2 were used to obtain each design.

CO_2 absorber section	**Variable**		**Unit**	**Cases defined in the CEMCAP common framework [5]**			
				Base case	**Constant low air leak**	**Optional extent of capture**	**Steam import**
NH_3 slip reduction	Diameter	D	m	6.5	5.6	6.5	6.5
	Height	H	m	1.5	1.5	1.5	1.5
CO_2 uptake	Diameter	D	m	10.0	8.8	10.0	10.0
	Height	H	m	22.0	34.0	26.5	22.0
	No. of intercoolers	N_{intcool}	-	3	4	4	3

The CO_2 absorber with intercooling of the liquid solvent at several column heights proposed in this report is an exemplary configuration among the different solutions that could be implemented. Other configurations for the CO_2 absorber of solvent-based post-combustion CO_2 capture processes have been proposed in the literature [16].

5.3.2 Design cases applied with non-design conditions

The CO_2 absorption columns proposed for the Design cases, whose sizing and design are shown in Table 5.3, were used to simulate each corresponding Non-design case. Namely, the CO_2 absorber was run at different flue gas conditions, as specified in Table 3.2, without changing the design of the process unit. More specifically, the CO_2 concentration in the flue gas was increased from 18 to 22%vol as a result of a lower air leak into the cement manufacturing process. Consequently, the operating conditions of the CAP were adapted accordingly with the aim of fulfilling the CO_2 capture efficiency specified for each case, departing from the optimum sets given in Table 5.2. The adaptation of the operating conditions was performed manually based on the results of the optimization of the process shown in Section 5.2, considering the experimental results of the pilot plant tests of the CO_2 absorber summarized in Section 4.5.2 and using the knowledge acquired during the CEMCAP project on the application of the CAP to cement plant-

This project has received funding from the European Union's Horizon2020 Research and Innovation Programme under Grant Agreement No 641185. This work was supported by the Swiss State Secretariat for Education, Research and Innovation (SERI) under contract number 15.0160

like flue gas conditions. The resulting sets of operating conditions for the Non-design cases are shown in Table 5.4.

Table 5.4: Operating conditions selected for the operation of each case defined in the CEMCAP common framework [5] run at flue gas conditions that are different to the flue gas conditions used for the design of the CAP. The CO_2 absorber size and design are those specified in Table 5.3 for each case.

Variable		Unit	Set of operating conditions of the CAP per case [5] adapted to lower air leak (Non-design cases)			
			Base case	Constant low air leak	Optional extent of capture	Steam import
			22%vol CO_2 90% CCR	N/A	22%vol CO_2 85% CCR	22%vol CO_2 90% CCR
CO_2-lean NH_3 concentration	$C_{NH_3}^{in}$	mol_{NH3}/kg_{water}	5.0	N/A	4.0	5.0
CO_2-lean CO_2 loading	$l_{CO_2}^{in}$	mol_{CO2}/mol_{NH3}	0.415	N/A	0.364	0.415
CO_2-lean to inlet flue gas flowrate ratio	L/G	kg/kg	9.0	N/A	7.0	9.0
Pumparound split fraction	f_s	-	0.12	N/A	0.12	0.12
Pumparound temperature	T_{pa}	°C	12	N/A	13	12
CO_2 desorber pressure	$P_{CO_2 des}$	bar	25.0	N/A	20.0	10.0
Cold-rich split fraction	f_{cr}	-	0.025	N/A	0.035	0.0375

After maintenance of the cement plant, the operating conditions of the CO_2 absorber (NH_3 concentration and CO_2 loading of the CO_2-lean stream, liquid-to-gas flowrate ratio, pumparound split fraction and temperature) and the cold-rich split fraction will have to be adapted from the values proposed for the medium rate of air leakage into the cement plant, shown in Table 5.2, to the values suggested for the low air leak case given in Table 5.4. The adaptation of the aforementioned operating conditions cannot be accomplished instantaneously, but requires a certain period that depends on the circulating liquid flowrate and the total volume of liquid within the process, including stored and circulating volume. The adaptation process can be speeded up acting upon the make-up flowrate of NH_3 and water to the CO_2 absorber. Similarly, the operating conditions of the CAP will require gradual adaptation over the year in order to cope with the decreasing CO_2 concentration in the inlet flue gas, to eventually end up in the operating conditions shown in Table 5.2 before the next shutting down of the cement plant for maintenance. The pressure of the CO_2 desorber has not been modified between the design case and the corresponding non-design case since the design of the column, i.e. the thickness of the wall, depends on this variable.

5.4 NH_3 absorber design

The design of the NH_3 absorber of the CAP applied to power plants for CO_2 capture is described in Section 4.5.3, as well as the typical NH_3 concentration in the flue gas along the column and the objectives of each packing section. Additionally, the results of the pilot plant tests of the NH_3

This project has received funding from the European Union's Horizon2020 Research and Innovation Programme under Grant Agreement No 641185. This work was supported by the Swiss State Secretariat for Education, Research and Innovation (SERI) under contract number 15.0160

absorber performed within the CEMCAP project showed that the NH_3 concentration in the flue gas leaving the top of the CO_2 desorber can be reduced from 12,500 to less than 200 ppm_v at the outlet of the NH_3 absorber when considering cement plant-like flue gas conditions. Taking into account the results of the pilot plant tests of the NH_3 absorber described in Section 4.5.3, and more specifically those obtained during Campaign 2, the NH_3 concentration in the flue gas can be decreased from 5,000 ppm_v to 200 ppm_v using a structured packing Koch Glitsch Flexipac M 350X of 3 m high with a gas superficial velocity of around 1.3-1.5 m/s if the inlet flue gas contains ≥3%vol CO_2. Specifically, it was found experimentally that an NH_3-lean solution containing 0.05 $kmol_{NH_3}/m^3$ and entering the top of the absorber at 15°C could be used, with a liquid-to-gas flowrate ratio of 0.2 kg/kg. The latter conditions are expected to minimize the energy consumption of the FG-WW section while fulfilling the NH_3 concentration limit in the exiting flue gas, i.e. 200 ppm_v.

The simulations of the CO_2 absorber of the CAP at the optimum set of operating conditions led to NH_3 concentrations below 5,000 ppm_v in the CO_2-depleted flue gas leaving the top of the CO_2 absorber, as shown in Table 5.5 for each optimized case. Therefore, the NH_3 absorber of the CAP applied to cement plants for CO_2 capture only requires the upper section of the typical design adopted for power plants. Such design is shown in Figure 5.10. The stream numbering corresponds to the stream identification given in the flow scheme of the full CAP shown in Figure 2.1. The NH_3-lean stream containing 0.05 $kmol_{NH_3}/m^3$ enters the top of the NH_3 absorber at 15°C, taking NH_3 (and CO_2) from the CO_2-depleted flue gas when flowing down the column in counter-current with respect to the gas. Consequently, a NH_3-rich solution is obtained at the bottom of the NH_3 absorber, that is sent to the NH_3 desorber. The NH_3-rich solution is regenerated in the NH_3 desorber using thermal energy and, after being cooled and chilled, is sent back as NH_3-lean stream to the top of the NH_3 absorber. Table 5.5 also shows the NH_3 concentration in the CO_2 and NH_3-depleted flue gas leaving the top of the NH_3 absorber that have been obtained for the simulations of the optimized CAP using: (i) the NH_3 absorber design shown in Figure 5.10, and (ii) the aforementioned operating conditions and packing type and dimensions. The simulation results shown in Table 5.5 for the NH_3 concentration in the flue gas leaving the top of the NH_3 absorber are in line with the results of the pilot plant tests performed at the same operating conditions: The simulations obtain NH_3 concentrations even lower than the 200 ppm_v obtained experimentally, because the NH_3 content in the simulated inlet flue gas is smaller than the NH_3 concentration tested experimentally, i.e. 5,000 ppm_v.

Table 5.5: NH_3 content in the flue gas leaving the top of the CO_2 desorber (and entering the bottom of the NH_3 absorber) and in the flue gas leaving the top of the NH_3 absorber, for the simulation of the CAP at the optimum set of operating conditions found for each case (see Table 5.2 and Table 5.4) defined in Table 3.2. The configuration of the NH_3 absorber shown in Figure 5.10 has been adopted in all simulations. The flue gas leaving the top of the CO_2 desorber (and entering the bottom of the NH_3 absorber) approximately contains 3-5%vol CO_2 in all cases, according to the simulation results.

Case			NH_3 content in the flue gas (ppm_v)	
Denomination	**Designed for**	**Run at**	**At the NH_3 absorber inlet**	**At the NH_3 absorber outlet**
Base case	Medium air leak	Low air leak	2,696	144
		Medium air leak	3,526	193
Constant low air leak	Low air leak	Low air leak	1,915	102
Optional extent of	Medium air	Low air leak	2,305	119

This project has received funding from the European Union's Horizon2020 Research and Innovation Programme under Grant Agreement No 641185. This work was supported by the Swiss State Secretariat for Education, Research and Innovation (SERI) under contract number 15.0160

capture	leak	Medium air leak	2,772	148
Steam import	Medium air leak	Low air leak	2,696	144
		Medium air leak	3,457	182

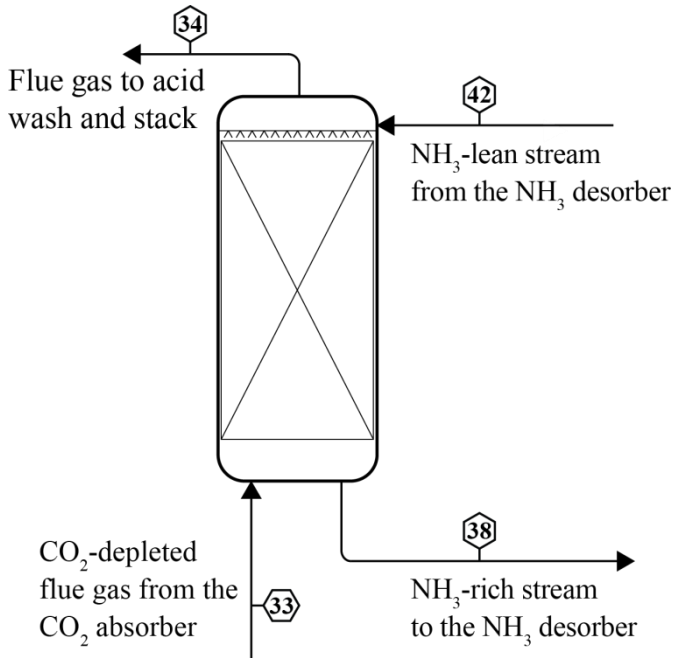

Figure 5.10: Schematic of the NH_3 absorber configuration selected for the CAP applied to CO_2 capture from cement plants. Stream numbers corresponds to those specified in the flow scheme of the full CAP shown in Figure 2.1.

5.5 Energetic assessment of the CAP applied to cement plants

Figure 5.11 shows the contribution of the key energy consumers to the overall SPECCA index obtained as a result of the optimization of the operating conditions of the CAP applied to cement plants for CO_2 capture. The cases defined in the CEMCAP common framework [5] and summarized in Table 3.2 are shown in Figure 5.11. The corresponding optimum sets of operating conditions that have been found to minimize the SPECCA index in each case are shown in Table 5.2 and Table 5.4 for the Design cases and for the Non-design cases, respectively. Figure 5.11 shows that in all cases the main contribution to the energy consumption of the CAP stems from the heat required in the CO_2 desorber. Consequently, the optimization of the operating conditions of the CAP has mainly been driven by the decrease of the reboiler duty of the CO_2 desorber: The pressure of the CO_2 desorber has been adapted accordingly taking into account its effect on the reboiler temperature and on the reboiler duty, and the opposing effect of those two variables on the value of the SPECCA index. The pressure of the CO_2 desorber also affects the balance between the SPECCA contribution stemming from the CO_2 compression and the SPECCA contribution associated with the auxiliaries, i.e. pumps and fans, of the CAP. In summary, higher pressure in the CO_2 desorber decreases the electrical demand of the CO_2 compression process, as well as the reboiler duty of the CO_2 desorber, at the cost of increasing the electrical demand to pump the CO_2-rich solution to the pressure level of the CO_2 desorber and increasing the temperature of the required steam in the reboiler. Additionally, available heat in the cement manufacturing process can be recovered to produce steam, as specified in the

This project has received funding from the European Union's Horizon2020 Research and Innovation Programme under Grant Agreement No 641185. This work was supported by the Swiss State Secretariat for Education, Research and Innovation (SERI) under contract number 15.0160

CEMCAP common framework [5], decreasing both the fuel requirements and the associated CO_2 emissions, and thus, leading to a decrease of the SPECCA.

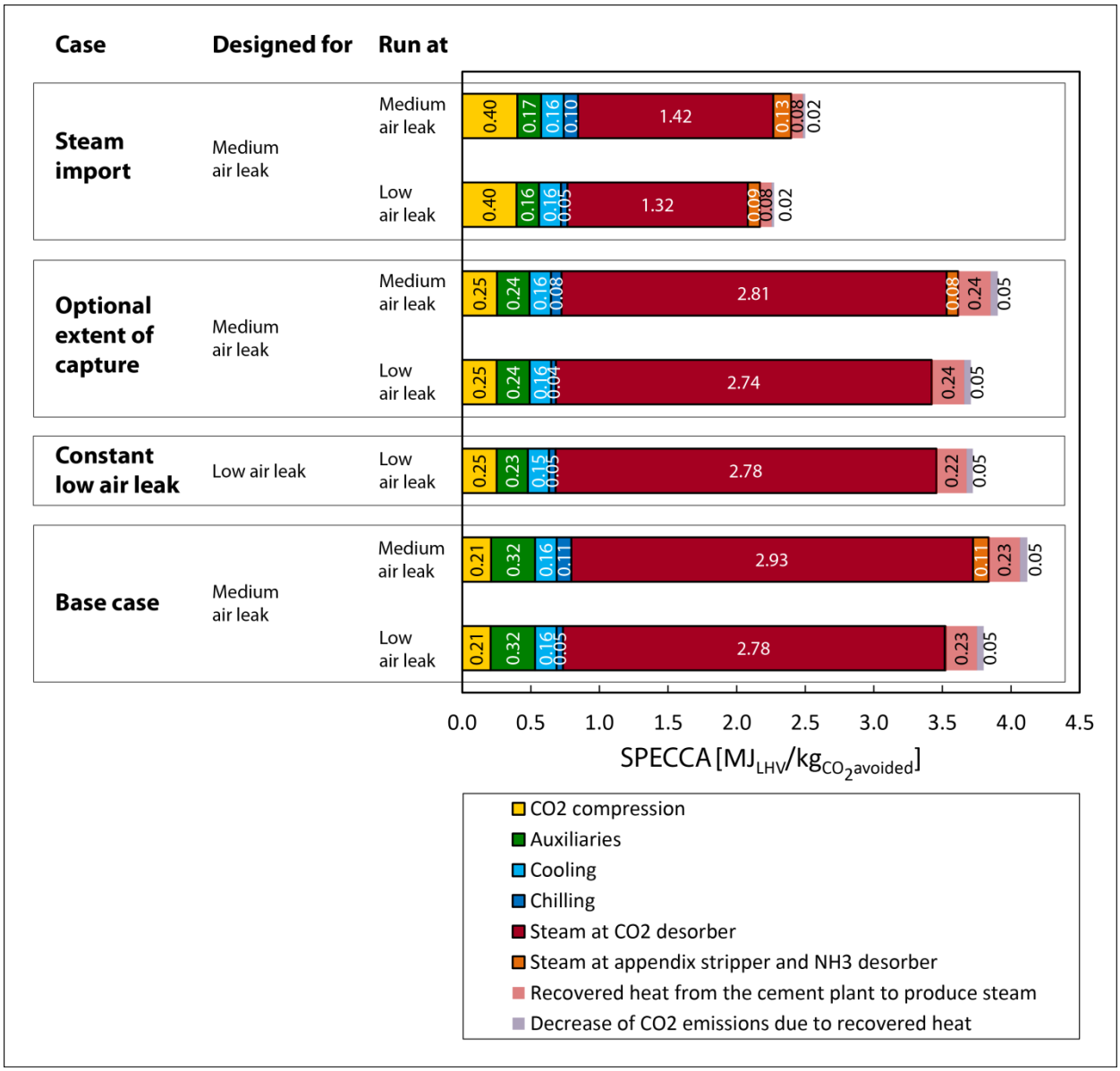

Figure 5.11: Energetic performance of the optimized CAP applied to the cases specified in Table 3.2. The resulting SPECCA after integrating the heat recovered from the cement plant is contained within the bars with solid black contour lines, while the lighter bar sections out of the solid black contour lines correspond to the energy saved by integrating the heat recovered from the cement plant. Recovered heat from the cement plant is used: (i) to produce steam for the Appendix Stripper and the NH_3 desorber when using an on-site NG boiler to produce the rest of the required steam, or (ii) to produce steam for the CO_2 desorber when the remaining required steam is imported from a CHP plant. The use of the heat recovered from the cement plant for the production of the steam required in the CAP decreases the CO_2 emissions associated with the fuel saved in the NG boiler or in the CHP plant, leading to a slight decrease of the SPECCA.

The Steam import case shows the most competitive energy performance among the cases presented in Figure 5.11. Consequently, the application of the CAP to cement plants will be

This project has received funding from the European Union's Horizon2020 Research and Innovation Programme under Grant Agreement No 641185. This work was supported by the Swiss State Secretariat for Education, Research and Innovation (SERI) under contract number 15.0160

favored by the existence of a thermal power plant in the vicinity of the cement plant. In addition, the increase of the CO_2 concentration in the flue gas, i.e. from 18 to 22%vol CO_2 as a consequence of lower air leak into the cement manufacturing process, improves the energy performance of the CAP as it has been already pointed out from the results of the heuristic optimization shown in Figure 5.7. Figure 5.11 confirms the reduced energy penalty for higher CO_2 concentrations even if the plant had not been designed for the high CO_2 concentrations, highlighting the importance of controlling the air leak into the cement plant through regular maintenance. The results shown in Figure 5.11 have also confirmed the decrease of the SPECCA index for lower CO_2 capture rates already revealed by Figure 5.7. Nevertheless, the latter effect has been shown to be more important for lower CO_2 concentration levels in the inlet flue gas to the CAP. Finally, no noticeable difference is found when comparing the SPECCA index obtained for the Constant low air leak case (designed and run for a flue gas containing 22%vol CO_2) with the result of the Base case run with a flue gas containing 22%vol CO_2 but using the design of the CAP obtained if the flue gas contains 18%vol CO_2. A lower air leak into the cement manufacturing process not only leads to a higher CO_2 concentration in the generated flue gas, but also to a lower flue gas flowrate. Consequently, the CO_2 absorber designed for medium air leak conditions increases the flue gas velocity along the column with respect to the Design case, which does not affect negatively the CO_2 absorption process.

Material and energy balances composed of stream tables and main energy consumers of the CAP flow scheme shown in Figure 2.1 applied to the optimized cases specified in Table 3.2 are given in the Annex. As aforementioned, the overall energy performance of the optimized CAP applied to each case is shown in Figure 5.11.

This project has received funding from the European Union's Horizon2020 Research and Innovation Programme under Grant Agreement No 641185. This work was supported by the Swiss State Secretariat for Education, Research and Innovation (SERI) under contract number 15.0160

6 SUMMARY AND CONCLUDING REMARKS

The CAP has been optimized for its application to cement plant-like flue gas conditions. Namely, the sets of operating conditions that minimize the energy consumption of the process for each case defined in the CEMCAP common framework [5] have been found. The specifications of each one of these cases are given in Table 3.2. The energetic performance of the CAP has been assessed by means of the SPECCA index, as defined in the CEMCAP common framework [5]. The average minimum SPECCA value found for each case defined in the CEMCAP common framework [5] is shown in Figure 6.1. A minimum average SPECCA value of 3.68 $MJ_{LHV}/kg_{CO_2avoided}$ has been found for the Base case. On the one hand, maintaining constant low air leak into the cement manufacturing process, and hence, generating a flue gas with higher CO_2 concentration during the whole year, i.e. 22%vol CO_2, decreases the SPECCA index of the CAP to 3.46 $MJ_{LHV}/kg_{CO_2avoided}$, improving the energetic performance of the CAP by 6% with respect to the Base case. On the other hand, decreasing the yearly average CO_2 capture rate of the CAP from 90%, as for the Base case, to 85.5%, as for the Optional extent of capture case, decreases the SPECCA index of the CAP to 3.52 $MJ_{LHV}/kg_{CO_2avoided}$, improving the energetic performance of the CAP by more than 4% with respect to the Base case. Additionally, importing steam from a CHP plant to be used in the reboilers of the CAP, as for the Steam import case, decreased the SPECCA index by 38% with respect to the Base case, where the steam is produced in an on-site NG boiler, obtaining a yearly average minimum SPECCA of 2.29 $MJ_{LHV}/kg_{CO_2avoided}$.

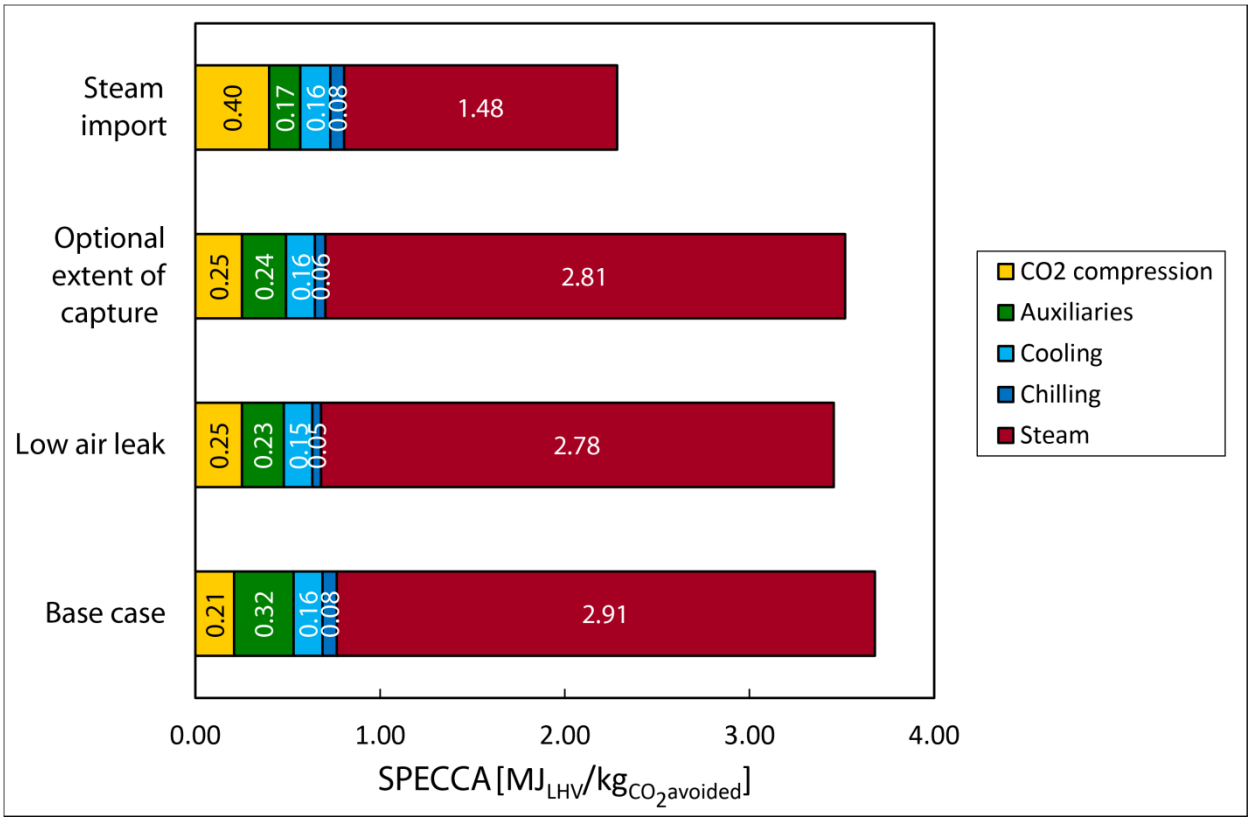

Figure 6.1: Average energetic performance of the CAP applied to the cases specified in the CEMCAP common framework [5]. The values shown here represent the average of the two values shown in Figure 5.11 for each case, respectively.

This project has received funding from the European Union's Horizon2020 Research and Innovation Programme under Grant Agreement No 641185. This work was supported by the Swiss State Secretariat for Education, Research and Innovation (SERI) under contract number 15.0160

Therefore, the application of the CAP to cement plants for CO_2 capture will be highly favored by the existence of a CHP plant in the vicinity of the cement plant or the building of such plant for the purpose of providing steam for the CAP plant. If steam is generated without the co-generation of electricity, primary energy consumption associated to the steam generation is higher and the SPECCA increases. Additionally, the optional capture of the CO_2 emissions generated in the NG boiler are expected to decrease the SPECCA of the CAP further compared to the Base case of this study, in which the CO_2 generated in the NG boiler is emitted to the atmosphere. Additionally, net negative CO_2 emissions for the overall process can be obtained if sustainably harvested biomass is used as fuel in the boiler and the biogenic CO_2 is captured and stored. Furthermore, lowering the air leak into the cement manufacturing process or the CO_2 capture rate specification, e.g. 85% instead of 90%, represent opportunities to improve the energetic performance of the CAP applied to cement plants for CO_2 capture. In addition, advanced CAP configurations developed as part of the CEMCAP project have shown very promising results to further improve the performance of the CAP applied to cement plants for CO_2 capture. This family of advanced CAP configurations is expected: (i) to decrease the OPEX of the process by reducing the energy consumption of the main energy consumer of the CAP, i.e. the reboiler duty of the CO_2 desorber, and/or (ii) to decrease the CAPEX by simplifying the capture process and decreasing the required number of unit operations.

The unit operations of the CAP that have to face the higher CO_2 concentration of the flue gas produced in the cement plant in comparison with the power plant case, namely the DCC of the flue gas cooling section, the CO_2 absorber and the NH_3 absorber, have been tested at pilot plant scale using cement plant-like flue gas conditions. On the one hand, the experimental setups of the SO_x uptake section of the DCC and of the NH_3 absorber were able to fulfill the specifications and constraints defined for the industrial unit. Therefore, packing heights and unit designs have been taken from the test rig used in each case, operating conditions have been selected from the analysis of the pilot plant tests and the simulations of the process have been adapted to reproduce the experimental results. On the other hand, the CO_2 absorber pilot plant tests have been used to obtain a rate-based model that allows for the design of the column, since no single CO_2 absorber pilot plant test was able to fulfill the CO_2 capture rate specification, as expected. Overall, it has been shown experimentally that the conditions of the flue gas generated by cement plants, according to the reference cement plant defined in the CEMCAP common framework [5], favor the operation of the CAP with respect to the power plant case: (i) the lower SO_2 content in the flue gas produced by the cement plant allows for the total removal of SO_2 before the CO_2 absorber using an aqueous ammonia solution and simplifying the flow scheme of the CAP, and (ii) the higher CO_2 concentration in the flue gas improves the removal of NH_3 in the FG-WW section. As far as the CO_2 absorption column is concerned, the higher CO_2 content in the flue gas is not expected to affect significantly the design and size of the column with respect to the power plant case. In fact, similar packing heights to those used in the power plant application are foreseen. On the contrary, the higher CO_2 concentration in the flue gas is expected to decrease the specific energy consumption of the CAP applied to cement plants in comparison with its application to power plants: Only the adaptation of the operating conditions of the CO_2 absorber is required to handle the higher CO_2 concentration in the entering flue gas. Overall, a 23.5 m high packing has been predicted for the CO_2 absorption column at the conditions of the Base case (and of the Steam import case), with additional 3 m high packing to be placed at the top as NH_3 absorber. The structured packing used for the pilot plant tests is proposed in both cases, i.e. Koch Glitsch Flexipac M 350X. As for the SO_x uptake section of the DCC of the Flue gas cooling section, a structured packing material Mellapak Plastic 125X with

This project has received funding from the European Union's Horizon2020 Research and Innovation Programme under Grant Agreement No 641185. This work was supported by the Swiss State Secretariat for Education, Research and Innovation (SERI) under contract number 15.0160

4.2 meter-height is proposed, as tested at pilot plant scale. Other packing sections of the process do not depend on the CO_2 concentration in the flue gas. Consequently, their design and size is expected to be similar to the design and size implemented in the CAP applied to power plants.

In conclusion, the results obtained in this study have shown that the CAP can be applied to cement plants for CO_2 capture with favorable energetic performance. The knowledge acquired and the results obtained during the CEMCAP project for the application of the CAP to cement plants, together with the previous experience on the application of the CAP to power plants, including the design and operation of demonstration plants [15], makes the CAP ready to be demonstrated at industrial scale at the cement plant [19].

This project has received funding from the European Union's Horizon2020 Research and Innovation Programme under Grant Agreement No 641185. This work was supported by the Swiss State Secretariat for Education, Research and Innovation (SERI) under contract number 15.0160

7 NOTATION

CAP	Chilled Ammonia Process
CCR	CO_2 capture rate, also referred to as CO_2 capture efficiency or Extent of capture within the report
CHP	Combined heat and power
CO_2-WW	CO_2 water-wash
D4.6	CEMCAP deliverable D4.6
D10.1	CEMCAP deliverable D10.1
D10.3	CEMCAP deliverable D10.3
DCC	Direct Contact Cooler
DCH	Direct Contact Heater
DTU	Technical University of Denmark
FG	Flue gas
FGD	Flue Gas Desulfurization
FG-WW	Flue gas water-wash
GE	General Electric
MEA	Monoethanol Amine
NG	Natural Gas
PFD	Process Flow Diagram
SPECCA	Specific primary energy consumption for CO_2 avoided
TCM	Technology Center Mongstad

This project has received funding from the European Union's Horizon2020 Research and Innovation Programme under Grant Agreement No 641185. This work was supported by the Swiss State Secretariat for Education, Research and Innovation (SERI) under contract number 15.0160

8 REFERENCES

[1] Bollinger R, Muraskin D, Hammond M, Kozak F, Spitznogle G, Cage M, Sherrick B, Varner M. CCS Project with Alstom's Chilled Ammonia Process at AEP's Mountaineer Plant. Alstom Technical Report, Paper No. 72.

[2] Baburao B, Kniesburger P, Lombardo G. Chilled Ammonia Process Operation and Results from Pilot Plant at Technology Centre Mongstad. Presentation at TCCS-8, Trondheim, Norway, 2015.

[3] Sutter D, Gazzani M, Mazzotti M. Formation of solids in ammonia-based CO_2 capture processes – Identification of criticalities through thermodynamic analysis of the CO_2-NH_3-H_2O system. Chem Eng Sci 2015; 133:170-180.

[4] Sutter D, Gazzani M, Mazzotti M. A low-energy chilled ammonia process exploiting controlled solid formation for post-combustions CO_2 capture. Faraday Discuss 2016; 192:59-83.

[5] Voldsund M, Anantharaman R, Berstad D, Cinti G, De Lena E, Gatti M, Gazzani M, Hoppe H, Martínez I, Garcia Moretz-Sohn Monteiro J, Romano M, Roussanaly S, Schols E, Spinelli M, Størset S, van Os P. CEMCAP framework for comparative techno-economic analysis of CO_2 capture from cement plants (D3.2) 2018.

[6] Yu H, Morgan S, Allport A, Cottrell A, Do T, McGregor J, Wardhaugh L, Feron P. Results from trialling aqueous NH_3 based post-combustion capture in a pilot plant at Munmorah power station: Absorption. Chem Eng Res Des 2011; 89:1204-1215.

[7] Pérez-Calvo J-F, Sutter D, Gazzani M, Mazzotti M. Application of a chilled ammonia-based process for CO_2 capture to cement plants. Energy Procedia 2017; 114:6197-6205.

[8] Thomsen K, Rasmussen P. Modeling of vapor–liquid–solid equilibrium in gas–aqueous electrolyte systems. Chem Eng Sci 1999; 54:1787–1802.

[9] Darde V, van Well WJM, Stenby EH, Thomsen K. Modeling of carbon dioxide absorption by aqueous ammonia solutions using the Extended UNIQUAC model. Ind Eng Chem Res 2010; 49:12663-12674

[10] Qi G, Wang S, Yu H, Wardhaugh L, Feron P, Chen C. Development of a rate-based model for CO_2 absorption using aqueous NH_3 in a packed column. Int. J. Greenh. Gas Control 2013; 17:450-461.

[11] Pinsent BRW, Pearson L, Roughton FJW. The kinetics of combination of carbon dioxide with hydroxide ions. Trans Faraday Soc 1956; 52:1512-1520.

[12] Pinsent BRW, Pearson L, Roughton FJW. The kinetics of combination of carbon dioxide with ammonia. Trans Faraday Soc 1956; 52:1594-1598.

[13] Bravo JL, Rocha JA, Fair JR. A comprehensive model for the performance of columns containing structured packings, distillation and absorption. Institution of Chemical Engineers Symposium Series 128; 1992. Institute Chem Eng, 1.

[14] Pérez-Calvo J-F, Sutter D, Gazzani M, Mazzotti M. Pilot Tests and Rate-Based Modelling of CO_2 Capture in Cement Plants Using an Aqueous Ammonia Solution. CET 2018;69(*in press*)

[15] Augustsson O, Baburao B, Dube S, Bedell S, Strunz P, Balfe M, Stallmann O. Chilled Ammonia Process Scale-up and Lessons Learned. Energy Procedia 2017;114:2293-5615.

[16] Le Moullec Y, Neveux T, Al Azki A, Chikukwa A, Hoff K A. Process modifications for solvent-based post-combustion CO_2 capture. Int J Greenh Gas Control 2014; 31:96-112.

[17] Lombardo G, Agarwal R, Askander J. Chilled Ammonia Process at Technology Center Mongstad – First Results. Energy Procedia 2014; 51:31-39.

[18] Cansolv Technologies, Inc. SaskPower Boundary Dam 3 – Project Update and some Lessons Learned. Presentation at PCCC-2, Bergen, Norway, 2013.

This project has received funding from the European Union's Horizon2020 Research and Innovation Programme under Grant Agreement No 641185. This work was supported by the Swiss State Secretariat for Education, Research and Innovation (SERI) under contract number 15.0160

[19] Augustsson O, Oskarsson A, Grubbström J, Sutter D. Feasibility study for CAP process scale-up (D10.4) (*in press*).

This project has received funding from the European Union's Horizon2020 Research and Innovation Programme under Grant Agreement No 641185. This work was supported by the Swiss State Secretariat for Education, Research and Innovation (SERI) under contract number 15.0160

9 ANNEX: MATERIAL AND ENERGY BALANCES

9.1 Base case

Table 9.1: Specifications of the streams of the CAP applied to the "Base" case defined in CEMCAP. Design at medium air leak, run at low air leak. First ½ of the year.

						Composition (mole frac.)												
#	F [kg/s]	T [°C]	P [bar]	N [kmol/s]	H [kJ/s]	H_2O	NH_3	CO_2	NH_4^+	H^+	OH^-	CO_3^{2-}	HCO_3^-	NH_2COO^-	Air	SO_2	$(NH_4)_2SO_4$	H_2SO_4
1	8.84E+01	130.0	1.10	2.90E+00	-3.19E+05	1.10E-01	0.00E+00	2.20E-01	0.00E+00	0.00E+00	0.00E+00	0.00E+00	0.00E+00	0.00E+00	6.70E-01	200 mg/Nm^3	0.00E+00	0.00E+00
2	1.86E+02	48.2	1.01	1.03E+01	-2.93E+06	1.00E+00	0.00E+00	7.94E-05	0.00E+00	8.36E-07	1.88E-11	1.27E-12	8.36E-07	0.00E+00	7.06E-06	0.00E+00	0.00E+00	0.00E+00
3	7.55E-01	34.3	1.01	4.19E-02	-1.19E+04	1.00E+00	0.00E+00	1.44E-05	0.00E+00	3.49E-07	1.85E-11	1.02E-12	3.49E-07	0.00E+00	1.12E-05	0.00E+00	0.00E+00	0.00E+00
4	1.81E+02	21.2	1.01	1.01E+01	-2.88E+06	1.00E+00	0.00E+00	7.94E-05	0.00E+00	7.74E-07	3.22E-12	8.01E-13	7.74E-07	0.00E+00	7.06E-06	0.00E+00	0.00E+00	0.00E+00
5[(1)]	3.46E-02	20.0	1.10	1.95E-03	-4.54E+02	7.39E-01	2.61E-01	0.00E+00	0.00E+00	0.00E+00	0.00E+00	0.00E+00	0.00E+00	0.00E+00	0.00E+00	0.00E+00	0.00E+00	0.00E+00
6[(1)]	5.95E-02	20.0	1.01	1.70E-03	-4.54E+02	8.50E-01	0.00E+00	0.00E+00	0.00E+00	0.00E+00	0.00E+00	0.00E+00	0.00E+00	0.00E+00	0.00E+00	0.00E+00	1.50E-01	0.00E+00
7	8.39E+01	22.2	1.01	2.66E+00	-2.69E+05	2.66E-02	0.00E+00	2.41E-01	0.00E+00	0.00E+00	0.00E+00	0.00E+00	0.00E+00	0.00E+00	7.33E-01	0.00E+00	0.00E+00	0.00E+00
8	8.39E+01	29.9	1.10	2.66E+00	-2.68E+05	2.66E-02	0.00E+00	2.41E-01	0.00E+00	0.00E+00	0.00E+00	0.00E+00	0.00E+00	0.00E+00	7.33E-01	0.00E+00	0.00E+00	0.00E+00
9	8.89E+02	24.8	1.05	4.42E+01	-1.29E+07	8.93E-01	4.52E-03	9.41E-05	5.39E-02	4.74E-11	1.22E-08	4.90E-03	1.99E-02	2.42E-02	5.59E-07	0.00E+00	0.00E+00	0.00E+00
10	1.07E+02	12.0	1.40	5.31E+00	-1.56E+06	8.91E-01	3.24E-03	1.83E-04	5.63E-02	2.19E-11	7.68E-09	7.38E-03	1.84E-02	2.31E-02	5.59E-07	0.00E+00	0.00E+00	0.00E+00
11	0.00E+00	na	na	0.00E+00	na	0.00E+00	0.00E+00	0.00E+00	0.00E+00	0.00E+00	0.00E+00	0.00E+00	0.00E+00	0.00E+00	0.00E+00	0.00E+00	0.00E+00	0.00E+00
12	0.00E+00	na	na	0.00E+00	na	0.00E+00	0.00E+00	0.00E+00	0.00E+00	0.00E+00	0.00E+00	0.00E+00	0.00E+00	0.00E+00	0.00E+00	0.00E+00	0.00E+00	0.00E+00
13	7.82E+02	25.6	25.40	3.89E+01	-1.14E+07	8.93E-01	4.60E-03	9.20E-05	5.38E-02	4.95E-11	1.25E-08	4.79E-03	2.00E-02	2.42E-02	5.59E-07	0.00E+00	0.00E+00	0.00E+00
14	7.62E+02	136.7	25.40	3.84E+01	-1.07E+07	8.80E-01	3.35E-02	1.08E-02	3.79E-02	3.43E-09	9.13E-08	2.00E-04	2.72E-02	1.03E-02	5.53E-07	0.00E+00	0.00E+00	0.00E+00
15	1.95E+01	25.6	25.40	9.73E-01	-2.84E+05	8.93E-01	4.60E-03	9.20E-05	5.38E-02	4.95E-11	1.26E-08	4.79E-03	2.00E-02	2.42E-02	5.59E-07	0.00E+00	0.00E+00	0.00E+00
16	7.57E+02	145.5	25.00	3.90E+01	-1.07E+07	8.92E-01	4.30E-02	3.15E-03	3.12E-02	3.57E-09	1.64E-07	1.61E-04	2.27E-02	8.19E-03	9.16E-10	0.00E+00	0.00E+00	0.00E+00
17	7.55E+02	29.3	25.00	3.88E+01	-1.11E+07	9.06E-01	2.03E-02	3.17E-06	3.89E-02	1.23E-11	1.18E-07	4.64E-03	6.24E-03	2.34E-02	9.19E-10	0.00E+00	0.00E+00	0.00E+00
18	7.55E+02	21.2	1.05	3.88E+01	-1.11E+07	9.06E-01	1.94E-02	2.61E-06	4.03E-02	6.61E-12	1.10E-07	5.98E-03	5.36E-03	2.30E-02	9.19E-10	0.00E+00	0.00E+00	0.00E+00
19[(1)]	1.02E-02	20.0	1.01	5.72E-04	-1.33E+02	7.39E-01	2.61E-01	0.00E+00	0.00E+00	0.00E+00	0.00E+00	0.00E+00	0.00E+00	0.00E+00	0.00E+00	0.00E+00	0.00E+00	0.00E+00

This project has received funding from the European Union's Horizon2020 Research and Innovation Programme under Grant Agreement No 641185. This work was supported by the Swiss State Secretariat for Education, Research and Innovation (SERI) under contract number 15.0160

20	2.54E+01	59.4	24.50	5.81E-01	-2.28E+05	8.81E-03	2.16E-04	9.91E-01	0.00E+00	0.00E+00	0.00E+00	0.00E+00	0.00E+00	0.00E+00	3.74E-05	0.00E+00	0.00E+00	0.00E+00
21	9.23E+00	56.8	24.50	4.52E-01	-1.34E+05	8.88E-01	4.66E-04	7.70E-03	5.19E-02	4.76E-09	5.39E-10	1.80E-04	4.90E-02	2.56E-03	1.87E-09	0.00E+00	0.00E+00	0.00E+00
22	4.76E-03	20.0	1.01	2.64E-04	-7.56E+01	1.00E+00	0.00E+00	0.00E+00	0.00E+00	1.50E-09	1.49E-09	0.00E+00	0.00E+00	0.00E+00	0.00E+00	0.00E+00	0.00E+00	0.00E+00
23	9.23E+00	50.0	24.50	4.52E-01	-1.34E+05	8.88E-01	3.75E-04	7.56E-03	5.21E-02	3.92E-09	4.21E-10	2.08E-04	4.92E-02	2.49E-03	1.87E-09	0.00E+00	0.00E+00	0.00E+00
24	2.54E+01	35.0	24.50	5.77E-01	-2.27E+05	2.97E-03	9.25E-07	9.97E-01	0.00E+00	0.00E+00	0.00E+00	0.00E+00	0.00E+00	0.00E+00	3.76E-05	0.00E+00	0.00E+00	0.00E+00
25	2.53E+01	28.2	110.00	5.76E-01	-2.33E+05	0.00E+00	0.00E+00	1.00E+00	0.00E+00	0.00E+00	0.00E+00	0.00E+00	0.00E+00	0.00E+00	0.00E+00	0.00E+00	0.00E+00	0.00E+00
26	4.06E-02	35.0	24.50	2.14E-03	-6.22E+02	9.57E-01	1.14E-05	1.29E-02	1.48E-02	1.44E-08	2.84E-10	5.25E-06	1.48E-02	2.75E-05	6.49E-09	0.00E+00	0.00E+00	0.00E+00
27	3.46E-02	56.8	24.50	1.69E-03	-5.03E+02	8.88E-01	4.66E-04	7.70E-03	5.19E-02	4.76E-09	5.39E-10	1.80E-04	4.90E-02	2.56E-03	1.87E-09	0.00E+00	0.00E+00	0.00E+00
28	1.29E+00	29.3	25.00	6.65E-02	-1.89E+04	9.06E-01	2.03E-02	3.17E-06	3.89E-02	1.23E-11	1.18E-07	4.64E-03	6.24E-03	2.34E-02	9.19E-10	0.00E+00	0.00E+00	0.00E+00
29	1.37E+00	72.0	24.50	7.02E-02	-1.98E+04	9.05E-01	2.38E-02	3.43E-05	3.61E-02	1.80E-10	1.18E-07	1.44E-03	1.32E-02	2.00E-02	1.11E-09	0.00E+00	0.00E+00	0.00E+00
30	5.50E-01	93.9	1.15	2.73E-02	-5.82E+03	7.05E-01	2.05E-01	8.93E-02	0.00E+00	0.00E+00	0.00E+00	0.00E+00	0.00E+00	0.00E+00	2.86E-09	0.00E+00	0.00E+00	0.00E+00
31	8.17E-01	105.0	1.25	4.54E-02	-1.27E+04	1.00E+00	1.68E-04	2.31E-08	8.38E-06	4.59E-11	5.11E-06	1.21E-07	3.02E-06	1.41E-08	1.00E-30	0.00E+00	0.00E+00	0.00E+00
32	8.17E-01	40.8	1.25	4.54E-02	-1.29E+04	1.00E+00	1.66E-04	3.63E-10	1.02E-05	1.79E-12	5.77E-06	1.29E-06	1.85E-06	4.35E-08	0.00E+00	0.00E+00	0.00E+00	0.00E+00
33	5.81E+01	12.4	1.01	2.05E+00	-3.45E+04	1.32E-02	2.70E-03	3.34E-02	0.00E+00	0.00E+00	0.00E+00	0.00E+00	0.00E+00	0.00E+00	9.51E-01	0.00E+00	0.00E+00	0.00E+00
34	5.80E+01	15.8	1.01	2.05E+00	-3.44E+04	1.78E-02	1.44E-04	3.11E-02	0.00E+00	0.00E+00	0.00E+00	0.00E+00	0.00E+00	0.00E+00	9.51E-01	0.00E+00	0.00E+00	0.00E+00
35	6.17E+01	47.3	1.01	2.25E+00	-8.25E+04	1.08E-01	0.00E+00	2.85E-02	0.00E+00	0.00E+00	0.00E+00	0.00E+00	0.00E+00	0.00E+00	8.64E-01	0.00E+00	0.00E+00	0.00E+00
36[(1)]	1.47E-02	20.0	1.10	1.63E-04	na	1.00E-01	0.00E+00	0.00E+00	0.00E+00	0.00E+00	0.00E+00	0.00E+00	0.00E+00	0.00E+00	0.00E+00	0.00E+00	0.00E+00	9.00E-01
37[(1)]	1.97E-02	20.0	1.01	1.63E-04	na	1.00E-01	0.00E+00	0.00E+00	0.00E+00	0.00E+00	0.00E+00	0.00E+00	0.00E+00	0.00E+00	0.00E+00	0.00E+00	9.00E-01	0.00E+00
38	1.18E+01	12.5	1.04	6.41E-01	-1.85E+05	9.84E-01	4.08E-04	4.77E-05	7.91E-03	6.86E-11	2.34E-08	3.35E-04	6.46E-03	7.82E-04	1.61E-05	0.00E+00	0.00E+00	0.00E+00
39	1.18E-04	1.5	1.20	6.41E-06	-1.85E+00	9.84E-01	3.09E-04	4.94E-05	8.02E-03	3.84E-11	1.48E-08	4.47E-04	6.36E-03	7.71E-04	1.61E-05	0.00E+00	0.00E+00	0.00E+00
40	1.18E+01	90.6	1.40	6.43E-01	-1.81E+05	9.84E-01	3.86E-03	3.04E-03	4.62E-03	5.47E-10	3.53E-07	5.91E-05	3.90E-03	5.99E-04	1.60E-05	0.00E+00	0.00E+00	0.00E+00
41	1.14E+01	98.8	1.01	6.33E-01	-1.77E+05	9.99E-01	9.28E-04	1.28E-07	4.00E-05	3.03E-11	5.92E-06	2.01E-06	2.91E-05	9.01E-07	3.68E-25	0.00E+00	0.00E+00	0.00E+00
42	1.16E+01	15.0	1.01	6.45E-01	-1.85E+05	9.99E-01	8.91E-04	3.21E-10	5.86E-05	3.21E-13	5.15E-06	2.19E-05	7.93E-06	1.76E-06	0.00E+00	0.00E+00	0.00E+00	0.00E+00
43	3.52E-01	68.0	1.01	1.28E-02	-2.78E+03	2.09E-01	4.09E-01	3.81E-01	0.00E+00	0.00E+00	0.00E+00	0.00E+00	0.00E+00	0.00E+00	8.08E-04	0.00E+00	0.00E+00	0.00E+00
44	2.18E-01	20.0	1.01	1.21E-02	-3.46E+03	1.00E+00	0.00E+00	0.00E+00	0.00E+00	1.49E-09	1.49E-09	0.00E+00	0.00E+00	0.00E+00	0.00E+00	0.00E+00	0.00E+00	0.00E+00
45	3.13E-02	32.5	24.50	1.74E-03	-4.96E+02	1.00E+00	0.00E+00	0.00E+00	0.00E+00	0.00E+00	0.00E+00	0.00E+00	0.00E+00	0.00E+00	0.00E+00	0.00E+00	0.00E+00	0.00E+00

(1) *Apparent composition*

This project has received funding from the European Union's Horizon2020 Research and Innovation Programme under Grant Agreement No 641185. This work was supported by the Swiss State Secretariat for Education, Research and Innovation (SERI) under contract number 15.0160

Table 9.2: Specifications of the streams of the CAP applied to the "Base" case defined in CEMCAP. Design at medium air leak, run at medium air leak. Second ½ of the year.

						Composition (mole frac.)													
#	F [kg/s]	T [°C]	P [bar]	N [kmol/s]	H [kJ/s]	H_2O	NH_3	CO_2	NH_4^+	H^+	OH^-	CO_3^{2-}	HCO_3^-	NH_2COO^-	Air	SO_2	$(NH_4)_2SO_4$	H_2SO_4
1	1.08E+02	110.0	1.10	3.59E+00	-3.23E+05	9.00E-02	0.00E+00	1.80E-01	0.00E+00	0.00E+00	0.00E+00	0.00E+00	0.00E+00	0.00E+00	7.30E-01	200 mg/Nm^3	0.00E+00	0.00E+00
2	2.24E+02	42.9	1.01	1.24E+01	-3.54E+06	1.00E+00	0.00E+00	7.24E-05	0.00E+00	7.97E-07	1.43E-11	1.18E-12	7.97E-07	0.00E+00	8.13E-06	0.00E+00	0.00E+00	0.00E+00
3	6.81E-01	31.4	1.01	3.78E-02	-1.08E+04	1.00E+00	0.00E+00	1.17E-05	0.00E+00	3.11E-07	1.70E-11	9.70E-13	3.11E-07	0.00E+00	1.18E-05	0.00E+00	0.00E+00	0.00E+00
4	2.20E+02	21.2	1.01	1.22E+01	-3.49E+06	1.00E+00	0.00E+00	7.25E-05	0.00E+00	7.39E-07	3.37E-12	8.00E-13	7.39E-07	0.00E+00	8.13E-06	0.00E+00	0.00E+00	0.00E+00
5[(1)]	4.07E-02	20.0	1.10	2.29E-03	-5.33E+02	7.39E-01	2.61E-01	0.00E+00	0.00E+00	0.00E+00	0.00E+00	0.00E+00	0.00E+00	0.00E+00	0.00E+00	0.00E+00	0.00E+00	0.00E+00
6[(1)]	7.00E-02	20.0	1.01	1.99E-03	-5.93E+02	8.50E-01	0.00E+00	0.00E+00	0.00E+00	0.00E+00	0.00E+00	0.00E+00	0.00E+00	0.00E+00	0.00E+00	0.00E+00	1.50E-01	0.00E+00
7	1.04E+02	21.8	1.01	3.36E+00	-2.76E+05	2.61E-02	0.00E+00	1.93E-01	0.00E+00	0.00E+00	0.00E+00	0.00E+00	0.00E+00	0.00E+00	7.81E-01	0.00E+00	0.00E+00	0.00E+00
8	1.04E+02	29.7	1.10	3.36E+00	-2.75E+05	2.61E-02	0.00E+00	1.93E-01	0.00E+00	0.00E+00	0.00E+00	0.00E+00	0.00E+00	0.00E+00	7.81E-01	0.00E+00	0.00E+00	0.00E+00
9	8.61E+02	26.0	1.05	4.24E+01	-1.24E+07	8.78E-01	6.54E-03	5.72E-05	6.05E-02	3.54E-11	1.37E-08	6.05E-03	1.80E-02	3.05E-02	3.30E-07	0.00E+00	0.00E+00	0.00E+00
10	1.55E+02	9.0	1.40	7.63E+00	-2.24E+06	8.76E-01	4.29E-03	1.52E-04	6.52E-02	1.14E-11	7.45E-09	1.09E-02	1.55E-02	2.80E-02	3.30E-07	0.00E+00	0.00E+00	0.00E+00
11	0.00E+00	na	na	0.00E+00	na	0.00E+00	0.00E+00	0.00E+00	0.00E+00	0.00E+00	0.00E+00	0.00E+00	0.00E+00	0.00E+00	0.00E+00	0.00E+00	0.00E+00	0.00E+00
12	0.00E+00	na	na	0.00E+00	na	0.00E+00	0.00E+00	0.00E+00	0.00E+00	0.00E+00	0.00E+00	0.00E+00	0.00E+00	0.00E+00	0.00E+00	0.00E+00	0.00E+00	0.00E+00
13	7.06E+02	26.8	25.40	3.48E+01	-1.01E+07	8.78E-01	6.65E-03	5.61E-05	6.04E-02	3.72E-11	1.40E-08	5.90E-03	1.81E-02	3.05E-02	3.30E-07	0.00E+00	0.00E+00	0.00E+00
14	6.81E+02	137.8	25.40	3.39E+01	-9.45E+06	8.63E-01	4.04E-02	1.11E-02	4.31E-02	3.38E-09	8.23E-08	2.42E-04	2.96E-02	1.30E-02	3.27E-07	0.00E+00	0.00E+00	0.00E+00
15	2.47E+01	26.8	25.40	1.22E+00	-3.55E+05	8.78E-01	6.66E-03	5.61E-05	6.04E-02	3.72E-11	1.40E-08	5.90E-03	1.81E-02	3.05E-02	3.30E-07	0.00E+00	0.00E+00	0.00E+00
16	6.80E+02	147.0	25.00	3.49E+01	-9.52E+06	8.75E-01	5.23E-02	2.94E-03	3.49E-02	3.55E-09	1.61E-07	1.97E-04	2.44E-02	1.01E-02	1.22E-09	0.00E+00	0.00E+00	0.00E+00
17	6.79E+02	30.5	25.00	3.47E+01	-9.82E+06	8.92E-01	2.78E-02	2.10E-06	4.28E-02	1.05E-11	1.08E-07	5.06E-03	5.74E-03	2.69E-02	1.22E-09	0.00E+00	0.00E+00	0.00E+00
18	6.79E+02	21.2	1.05	3.47E+01	-9.85E+06	8.91E-01	2.69E-02	1.66E-06	4.45E-02	5.02E-12	1.01E-07	6.75E-03	4.79E-03	2.62E-02	1.22E-09	0.00E+00	0.00E+00	0.00E+00
19[(1)]	3.04E-02	20.0	1.01	1.71E-03	-3.99E+02	7.39E-01	2.61E-01	0.00E+00	0.00E+00	0.00E+00	0.00E+00	0.00E+00	0.00E+00	0.00E+00	0.00E+00	0.00E+00	0.00E+00	0.00E+00
20	2.58E+01	54.3	24.50	5.88E-01	-2.31E+05	6.79E-03	1.62E-04	9.93E-01	0.00E+00	0.00E+00	0.00E+00	0.00E+00	0.00E+00	0.00E+00	1.95E-05	0.00E+00	0.00E+00	0.00E+00
21	9.35E+00	52.9	24.50	4.57E-01	-1.36E+05	8.87E-01	3.48E-04	8.95E-03	5.18E-02	4.97E-09	3.86E-10	1.62E-04	4.94E-02	2.12E-03	1.05E-09	0.00E+00	0.00E+00	0.00E+00
22	1.45E-02	20.0	1.01	8.05E-04	-2.30E+02	1.00E+00	0.00E+00	0.00E+00	0.00E+00	1.50E-09	1.50E-09	0.00E+00	0.00E+00	0.00E+00	0.00E+00	0.00E+00	0.00E+00	0.00E+00

This project has received funding from the European Union's Horizon2020 Research and Innovation Programme under Grant Agreement No 641185. This work was supported by the Swiss State Secretariat for Education, Research and Innovation (SERI) under contract number 15.0160

23	9.37E+00	50.0	24.50	4.58E-01	-1.36E+05	8.87E-01	3.18E-04	8.89E-03	5.18E-02	4.56E-09	3.50E-10	1.72E-04	4.94E-02	2.09E-03	1.05E-09	0.00E+00	0.00E+00	0.00E+00
24	2.57E+01	35.0	24.50	5.85E-01	-2.30E+05	2.98E-03	8.62E-07	9.97E-01	0.00E+00	0.00E+00	0.00E+00	0.00E+00	0.00E+00	0.00E+00	1.95E-05	0.00E+00	0.00E+00	0.00E+00
25	2.57E+01	28.2	110.00	5.83E-01	-2.36E+05	0.00E+00	0.00E+00	1.00E+00	0.00E+00	0.00E+00	0.00E+00	0.00E+00	0.00E+00	0.00E+00	0.00E+00	0.00E+00	0.00E+00	0.00E+00
26	3.70E-02	35.0	24.50	1.95E-03	-5.66E+02	9.59E-01	1.06E-05	1.28E-02	1.41E-02	1.49E-08	2.85E-10	4.73E-06	1.41E-02	2.43E-05	3.41E-09	0.00E+00	0.00E+00	0.00E+00
27	2.53E-02	52.9	24.50	1.23E-03	-3.67E+02	8.87E-01	3.48E-04	8.95E-03	5.18E-02	4.97E-09	3.86E-10	1.62E-04	4.94E-02	2.12E-03	1.05E-09	0.00E+00	0.00E+00	0.00E+00
28	1.85E+00	30.5	25.00	9.43E-02	-2.67E+04	8.92E-01	2.78E-02	2.10E-06	4.28E-02	1.05E-11	1.08E-07	5.06E-03	5.74E-03	2.69E-02	1.22E-09	0.00E+00	0.00E+00	0.00E+00
29	1.91E+00	75.4	24.50	9.74E-02	-2.73E+04	8.90E-01	3.27E-02	2.66E-05	3.94E-02	1.74E-10	1.09E-07	1.58E-03	1.30E-02	2.33E-02	1.26E-09	0.00E+00	0.00E+00	0.00E+00
30	8.12E-01	92.9	1.15	4.02E-02	-8.38E+03	6.78E-01	2.31E-01	9.16E-02	0.00E+00	0.00E+00	0.00E+00	0.00E+00	0.00E+00	0.00E+00	3.05E-09	0.00E+00	0.00E+00	0.00E+00
31	1.10E+00	105.0	1.25	6.09E-02	-1.70E+04	1.00E+00	1.75E-04	2.41E-08	8.30E-06	4.41E-11	4.81E-06	1.31E-07	3.22E-06	1.60E-08	1.03E-27	0.00E+00	0.00E+00	0.00E+00
32	1.10E+00	34.3	1.25	6.09E-02	-1.74E+04	1.00E+00	1.73E-04	2.29E-10	1.07E-05	1.19E-12	5.71E-06	1.63E-06	1.71E-06	4.86E-08	0.00E+00	0.00E+00	0.00E+00	0.00E+00
33	7.74E+01	10.5	1.01	2.74E+00	-3.74E+04	1.15E-02	3.53E-03	2.61E-02	0.00E+00	0.00E+00	0.00E+00	0.00E+00	0.00E+00	0.00E+00	9.59E-01	0.00E+00	0.00E+00	0.00E+00
34	7.72E+01	15.1	1.01	2.73E+00	-3.72E+04	1.71E-02	1.93E-04	2.32E-02	0.00E+00	0.00E+00	0.00E+00	0.00E+00	0.00E+00	0.00E+00	9.59E-01	0.00E+00	0.00E+00	0.00E+00
35	8.07E+01	42.4	1.01	2.93E+00	-8.29E+04	8.33E-02	0.00E+00	2.19E-02	0.00E+00	0.00E+00	0.00E+00	0.00E+00	0.00E+00	0.00E+00	8.95E-01	0.00E+00	0.00E+00	0.00E+00
36[(1)]	2.64E-02	20.0	1.10	2.93E-04	na	1.00E-01	0.00E+00	0.00E+00	0.00E+00	0.00E+00	0.00E+00	0.00E+00	0.00E+00	0.00E+00	0.00E+00	0.00E+00	0.00E+00	9.00E-01
37[(1)]	3.53E-02	20.0	1.01	2.93E-04	na	1.00E-01	0.00E+00	0.00E+00	0.00E+00	0.00E+00	0.00E+00	0.00E+00	0.00E+00	0.00E+00	0.00E+00	0.00E+00	9.00E-01	0.00E+00
38	1.57E+01	10.8	1.04	8.54E-01	-2.46E+05	9.80E-01	5.80E-04	4.46E-05	9.73E-03	4.97E-11	2.60E-08	5.55E-04	7.29E-03	1.33E-03	1.53E-05	0.00E+00	0.00E+00	0.00E+00
39	1.57E-04	1.5	1.20	8.54E-06	-2.47E+00	9.80E-01	4.56E-04	4.96E-05	9.87E-03	3.05E-11	1.75E-08	7.06E-04	7.15E-03	1.31E-03	1.53E-05	0.00E+00	0.00E+00	0.00E+00
40	1.57E+01	89.6	1.40	8.56E-01	-2.41E+05	9.80E-01	4.89E-03	3.49E-03	5.78E-03	5.10E-10	3.53E-07	8.47E-05	4.68E-03	9.30E-04	1.52E-05	0.00E+00	0.00E+00	0.00E+00
41	1.51E+01	98.8	1.01	8.40E-01	-2.35E+05	9.99E-01	9.27E-04	1.29E-07	4.00E-05	3.03E-11	5.91E-06	2.01E-06	2.92E-05	9.02E-07	3.20E-25	0.00E+00	0.00E+00	0.00E+00
42	1.55E+01	13.9	1.01	8.60E-01	-2.46E+05	9.99E-01	8.86E-04	2.91E-10	5.87E-05	2.97E-13	5.07E-06	2.21E-05	7.63E-06	1.73E-06	0.00E+00	0.00E+00	0.00E+00	0.00E+00
43	5.81E-01	68.0	1.01	2.14E-02	-4.55E+03	2.08E-01	4.26E-01	3.66E-01	0.00E+00	0.00E+00	0.00E+00	0.00E+00	0.00E+00	0.00E+00	6.08E-04	0.00E+00	0.00E+00	0.00E+00
44	3.54E-01	20.0	1.01	1.96E-02	-5.62E+03	1.00E+00	0.00E+00	0.00E+00	0.00E+00	1.49E-09	1.49E-09	0.00E+00	0.00E+00	0.00E+00	0.00E+00	0.00E+00	0.00E+00	0.00E+00
45	3.16E-02	32.5	24.50	1.75E-03	-5.01E+02	1.00E+00	0.00E+00	0.00E+00	0.00E+00	0.00E+00	0.00E+00	0.00E+00	0.00E+00	0.00E+00	0.00E+00	0.00E+00	0.00E+00	0.00E+00

(1) *Apparent composition*

This project has received funding from the European Union's Horizon2020 Research and Innovation Programme under Grant Agreement No 641185. This work was supported by the Swiss State Secretariat for Education, Research and Innovation (SERI) under contract number 15.0160

Table 9.3: Main energy consumers of the CAP applied to the "Base" case defined in CEMCAP. Design at medium air leak, run at low air leak. First ½ of the year.

Variable	Value
$\dot{Q}_{\mathrm{heat,tot}}$ [MW_{th}]	58.22
$\dot{Q}_{\mathrm{heat,Reb-1}}$ [MW_{th}]	53.68
$T_{\mathrm{Reb-1}}$ [°C]	145
$\dot{Q}_{\mathrm{heat,Reb-2}}$ [MW_{th}]	3.21
$T_{\mathrm{Reb-2}}$ [°C]	99
$\dot{Q}_{\mathrm{heat,Reb-3}}$ [MW_{th}]	1.33
$T_{\mathrm{Reb-3}}$ [°C]	105
$\dot{Q}_{\mathrm{cool,tot}}$ [MW_{th}]	76.74
$\dot{Q}_{\mathrm{cool,Cond-1}}$ [MW_{th}]	0
$T_{\mathrm{out,Cond-1}}$ [°C]	-
$\dot{Q}_{\mathrm{cool,Cond-2}}$ [MW_{th}]	2.42
$T_{\mathrm{out,Cond-2}}$ [°C]	68.0
$\dot{Q}_{\mathrm{cool,Cool-1}}$ [MW_{th}]	9.71
$T_{\mathrm{out,Cool-1}}$ [°C]	21.2
$\dot{Q}_{\mathrm{cool,Cool-2}}$ [MW_{th}]	1.54
$T_{\mathrm{out,Cool-2}}$ [°C]	21.2
$\dot{Q}_{\mathrm{cool,Cool-3}}$ [MW_{th}]	24.08
$T_{\mathrm{out,Cool-3}}$ [°C]	21.2
$\dot{Q}_{\mathrm{cool,Cool-4}}$ [MW_{th}]	0.25
$T_{\mathrm{out,Cool-4}}$ [°C]	50.0
$\dot{Q}_{\mathrm{cool,Cool-5}}$ [MW_{th}]	0.53
$T_{\mathrm{out,Cool-5}}$ [°C]	35.0
$\dot{Q}_{\mathrm{cool,Cool-6}}$ [MW_{th}]	7.80
$T_{\mathrm{out,Cool-6}}$ [°C]	28.2
$\dot{Q}_{\mathrm{cool,Cool-7}}$ [MW_{th}]	30.41
$T_{\mathrm{out,Cool-7}}$ [°C]	21.2
$\dot{Q}_{\mathrm{chill,tot}}$ [MW_{th}]	4.07
$\dot{Q}_{\mathrm{chill,Chill-1}}$ [MW_{th}]	4.04
$T_{\mathrm{out,Chill-1}}$ [°C]	12.0
$\dot{Q}_{\mathrm{chill,Chill-2}}$ [MW_{th}]	0
$T_{\mathrm{out,Chill-2}}$ [°C]	-
$\dot{Q}_{\mathrm{chill,Chill-3}}$ [MW_{th}]	0.03
$T_{\mathrm{out,Chill-3}}$ [°C]	15.0
$\dot{W}_{\mathrm{aux,tot}}$ [MW_{el}]	3.19

This project has received funding from the European Union's Horizon2020 Research and Innovation Programme under Grant Agreement No 641185. This work was supported by the Swiss State Secretariat for Education, Research and Innovation (SERI) under contract number 15.0160

$\dot{W}_{\mathrm{aux,Fan-1}}$ [MW$_{el}$]	0.67
$\dot{W}_{\mathrm{aux,Pump-1}}$ [MW$_{el}$]	2.51
$\dot{W}_{\mathrm{CO_2comp,Comp-1}}$ [MW$_{el}$]	2.04

This project has received funding from the European Union's Horizon2020 Research and Innovation Programme under Grant Agreement No 641185. This work was supported by the Swiss State Secretariat for Education, Research and Innovation (SERI) under contract number 15.0160

Table 9.4: Main energy consumers of the CAP applied to the "Base" case defined in CEMCAP. Design at medium air leak, run at medium air leak. Second ½ of the year.

Variable	Value
$\dot{Q}_{\mathrm{heat,tot}}$ [MW_{th}]	63.11
$\dot{Q}_{\mathrm{heat,Reb-1}}$ [MW_{th}]	56.50
$T_{\mathrm{Reb-1}}$ [°C]	147
$\dot{Q}_{\mathrm{heat,Reb-2}}$ [MW_{th}]	4.70
$T_{\mathrm{Reb-2}}$ [°C]	99
$\dot{Q}_{\mathrm{heat,Reb-3}}$ [MW_{th}]	1.92
$T_{\mathrm{Reb-3}}$ [°C]	105
$\dot{Q}_{\mathrm{cool,tot}}$ [MW_{th}]	84.17
$\dot{Q}_{\mathrm{cool,Cond-1}}$ [MW_{th}]	0
$T_{\mathrm{out,Cond-1}}$ [°C]	-
$\dot{Q}_{\mathrm{cool,Cond-2}}$ [MW_{th}]	3.42
$T_{\mathrm{out,Cond-2}}$ [°C]	68.0
$\dot{Q}_{\mathrm{cool,Cool-1}}$ [MW_{th}]	9.23
$T_{\mathrm{out,Cool-1}}$ [°C]	21.2
$\dot{Q}_{\mathrm{cool,Cool-2}}$ [MW_{th}]	3.00
$T_{\mathrm{out,Cool-2}}$ [°C]	21.2
$\dot{Q}_{\mathrm{cool,Cool-3}}$ [MW_{th}]	24.57
$T_{\mathrm{out,Cool-3}}$ [°C]	21.2
$\dot{Q}_{\mathrm{cool,Cool-4}}$ [MW_{th}]	0.11
$T_{\mathrm{out,Cool-4}}$ [°C]	50.0
$\dot{Q}_{\mathrm{cool,Cool-5}}$ [MW_{th}]	0.49
$T_{\mathrm{out,Cool-5}}$ [°C]	35.0
$\dot{Q}_{\mathrm{cool,Cool-6}}$ [MW_{th}]	7.91
$T_{\mathrm{out,Cool-6}}$ [°C]	28.2
$\dot{Q}_{\mathrm{cool,Cool-7}}$ [MW_{th}]	29.02
$T_{\mathrm{out,Cool-7}}$ [°C]	21.2
$\dot{Q}_{\mathrm{chill,tot}}$ [MW_{th}]	7.98
$\dot{Q}_{\mathrm{chill,Chill-1}}$ [MW_{th}]	7.98
$T_{\mathrm{out,Chill-1}}$ [°C]	9.0
$\dot{Q}_{\mathrm{chill,Chill-2}}$ [MW_{th}]	0
$T_{\mathrm{out,Chill-2}}$ [°C]	-
$\dot{Q}_{\mathrm{chill,Chill-3}}$ [MW_{th}]	0
$T_{\mathrm{out,Chill-3}}$ [°C]	-
$\dot{W}_{\mathrm{aux,tot}}$ [MW_{el}]	3.15

This project has received funding from the European Union's Horizon2020 Research and Innovation Programme under Grant Agreement No 641185. This work was supported by the Swiss State Secretariat for Education, Research and Innovation (SERI) under contract number 15.0160

$\dot{W}_{\mathrm{aux,Fan-1}}$ [MW$_{el}$]	0.85
$\dot{W}_{\mathrm{aux,Pump-1}}$ [MW$_{el}$]	2.30
$\dot{W}_{\mathrm{CO_2comp,Comp-1}}$ [MW$_{el}$]	2.07

This project has received funding from the European Union's Horizon2020 Research and Innovation Programme under Grant Agreement No 641185. This work was supported by the Swiss State Secretariat for Education, Research and Innovation (SERI) under contract number 15.0160

9.2 Constant low air leak

Table 9.5: Specifications of the streams of the CAP applied to the "Constant low air leak" case defined in CEMCAP.

						Composition (mole frac.)												
#	F [kg/s]	T [°C]	P [bar]	N [kmol/s]	H [kJ/s]	H_2O	NH_3	CO_2	NH_4^+	H^+	OH^-	CO_3^{2-}	HCO_3^-	NH_2COO^-	Air	SO_2	$(NH_4)_2SO_4$	H_2SO_4
1	8.84E+01	130.0	1.10	2.90E+00	-3.19E+05	1.10E-01	0.00E+00	2.20E-01	0.00E+00	0.00E+00	0.00E+00	0.00E+00	0.00E+00	0.00E+00	6.70E-01	200 mg/Nm^3	0.00E+00	0.00E+00
2	1.86E+02	48.2	1.01	1.03E+01	-2.93E+06	1.00E+00	0.00E+00	7.94E-05	0.00E+00	8.36E-07	1.88E-11	1.27E-12	8.36E-07	0.00E+00	7.06E-06	0.00E+00	0.00E+00	0.00E+00
3	7.37E-01	34.2	1.01	4.09E-02	-1.17E+04	1.00E+00	0.00E+00	1.45E-05	0.00E+00	3.50E-07	1.83E-11	1.02E-12	3.50E-07	0.00E+00	1.12E-05	0.00E+00	0.00E+00	0.00E+00
4	1.81E+02	21.2	1.01	1.01E+01	-2.88E+06	1.00E+00	0.00E+00	7.94E-05	0.00E+00	7.74E-07	3.22E-12	8.01E-13	7.74E-07	0.00E+00	7.06E-06	0.00E+00	0.00E+00	0.00E+00
5[(1)]	3.46E-02	20.0	1.10	1.95E-03	-4.54E+02	7.39E-01	2.61E-01	0.00E+00	0.00E+00	0.00E+00	0.00E+00	0.00E+00	0.00E+00	0.00E+00	0.00E+00	0.00E+00	0.00E+00	0.00E+00
6[(1)]	5.95E-02	20.0	1.01	1.70E-03	-4.54E+02	8.50E-01	0.00E+00	0.00E+00	0.00E+00	0.00E+00	0.00E+00	0.00E+00	0.00E+00	0.00E+00	0.00E+00	0.00E+00	1.50E-01	0.00E+00
7	8.39E+01	22.2	1.01	2.66E+00	-2.69E+05	2.66E-02	0.00E+00	2.41E-01	0.00E+00	0.00E+00	0.00E+00	0.00E+00	0.00E+00	0.00E+00	7.33E-01	0.00E+00	0.00E+00	0.00E+00
8	8.39E+01	29.9	1.10	2.66E+00	-2.68E+05	2.66E-02	0.00E+00	2.41E-01	0.00E+00	0.00E+00	0.00E+00	0.00E+00	0.00E+00	0.00E+00	7.33E-01	0.00E+00	0.00E+00	0.00E+00
9	7.24E+02	24.4	1.05	3.66E+01	-1.07E+07	9.10E-01	3.65E-03	9.75E-05	4.51E-02	5.44E-11	1.55E-08	3.83E-03	1.89E-02	1.85E-02	1.09E-06	0.00E+00	0.00E+00	0.00E+00
10	1.09E+02	12.0	1.40	5.49E+00	-1.61E+06	9.09E-01	2.65E-03	1.70E-04	4.67E-02	2.68E-11	9.94E-09	5.58E-03	1.78E-02	1.78E-02	1.09E-06	0.00E+00	0.00E+00	0.00E+00
11	0.00E+00	na	na	0.00E+00	na	0.00E+00	0.00E+00	0.00E+00	0.00E+00	0.00E+00	0.00E+00	0.00E+00	0.00E+00	0.00E+00	0.00E+00	0.00E+00	0.00E+00	0.00E+00
12	0.00E+00	na	na	0.00E+00	na	0.00E+00	0.00E+00	0.00E+00	0.00E+00	0.00E+00	0.00E+00	0.00E+00	0.00E+00	0.00E+00	0.00E+00	0.00E+00	0.00E+00	0.00E+00
13	6.15E+02	25.0	20.40	3.11E+01	-9.08E+06	9.10E-01	3.70E-03	9.61E-05	4.50E-02	5.62E-11	1.58E-08	3.76E-03	1.90E-02	1.85E-02	1.09E-06	0.00E+00	0.00E+00	0.00E+00
14	5.91E+02	137.4	20.40	3.03E+01	-8.42E+06	9.00E-01	3.12E-02	1.29E-02	2.81E-02	3.01E-09	1.46E-07	1.57E-04	2.07E-02	7.05E-03	1.08E-06	0.00E+00	0.00E+00	0.00E+00
15	2.46E+01	25.0	20.40	1.25E+00	-3.63E+05	9.10E-01	3.71E-03	9.61E-05	4.50E-02	5.62E-11	1.59E-08	3.76E-03	1.90E-02	1.85E-02	1.09E-06	0.00E+00	0.00E+00	0.00E+00
16	5.90E+02	148.8	20.00	3.12E+01	-8.50E+06	9.15E-01	4.17E-02	2.37E-03	2.06E-02	3.06E-09	2.91E-07	1.11E-04	1.56E-02	4.77E-03	1.54E-09	0.00E+00	0.00E+00	0.00E+00
17	5.89E+02	29.6	20.00	3.11E+01	-8.78E+06	9.26E-01	2.53E-02	1.21E-06	2.60E-02	8.96E-12	2.40E-07	3.14E-03	3.85E-03	1.59E-02	1.54E-09	0.00E+00	0.00E+00	0.00E+00
18	5.89E+02	21.2	1.05	3.11E+01	-8.80E+06	9.26E-01	2.48E-02	8.49E-07	2.69E-02	4.73E-12	2.27E-07	3.98E-03	3.30E-03	1.56E-02	1.54E-09	0.00E+00	0.00E+00	0.00E+00
19[(1)]	1.14E-02	20.0	1.01	6.44E-04	-1.50E+02	7.39E-01	2.61E-01	0.00E+00	0.00E+00	0.00E+00	0.00E+00	0.00E+00	0.00E+00	0.00E+00	0.00E+00	0.00E+00	0.00E+00	0.00E+00
20	2.54E+01	47.5	19.50	5.79E-01	-2.27E+05	6.16E-03	6.43E-05	9.94E-01	0.00E+00	0.00E+00	0.00E+00	0.00E+00	0.00E+00	0.00E+00	5.86E-05	0.00E+00	0.00E+00	0.00E+00
21	7.85E+00	46.7	19.50	4.24E-01	-1.22E+05	9.78E-01	1.46E-05	6.82E-03	7.55E-03	1.70E-08	8.98E-10	2.29E-06	7.54E-03	1.35E-05	8.90E-09	0.00E+00	0.00E+00	0.00E+00

This project has received funding from the European Union's Horizon2020 Research and Innovation Programme under Grant Agreement No 641185. This work was supported by the Swiss State Secretariat for Education, Research and Innovation (SERI) under contract number 15.0160

22	8.41E-02	20.0	1.01	4.67E-03	-1.34E+03	1.00E+00	0.00E+00	0.00E+00	0.00E+00	1.50E-09	1.50E-09	0.00E+00	0.00E+00	0.00E+00	0.00E+00	0.00E+00	0.00E+00	0.00E+00
23	7.94E+00	45.0	19.50	4.29E-01	-1.23E+05	9.78E-01	1.31E-05	6.74E-03	7.47E-03	1.67E-08	8.26E-10	2.25E-06	7.47E-03	1.25E-05	8.80E-09	0.00E+00	0.00E+00	0.00E+00
24	2.54E+01	35.0	19.50	5.77E-01	-2.27E+05	3.59E-03	8.65E-09	9.96E-01	0.00E+00	0.00E+00	0.00E+00	0.00E+00	0.00E+00	0.00E+00	5.87E-05	0.00E+00	0.00E+00	0.00E+00
25	2.53E+01	28.2	110.00	5.75E-01	-2.32E+05	0.00E+00	0.00E+00	1.00E+00	0.00E+00	0.00E+00	0.00E+00	0.00E+00	0.00E+00	0.00E+00	0.00E+00	0.00E+00	0.00E+00	0.00E+00
26	2.67E-02	35.0	19.50	1.46E-03	-4.19E+02	9.90E-01	9.13E-08	8.33E-03	7.40E-04	1.22E-07	5.33E-11	9.42E-09	7.41E-04	1.03E-08	1.01E-08	0.00E+00	0.00E+00	0.00E+00
27	8.83E-02	46.7	19.50	4.77E-03	-1.37E+03	9.78E-01	1.46E-05	6.82E-03	7.55E-03	1.70E-08	8.98E-10	2.29E-06	7.54E-03	1.35E-05	8.90E-09	0.00E+00	0.00E+00	0.00E+00
28	1.23E+00	29.6	20.00	6.50E-02	-1.84E+04	9.26E-01	2.53E-02	1.21E-06	2.60E-02	8.96E-12	2.40E-07	3.14E-03	3.85E-03	1.59E-02	1.54E-09	0.00E+00	0.00E+00	0.00E+00
29	1.35E+00	74.2	19.50	7.11E-02	-1.99E+04	9.29E-01	2.62E-02	2.18E-05	2.30E-02	1.41E-10	2.57E-07	9.87E-04	8.30E-03	1.27E-02	2.21E-09	0.00E+00	0.00E+00	0.00E+00
30	4.90E-01	95.8	1.15	2.52E-02	-5.41E+03	7.63E-01	1.74E-01	6.22E-02	0.00E+00	0.00E+00	0.00E+00	0.00E+00	0.00E+00	0.00E+00	6.24E-09	0.00E+00	0.00E+00	0.00E+00
31	8.56E-01	105.0	1.25	4.75E-02	-1.33E+04	1.00E+00	1.58E-04	2.02E-08	7.46E-06	4.34E-11	5.40E-06	1.18E-07	2.80E-06	1.23E-08	2.98E-26	0.00E+00	0.00E+00	0.00E+00
32	8.56E-01	41.5	1.25	4.75E-02	-1.35E+04	1.00E+00	1.57E-04	3.36E-10	9.21E-06	1.79E-12	6.04E-06	1.20E-06	1.71E-06	3.73E-08	0.00E+00	0.00E+00	0.00E+00	0.00E+00
33	5.81E+01	12.8	1.01	2.05E+00	-3.44E+04	1.38E-02	1.91E-03	3.30E-02	0.00E+00	0.00E+00	0.00E+00	0.00E+00	0.00E+00	0.00E+00	9.51E-01	0.00E+00	0.00E+00	0.00E+00
34	5.80E+01	15.4	1.01	2.05E+00	-3.43E+04	1.74E-02	1.02E-04	3.12E-02	0.00E+00	0.00E+00	0.00E+00	0.00E+00	0.00E+00	0.00E+00	9.51E-01	0.00E+00	0.00E+00	0.00E+00
35	6.17E+01	47.3	1.01	2.25E+00	-8.26E+04	1.08E-01	0.00E+00	2.86E-02	0.00E+00	0.00E+00	0.00E+00	0.00E+00	0.00E+00	0.00E+00	8.64E-01	0.00E+00	0.00E+00	0.00E+00
36[(1)]	1.05E-02	20.0	1.10	1.16E-04	na	1.00E-01	0.00E+00	0.00E+00	0.00E+00	0.00E+00	0.00E+00	0.00E+00	0.00E+00	0.00E+00	0.00E+00	0.00E+00	0.00E+00	9.00E-01
37[(1)]	1.41E-02	20.0	1.01	1.16E-04	na	1.00E-01	0.00E+00	0.00E+00	0.00E+00	0.00E+00	0.00E+00	0.00E+00	0.00E+00	0.00E+00	0.00E+00	0.00E+00	9.00E-01	0.00E+00
38	1.17E+01	12.9	1.04	6.41E-01	-1.85E+05	9.88E-01	2.87E-04	4.18E-05	6.02E-03	7.92E-11	2.22E-08	2.04E-04	5.19E-03	4.28E-04	1.68E-05	0.00E+00	0.00E+00	0.00E+00
39	1.17E-04	1.5	1.20	6.41E-06	-1.85E+00	9.88E-01	2.17E-04	3.94E-05	6.10E-03	4.32E-11	1.40E-08	2.77E-04	5.12E-03	4.22E-04	1.68E-05	0.00E+00	0.00E+00	0.00E+00
40	1.17E+01	91.7	1.40	6.43E-01	-1.81E+05	9.88E-01	2.86E-03	2.36E-03	3.52E-03	6.00E-10	3.46E-07	3.77E-05	3.10E-03	3.44E-04	1.67E-05	0.00E+00	0.00E+00	0.00E+00
41	1.15E+01	98.8	1.01	6.36E-01	-1.78E+05	9.99E-01	9.27E-04	1.28E-07	4.00E-05	3.03E-11	5.92E-06	2.01E-06	2.91E-05	9.00E-07	5.54E-25	0.00E+00	0.00E+00	0.00E+00
42	1.16E+01	15.0	1.01	6.45E-01	-1.85E+05	9.99E-01	8.94E-04	3.22E-10	5.88E-05	3.21E-13	5.15E-06	2.20E-05	7.96E-06	1.77E-06	0.00E+00	0.00E+00	0.00E+00	0.00E+00
43	2.64E-01	68.0	1.01	9.45E-03	-2.11E+03	2.11E-01	3.92E-01	3.96E-01	0.00E+00	0.00E+00	0.00E+00	0.00E+00	0.00E+00	0.00E+00	1.14E-03	0.00E+00	0.00E+00	0.00E+00
44	1.66E-01	20.0	1.01	9.22E-03	-2.64E+03	1.00E+00	0.00E+00	0.00E+00	0.00E+00	1.49E-09	1.49E-09	0.00E+00	0.00E+00	0.00E+00	0.00E+00	0.00E+00	0.00E+00	0.00E+00
45	3.80E-02	32.3	19.50	2.11E-03	-6.02E+02	1.00E+00	0.00E+00	0.00E+00	0.00E+00	0.00E+00	0.00E+00	0.00E+00	0.00E+00	0.00E+00	0.00E+00	0.00E+00	0.00E+00	0.00E+00

(1) *Apparent composition*

This project has received funding from the European Union's Horizon2020 Research and Innovation Programme under Grant Agreement No 641185. This work was supported by the Swiss State Secretariat for Education, Research and Innovation (SERI) under contract number 15.0160

Table 9.6: Main energy consumers of the CAP applied to the "Constant low air leak" case defined in CEMCAP.

Variable	Value
$\dot{Q}_{\mathrm{heat,tot}}$ [MW_{th}]	57.91
$\dot{Q}_{\mathrm{heat,Reb-1}}$ [MW_{th}]	53.85
$T_{\mathrm{Reb-1}}$ [°C]	149.0
$\dot{Q}_{\mathrm{heat,Reb-2}}$ [MW_{th}]	2.85
$T_{\mathrm{Reb-2}}$ [°C]	99.0
$\dot{Q}_{\mathrm{heat,Reb-3}}$ [MW_{th}]	1.21
$T_{\mathrm{Reb-3}}$ [°C]	105.0
$\dot{Q}_{\mathrm{cool,tot}}$ [MW_{th}]	84.17
$\dot{Q}_{\mathrm{cool,Cond-1}}$ [MW_{th}]	0
$T_{\mathrm{out,Cond-1}}$ [°C]	-
$\dot{Q}_{\mathrm{cool,Cond-2}}$ [MW_{th}]	2.23
$T_{\mathrm{out,Cond-2}}$ [°C]	68.0
$\dot{Q}_{\mathrm{cool,Cool-1}}$ [MW_{th}]	9.65
$T_{\mathrm{out,Cool-1}}$ [°C]	21.2
$\dot{Q}_{\mathrm{cool,Cool-2}}$ [MW_{th}]	1.39
$T_{\mathrm{out,Cool-2}}$ [°C]	21.2
$\dot{Q}_{\mathrm{cool,Cool-3}}$ [MW_{th}]	19.68
$T_{\mathrm{out,Cool-3}}$ [°C]	21.2
$\dot{Q}_{\mathrm{cool,Cool-4}}$ [MW_{th}]	0.05
$T_{\mathrm{out,Cool-4}}$ [°C]	45.0
$\dot{Q}_{\mathrm{cool,Cool-5}}$ [MW_{th}]	0.32
$T_{\mathrm{out,Cool-5}}$ [°C]	35.0
$\dot{Q}_{\mathrm{cool,Cool-6}}$ [MW_{th}]	8.33
$T_{\mathrm{out,Cool-6}}$ [°C]	28.2
$\dot{Q}_{\mathrm{cool,Cool-7}}$ [MW_{th}]	34.21
$T_{\mathrm{out,Cool-7}}$ [°C]	21.2
$\dot{Q}_{\mathrm{chill,tot}}$ [MW_{th}]	4.12
$\dot{Q}_{\mathrm{chill,Chill-1}}$ [MW_{th}]	4.07
$T_{\mathrm{out,Chill-1}}$ [°C]	12.0
$\dot{Q}_{\mathrm{chill,Chill-2}}$ [MW_{th}]	0
$T_{\mathrm{out,Chill-2}}$ [°C]	-
$\dot{Q}_{\mathrm{chill,Chill-3}}$ [MW_{th}]	0.05
$T_{\mathrm{out,Chill-3}}$ [°C]	15.0
$\dot{W}_{\mathrm{aux,tot}}$ [MW_{el}]	2.24

This project has received funding from the European Union's Horizon2020 Research and Innovation Programme under Grant Agreement No 641185. This work was supported by the Swiss State Secretariat for Education, Research and Innovation (SERI) under contract number 15.0160

$\dot{W}_{\mathrm{aux,Fan-1}}$ [MW$_{el}$]	0.67
$\dot{W}_{\mathrm{aux,Pump-1}}$ [MW$_{el}$]	1.56
$\dot{W}_{\mathrm{CO_2comp,Comp-1}}$ [MW$_{el}$]	2.48

This project has received funding from the European Union's Horizon2020 Research and Innovation Programme under Grant Agreement No 641185. This work was supported by the Swiss State Secretariat for Education, Research and Innovation (SERI) under contract number 15.0160

9.3 Optional extent of capture

Table 9.7: Specifications of the streams of the CAP applied to the "Optional extent of capture" case defined in CEMCAP. Design at medium air leak, run at low air leak. First ½ of the year.

						Composition (mole frac.)												
#	F [kg/s]	T [°C]	P [bar]	N [kmol/s]	H [kJ/s]	H_2O	NH_3	CO_2	NH_4^+	H^+	OH^-	CO_3^{2-}	HCO_3^-	NH_2COO^-	Air	SO_2	$(NH_4)_2SO_4$	H_2SO_4
1	8.84E+01	130.0	1.10	2.90E+00	-3.19E+05	1.10E-01	0.00E+00	2.20E-01	0.00E+00	0.00E+00	0.00E+00	0.00E+00	0.00E+00	0.00E+00	6.70E-01	200 mg/Nm^3	0.00E+00	0.00E+00
2	1.86E+02	48.2	1.01	1.03E+01	-2.93E+06	1.00E+00	0.00E+00	7.94E-05	0.00E+00	8.36E-07	1.88E-11	1.27E-12	8.36E-07	0.00E+00	7.06E-06	0.00E+00	0.00E+00	0.00E+00
3	7.47E-01	34.3	1.01	4.15E-02	-1.18E+04	1.00E+00	0.00E+00	2.16E-05	0.00E+00	4.27E-07	1.51E-11	1.02E-12	4.27E-07	0.00E+00	1.10E-05	0.00E+00	0.00E+00	0.00E+00
4	1.81E+02	21.2	1.01	1.01E+01	-2.88E+06	1.00E+00	0.00E+00	7.94E-05	0.00E+00	7.74E-07	3.22E-12	8.01E-13	7.74E-07	0.00E+00	7.06E-06	0.00E+00	0.00E+00	0.00E+00
5(1)	3.46E-02	20.0	1.10	1.95E-03	-4.53E+02	7.39E-01	2.61E-01	0.00E+00	0.00E+00	0.00E+00	0.00E+00	0.00E+00	0.00E+00	0.00E+00	0.00E+00	0.00E+00	0.00E+00	0.00E+00
6(1)	5.95E-02	20.0	1.01	1.69E-03	-4.53E+02	8.50E-01	0.00E+00	0.00E+00	0.00E+00	0.00E+00	0.00E+00	0.00E+00	0.00E+00	0.00E+00	0.00E+00	0.00E+00	1.50E-01	0.00E+00
7	8.39E+01	22.2	1.01	2.66E+00	-2.69E+05	2.66E-02	0.00E+00	2.41E-01	0.00E+00	0.00E+00	0.00E+00	0.00E+00	0.00E+00	0.00E+00	7.33E-01	0.00E+00	0.00E+00	0.00E+00
8	8.39E+01	29.9	1.10	2.66E+00	-2.68E+05	2.66E-02	0.00E+00	2.41E-01	0.00E+00	0.00E+00	0.00E+00	0.00E+00	0.00E+00	0.00E+00	7.33E-01	0.00E+00	0.00E+00	0.00E+00
9	7.00E+02	24.5	1.05	3.54E+01	-1.03E+07	9.09E-01	3.44E-03	1.12E-04	4.55E-02	5.91E-11	1.39E-08	3.73E-03	1.98E-02	1.82E-02	1.09E-06	0.00E+00	0.00E+00	0.00E+00
10	8.40E+01	13.0	1.40	4.25E+00	-1.24E+06	9.09E-01	2.55E-03	1.87E-04	4.70E-02	3.10E-11	9.18E-09	5.27E-03	1.88E-02	1.77E-02	1.09E-06	0.00E+00	0.00E+00	0.00E+00
11	0.00E+00	na	na	0.00E+00	na	0.00E+00	0.00E+00	0.00E+00	0.00E+00	0.00E+00	0.00E+00	0.00E+00	0.00E+00	0.00E+00	0.00E+00	0.00E+00	0.00E+00	0.00E+00
12	0.00E+00	na	na	0.00E+00	na	0.00E+00	0.00E+00	0.00E+00	0.00E+00	0.00E+00	0.00E+00	0.00E+00	0.00E+00	0.00E+00	0.00E+00	0.00E+00	0.00E+00	0.00E+00
13	6.16E+02	25.1	20.40	3.11E+01	-9.08E+06	9.09E-01	3.49E-03	1.10E-04	4.54E-02	6.11E-11	1.42E-08	3.67E-03	1.98E-02	1.83E-02	1.09E-06	0.00E+00	0.00E+00	0.00E+00
14	5.95E+02	135.7	20.40	3.04E+01	-8.48E+06	9.00E-01	2.97E-02	1.23E-02	2.92E-02	3.00E-09	1.32E-07	1.65E-04	2.15E-02	7.40E-03	1.07E-06	0.00E+00	0.00E+00	0.00E+00
15	2.16E+01	25.1	20.40	1.09E+00	-3.18E+05	9.09E-01	3.49E-03	1.10E-04	4.54E-02	6.11E-11	1.42E-08	3.67E-03	1.98E-02	1.82E-02	1.09E-06	0.00E+00	0.00E+00	0.00E+00
16	5.92E+02	146.5	20.00	3.12E+01	-8.53E+06	9.14E-01	3.97E-02	2.41E-03	2.21E-02	3.05E-09	2.54E-07	1.21E-04	1.66E-02	5.27E-03	7.60E-10	0.00E+00	0.00E+00	0.00E+00
17	5.91E+02	29.5	20.00	3.11E+01	-8.80E+06	9.25E-01	2.26E-02	1.62E-06	2.78E-02	1.01E-11	2.14E-07	3.34E-03	4.36E-03	1.68E-02	7.62E-10	0.00E+00	0.00E+00	0.00E+00
18	5.91E+02	21.2	1.05	3.11E+01	-8.82E+06	9.25E-01	2.20E-02	1.18E-06	2.87E-02	5.36E-12	2.02E-07	4.25E-03	3.74E-03	1.65E-02	7.62E-10	0.00E+00	0.00E+00	0.00E+00
19(1)	1.36E-02	20.0	1.01	7.67E-04	-1.78E+02	7.39E-01	2.61E-01	0.00E+00	0.00E+00	0.00E+00	0.00E+00	0.00E+00	0.00E+00	0.00E+00	0.00E+00	0.00E+00	0.00E+00	0.00E+00
20	2.39E+01	50.1	19.50	5.46E-01	-2.14E+05	7.00E-03	8.65E-05	9.93E-01	0.00E+00	0.00E+00	0.00E+00	0.00E+00	0.00E+00	0.00E+00	6.18E-05	0.00E+00	0.00E+00	0.00E+00
21	8.43E+00	48.5	19.50	4.20E-01	-1.24E+05	9.07E-01	2.27E-04	8.25E-03	4.24E-02	4.99E-09	5.15E-10	1.16E-04	4.09E-02	1.26E-03	4.06E-09	0.00E+00	0.00E+00	0.00E+00

This project has received funding from the European Union's Horizon2020 Research and Innovation Programme under Grant Agreement No 641185. This work was supported by the Swiss State Secretariat for Education, Research and Innovation (SERI) under contract number 15.0160

22	1.67E-03	20.0	1.01	9.29E-05	-2.66E+01	1.00E+00	0.00E+00	0.00E+00	0.00E+00	1.50E-09	1.50E-09	0.00E+00	0.00E+00	0.00E+00	0.00E+00	0.00E+00	0.00E+00	0.00E+00
23	8.43E+00	45.0	19.50	4.21E-01	-1.24E+05	9.07E-01	2.02E-04	8.22E-03	4.24E-02	4.45E-09	4.56E-10	1.26E-04	4.09E-02	1.25E-03	4.06E-09	0.00E+00	0.00E+00	0.00E+00
24	2.39E+01	35.0	19.50	5.44E-01	-2.14E+05	3.53E-03	9.56E-07	9.96E-01	0.00E+00	0.00E+00	0.00E+00	0.00E+00	0.00E+00	0.00E+00	6.21E-05	0.00E+00	0.00E+00	0.00E+00
25	2.39E+01	28.2	110.00	5.42E-01	-2.19E+05	0.00E+00	0.00E+00	1.00E+00	0.00E+00	0.00E+00	0.00E+00	0.00E+00	0.00E+00	0.00E+00	0.00E+00	0.00E+00	0.00E+00	0.00E+00
26	2.53E-02	35.0	19.50	1.35E-03	-3.90E+02	9.67E-01	9.89E-06	1.00E-02	1.15E-02	1.45E-08	3.67E-10	3.88E-06	1.15E-02	1.86E-05	9.68E-09	0.00E+00	0.00E+00	0.00E+00
27	1.43E-02	48.5	19.50	7.11E-04	-2.10E+02	9.07E-01	2.27E-04	8.25E-03	4.24E-02	4.99E-09	5.16E-10	1.16E-04	4.09E-02	1.26E-03	4.06E-09	0.00E+00	0.00E+00	0.00E+00
28	1.11E+00	29.5	20.00	5.84E-02	-1.66E+04	9.25E-01	2.26E-02	1.62E-06	2.78E-02	1.01E-11	2.14E-07	3.34E-03	4.36E-03	1.68E-02	7.62E-10	0.00E+00	0.00E+00	0.00E+00
29	1.15E+00	73.4	19.50	6.05E-02	-1.70E+04	9.24E-01	2.56E-02	2.39E-05	2.58E-02	1.48E-10	2.17E-07	1.09E-03	9.28E-03	1.43E-02	1.00E-09	0.00E+00	0.00E+00	0.00E+00
30	4.29E-01	95.4	1.15	2.19E-02	-4.69E+03	7.50E-01	1.81E-01	6.83E-02	0.00E+00	0.00E+00	0.00E+00	0.00E+00	0.00E+00	0.00E+00	2.76E-09	0.00E+00	0.00E+00	0.00E+00
31	7.22E-01	105.0	1.25	4.01E-02	-1.12E+04	1.00E+00	1.60E-04	2.07E-08	8.01E-06	4.61E-11	5.08E-06	1.07E-07	2.70E-06	1.20E-08	1.00E-30	0.00E+00	0.00E+00	0.00E+00
32	7.22E-01	40.3	1.25	4.01E-02	-1.14E+04	1.00E+00	1.58E-04	3.13E-10	9.76E-06	1.74E-12	5.76E-06	1.17E-06	1.64E-06	3.72E-08	0.00E+00	0.00E+00	0.00E+00	0.00E+00
33	5.96E+01	14.4	1.01	2.08E+00	-4.84E+04	1.53E-02	2.31E-03	4.86E-02	0.00E+00	0.00E+00	0.00E+00	0.00E+00	0.00E+00	0.00E+00	9.34E-01	0.00E+00	0.00E+00	0.00E+00
34	5.95E+01	16.7	1.01	2.08E+00	-4.81E+04	1.89E-02	1.19E-04	4.64E-02	0.00E+00	0.00E+00	0.00E+00	0.00E+00	0.00E+00	0.00E+00	9.35E-01	0.00E+00	0.00E+00	0.00E+00
35	6.32E+01	47.3	1.01	2.29E+00	-9.62E+04	1.07E-01	0.00E+00	4.25E-02	0.00E+00	0.00E+00	0.00E+00	0.00E+00	0.00E+00	0.00E+00	8.50E-01	0.00E+00	0.00E+00	0.00E+00
36[(1)]	1.24E-02	20.0	1.10	1.38E-04	na	1.00E-01	0.00E+00	0.00E+00	0.00E+00	0.00E+00	0.00E+00	0.00E+00	0.00E+00	0.00E+00	0.00E+00	0.00E+00	0.00E+00	9.00E-01
37[(1)]	1.66E-02	20.0	1.01	1.38E-04	na	1.00E-01	0.00E+00	0.00E+00	0.00E+00	0.00E+00	0.00E+00	0.00E+00	0.00E+00	0.00E+00	0.00E+00	0.00E+00	9.00E-01	0.00E+00
38	1.21E+01	14.5	1.04	6.59E-01	-1.90E+05	9.86E-01	2.93E-04	6.07E-05	7.07E-03	1.01E-10	1.93E-08	2.14E-04	6.14E-03	5.05E-04	1.59E-05	0.00E+00	0.00E+00	0.00E+00
39	1.21E-04	1.5	1.20	6.59E-06	-1.91E+00	9.86E-01	2.12E-04	5.96E-05	7.16E-03	5.13E-11	1.13E-08	3.01E-04	6.06E-03	4.98E-04	1.59E-05	0.00E+00	0.00E+00	0.00E+00
40	1.21E+01	91.0	1.40	6.61E-01	-1.86E+05	9.86E-01	3.31E-03	2.87E-03	4.07E-03	5.75E-10	3.46E-07	4.76E-05	3.52E-03	4.59E-04	1.58E-05	0.00E+00	0.00E+00	0.00E+00
41	1.18E+01	98.8	1.01	6.52E-01	-1.83E+05	9.99E-01	9.27E-04	1.28E-07	4.00E-05	3.03E-11	5.92E-06	2.01E-06	2.91E-05	9.01E-07	4.28E-25	0.00E+00	0.00E+00	0.00E+00
42	1.19E+01	15.0	1.01	6.62E-01	-1.90E+05	9.99E-01	8.93E-04	3.22E-10	5.88E-05	3.21E-13	5.15E-06	2.20E-05	7.96E-06	1.77E-06	0.00E+00	0.00E+00	0.00E+00	0.00E+00
43	3.21E-01	68.0	1.01	1.15E-02	-2.57E+03	2.11E-01	3.95E-01	3.94E-01	0.00E+00	0.00E+00	0.00E+00	0.00E+00	0.00E+00	0.00E+00	9.09E-04	0.00E+00	0.00E+00	0.00E+00
44	1.80E-01	20.0	1.01	9.97E-03	-2.85E+03	1.00E+00	0.00E+00	0.00E+00	0.00E+00	1.49E-09	1.49E-09	0.00E+00	0.00E+00	0.00E+00	0.00E+00	0.00E+00	0.00E+00	0.00E+00
45	3.52E-02	32.2	19.50	1.96E-03	-5.58E+02	1.00E+00	0.00E+00	0.00E+00	0.00E+00	0.00E+00	0.00E+00	0.00E+00	0.00E+00	0.00E+00	0.00E+00	0.00E+00	0.00E+00	0.00E+00

(1) Apparent composition

This project has received funding from the European Union's Horizon2020 Research and Innovation Programme under Grant Agreement No 641185. This work was supported by the Swiss State Secretariat for Education, Research and Innovation (SERI) under contract number 15.0160

Table 9.8: Specifications of the streams of the CAP applied to the "Optional extent of capture" case defined in CEMCAP. Design at medium air leak, run at medium air leak. Second ½ of the year.

						Composition (mole frac.)													
#	F [kg/s]	T [°C]	P [bar]	N [kmol/s]	H [kJ/s]	H_2O	NH_3	CO_2	NH_4^+	H^+	OH^-	CO_3^{2-}	HCO_3^-	NH_2COO^-	Air	SO_2	$(NH_4)_2SO_4$	H_2SO_4
1	1.08E+02	110.0	1.10	3.59E+00	-3.23E+05	9.00E-02	0.00E+00	1.80E-01	0.00E+00	0.00E+00	0.00E+00	0.00E+00	0.00E+00	0.00E+00	7.30E-01	200 mg/Nm^3	0.00E+00	0.00E+00
2	2.24E+02	42.9	1.01	1.24E+01	-3.54E+06	1.00E+00	0.00E+00	7.24E-05	0.00E+00	7.97E-07	1.43E-11	1.18E-12	7.97E-07	0.00E+00	8.13E-06	0.00E+00	0.00E+00	0.00E+00
3	7.01E-01	31.5	1.01	3.89E-02	-1.11E+04	1.00E+00	0.00E+00	1.61E-05	0.00E+00	3.65E-07	1.46E-11	9.74E-13	3.65E-07	0.00E+00	1.16E-05	0.00E+00	0.00E+00	0.00E+00
4	2.20E+02	21.2	1.01	1.22E+01	-3.49E+06	1.00E+00	0.00E+00	7.25E-05	0.00E+00	7.39E-07	3.37E-12	8.00E-13	7.39E-07	0.00E+00	8.13E-06	0.00E+00	0.00E+00	0.00E+00
5[(1)]	4.07E-02	20.0	1.10	2.29E-03	-5.33E+02	7.39E-01	2.61E-01	0.00E+00	0.00E+00	0.00E+00	0.00E+00	0.00E+00	0.00E+00	0.00E+00	0.00E+00	0.00E+00	0.00E+00	0.00E+00
6[(1)]	7.00E-02	20.0	1.01	1.99E-03	-5.93E+02	8.50E-01	0.00E+00	0.00E+00	0.00E+00	0.00E+00	0.00E+00	0.00E+00	0.00E+00	0.00E+00	0.00E+00	0.00E+00	1.50E-01	0.00E+00
7	1.04E+02	21.8	1.01	3.36E+00	-2.76E+05	2.61E-02	0.00E+00	1.93E-01	0.00E+00	0.00E+00	0.00E+00	0.00E+00	0.00E+00	0.00E+00	7.81E-01	0.00E+00	0.00E+00	0.00E+00
8	1.04E+02	29.7	1.10	3.36E+00	-2.75E+05	2.61E-02	0.00E+00	1.93E-01	0.00E+00	0.00E+00	0.00E+00	0.00E+00	0.00E+00	0.00E+00	7.81E-01	0.00E+00	0.00E+00	0.00E+00
9	6.91E+02	24.1	1.05	3.44E+01	-1.00E+07	8.92E-01	4.41E-03	9.77E-05	5.40E-02	4.60E-11	1.18E-08	5.00E-03	1.99E-02	2.41E-02	6.44E-07	0.00E+00	0.00E+00	0.00E+00
10	1.45E+02	12.0	1.40	7.22E+00	-2.12E+06	8.91E-01	3.22E-03	1.87E-04	5.63E-02	2.21E-11	7.58E-09	7.36E-03	1.85E-02	2.31E-02	6.44E-07	0.00E+00	0.00E+00	0.00E+00
11	0.00E+00	na	na	0.00E+00	na	0.00E+00	0.00E+00	0.00E+00	0.00E+00	0.00E+00	0.00E+00	0.00E+00	0.00E+00	0.00E+00	0.00E+00	0.00E+00	0.00E+00	0.00E+00
12	0.00E+00	na	na	0.00E+00	na	0.00E+00	0.00E+00	0.00E+00	0.00E+00	0.00E+00	0.00E+00	0.00E+00	0.00E+00	0.00E+00	0.00E+00	0.00E+00	0.00E+00	0.00E+00
13	5.46E+02	24.7	20.40	2.71E+01	-7.93E+06	8.92E-01	4.47E-03	9.58E-05	5.40E-02	4.76E-11	1.20E-08	4.91E-03	2.00E-02	2.42E-02	6.44E-07	0.00E+00	0.00E+00	0.00E+00
14	5.24E+02	134.9	20.40	2.64E+01	-7.36E+06	8.80E-01	3.54E-02	1.30E-02	3.58E-02	2.90E-09	1.06E-07	2.24E-04	2.50E-02	1.04E-02	6.35E-07	0.00E+00	0.00E+00	0.00E+00
15	2.18E+01	24.7	20.40	1.09E+00	-3.17E+05	8.92E-01	4.47E-03	9.58E-05	5.40E-02	4.76E-11	1.21E-08	4.91E-03	2.00E-02	2.42E-02	6.44E-07	0.00E+00	0.00E+00	0.00E+00
16	5.21E+02	146.6	20.00	2.72E+01	-7.41E+06	8.96E-01	4.88E-02	2.23E-03	2.65E-02	3.00E-09	2.31E-07	1.66E-04	1.89E-02	7.21E-03	5.27E-10	0.00E+00	0.00E+00	0.00E+00
17	5.19E+02	28.7	20.00	2.71E+01	-7.64E+06	9.09E-01	2.97E-02	1.18E-06	3.26E-02	7.99E-12	1.76E-07	4.03E-03	4.21E-03	2.03E-02	5.28E-10	0.00E+00	0.00E+00	0.00E+00
18	5.19E+02	21.2	1.05	2.71E+01	-7.65E+06	9.09E-01	2.91E-02	9.03E-07	3.36E-02	4.42E-12	1.67E-07	5.02E-03	3.66E-03	1.99E-02	5.28E-10	0.00E+00	0.00E+00	0.00E+00
19[(1)]	3.23E-02	20.0	1.01	1.82E-03	-4.24E+02	7.39E-01	2.61E-01	0.00E+00	0.00E+00	0.00E+00	0.00E+00	0.00E+00	0.00E+00	0.00E+00	0.00E+00	0.00E+00	0.00E+00	0.00E+00
20	2.47E+01	64.6	19.50	5.66E-01	-2.21E+05	1.33E-02	5.26E-04	9.86E-01	0.00E+00	0.00E+00	0.00E+00	0.00E+00	0.00E+00	0.00E+00	3.08E-05	0.00E+00	0.00E+00	0.00E+00
21	8.53E+00	61.9	19.50	4.29E-01	-1.26E+05	9.14E-01	5.59E-04	5.17E-03	4.03E-02	4.43E-09	1.68E-09	1.47E-04	3.79E-02	2.08E-03	1.71E-09	0.00E+00	0.00E+00	0.00E+00
22	5.54E-02	20.0	1.01	3.07E-03	-8.79E+02	1.00E+00	0.00E+00	0.00E+00	0.00E+00	1.50E-09	1.50E-09	0.00E+00	0.00E+00	0.00E+00	0.00E+00	0.00E+00	0.00E+00	0.00E+00

This project has received funding from the European Union's Horizon2020 Research and Innovation Programme under Grant Agreement No 641185. This work was supported by the Swiss State Secretariat for Education, Research and Innovation (SERI) under contract number 15.0160

23	8.59E+00	50.0	19.50	4.32E-01	-1.27E+05	9.14E-01	3.70E-04	4.82E-03	4.03E-02	3.32E-09	1.08E-09	1.78E-04	3.81E-02	1.91E-03	1.70E-09	0.00E+00	0.00E+00	0.00E+00
24	2.46E+01	35.0	19.50	5.60E-01	-2.20E+05	3.52E-03	1.10E-06	9.96E-01	0.00E+00	0.00E+00	0.00E+00	0.00E+00	0.00E+00	0.00E+00	3.12E-05	0.00E+00	0.00E+00	0.00E+00
25	2.46E+01	28.2	110.00	5.58E-01	-2.26E+05	0.00E+00	0.00E+00	1.00E+00	0.00E+00	0.00E+00	0.00E+00	0.00E+00	0.00E+00	0.00E+00	0.00E+00	0.00E+00	0.00E+00	0.00E+00
26	5.53E-02	35.0	19.50	2.94E-03	-8.51E+02	9.64E-01	1.14E-05	1.02E-02	1.26E-02	1.35E-08	3.70E-10	4.78E-06	1.26E-02	2.38E-05	4.79E-09	0.00E+00	0.00E+00	0.00E+00
27	1.21E-01	61.9	19.50	6.06E-03	-1.78E+03	9.14E-01	5.59E-04	5.17E-03	4.03E-02	4.43E-09	1.68E-09	1.47E-04	3.79E-02	2.08E-03	1.71E-09	0.00E+00	0.00E+00	0.00E+00
28	1.51E+00	28.7	20.00	7.88E-02	-2.22E+04	9.09E-01	2.97E-02	1.18E-06	3.26E-02	7.99E-12	1.76E-07	4.03E-03	4.21E-03	2.03E-02	5.28E-10	0.00E+00	0.00E+00	0.00E+00
29	1.69E+00	77.4	19.50	8.78E-02	-2.46E+04	9.10E-01	2.96E-02	2.98E-05	3.07E-02	1.83E-10	1.68E-07	1.19E-03	1.10E-02	1.73E-02	7.53E-10	0.00E+00	0.00E+00	0.00E+00
30	6.69E-01	94.4	1.15	3.38E-02	-7.15E+03	7.22E-01	2.01E-01	7.68E-02	0.00E+00	0.00E+00	0.00E+00	0.00E+00	0.00E+00	0.00E+00	1.96E-09	0.00E+00	0.00E+00	0.00E+00
31	1.02E+00	105.0	1.25	5.66E-02	-1.58E+04	1.00E+00	1.67E-04	2.19E-08	7.93E-06	4.43E-11	4.78E-06	1.17E-07	2.90E-06	1.37E-08	4.46E-28	0.00E+00	0.00E+00	0.00E+00
32	1.02E+00	35.5	1.25	5.66E-02	-1.61E+04	1.00E+00	1.64E-04	2.28E-10	1.02E-05	1.28E-12	5.72E-06	1.42E-06	1.59E-06	4.18E-08	0.00E+00	0.00E+00	0.00E+00	0.00E+00
33	7.85E+01	12.6	1.01	2.76E+00	-4.79E+04	1.34E-02	2.77E-03	3.45E-02	0.00E+00	0.00E+00	0.00E+00	0.00E+00	0.00E+00	0.00E+00	9.49E-01	0.00E+00	0.00E+00	0.00E+00
34	7.83E+01	16.0	1.01	2.76E+00	-4.78E+04	1.81E-02	1.48E-04	3.21E-02	0.00E+00	0.00E+00	0.00E+00	0.00E+00	0.00E+00	0.00E+00	9.50E-01	0.00E+00	0.00E+00	0.00E+00
35	8.19E+01	42.4	1.01	2.96E+00	-9.33E+04	8.33E-02	0.00E+00	3.02E-02	0.00E+00	0.00E+00	0.00E+00	0.00E+00	0.00E+00	0.00E+00	8.87E-01	0.00E+00	0.00E+00	0.00E+00
36[(1)]	2.04E-02	20.0	1.10	2.27E-04	na	1.00E-01	0.00E+00	0.00E+00	0.00E+00	0.00E+00	0.00E+00	0.00E+00	0.00E+00	0.00E+00	0.00E+00	0.00E+00	0.00E+00	9.00E-01
37[(1)]	2.74E-02	20.0	1.01	2.27E-04	na	1.00E-01	0.00E+00	0.00E+00	0.00E+00	0.00E+00	0.00E+00	0.00E+00	0.00E+00	0.00E+00	0.00E+00	0.00E+00	9.00E-01	0.00E+00
38	1.59E+01	12.7	1.04	8.67E-01	-2.50E+05	9.84E-01	4.17E-04	4.92E-05	8.10E-03	6.96E-11	2.34E-08	3.43E-04	6.60E-03	8.14E-04	1.59E-05	0.00E+00	0.00E+00	0.00E+00
39	1.59E-04	1.5	1.20	8.67E-06	-2.51E+00	9.84E-01	3.14E-04	5.13E-05	8.21E-03	3.86E-11	1.46E-08	4.60E-04	6.49E-03	8.02E-04	1.59E-05	0.00E+00	0.00E+00	0.00E+00
40	1.59E+01	90.5	1.40	8.69E-01	-2.45E+05	9.84E-01	3.95E-03	3.11E-03	4.73E-03	5.44E-10	3.53E-07	6.13E-05	3.98E-03	6.26E-04	1.59E-05	0.00E+00	0.00E+00	0.00E+00
41	1.54E+01	98.8	1.01	8.56E-01	-2.40E+05	9.99E-01	9.28E-04	1.28E-07	4.00E-05	3.03E-11	5.92E-06	2.01E-06	2.92E-05	9.02E-07	3.93E-25	0.00E+00	0.00E+00	0.00E+00
42	1.57E+01	15.0	1.01	8.72E-01	-2.50E+05	9.99E-01	8.91E-04	3.21E-10	5.86E-05	3.21E-13	5.15E-06	2.19E-05	7.94E-06	1.76E-06	0.00E+00	0.00E+00	0.00E+00	0.00E+00
43	4.87E-01	68.0	1.01	1.77E-02	-3.85E+03	2.09E-01	4.10E-01	3.80E-01	0.00E+00	0.00E+00	0.00E+00	0.00E+00	0.00E+00	0.00E+00	7.79E-04	0.00E+00	0.00E+00	0.00E+00
44	2.97E-01	20.0	1.01	1.65E-02	-4.72E+03	1.00E+00	0.00E+00	0.00E+00	0.00E+00	1.49E-09	1.49E-09	0.00E+00	0.00E+00	0.00E+00	0.00E+00	0.00E+00	0.00E+00	0.00E+00
45	3.59E-02	32.2	19.50	1.99E-03	-5.69E+02	1.00E+00	0.00E+00	0.00E+00	0.00E+00	0.00E+00	0.00E+00	0.00E+00	0.00E+00	0.00E+00	0.00E+00	0.00E+00	0.00E+00	0.00E+00

(1) *Apparent composition*

This project has received funding from the European Union's Horizon2020 Research and Innovation Programme under Grant Agreement No 641185. This work was supported by the Swiss State Secretariat for Education, Research and Innovation (SERI) under contract number 15.0160

Table 9.9: Main energy consumers of the CAP applied to the "Optional extent of capture" case defined in CEMCAP. Design at medium air leak, run at low air leak. First ½ of the year.

Variable	Value
$\dot{Q}_{\mathrm{heat,tot}}$ [MW_{th}]	54.31
$\dot{Q}_{\mathrm{heat,Reb-1}}$ [MW_{th}]	50.13
$T_{\mathrm{Reb-1}}$ [°C]	147
$\dot{Q}_{\mathrm{heat,Reb-2}}$ [MW_{th}]	3.13
$T_{\mathrm{Reb-2}}$ [°C]	99
$\dot{Q}_{\mathrm{heat,Reb-3}}$ [MW_{th}]	1.06
$T_{\mathrm{Reb-3}}$ [°C]	105
$\dot{Q}_{\mathrm{cool,tot}}$ [MW_{th}]	72.80
$\dot{Q}_{\mathrm{cool,Cond-1}}$ [MW_{th}]	0
$T_{\mathrm{out,Cond-1}}$ [°C]	-
$\dot{Q}_{\mathrm{cool,Cond-2}}$ [MW_{th}]	2.39
$T_{\mathrm{out,Cond-2}}$ [°C]	68.0
$\dot{Q}_{\mathrm{cool,Cool-1}}$ [MW_{th}]	9.71
$T_{\mathrm{out,Cool-1}}$ [°C]	21.2
$\dot{Q}_{\mathrm{cool,Cool-2}}$ [MW_{th}]	1.11
$T_{\mathrm{out,Cool-2}}$ [°C]	21.2
$\dot{Q}_{\mathrm{cool,Cool-3}}$ [MW_{th}]	19.55
$T_{\mathrm{out,Cool-3}}$ [°C]	21.2
$\dot{Q}_{\mathrm{cool,Cool-4}}$ [MW_{th}]	0.12
$T_{\mathrm{out,Cool-4}}$ [°C]	45.0
$\dot{Q}_{\mathrm{cool,Cool-5}}$ [MW_{th}]	0.31
$T_{\mathrm{out,Cool-5}}$ [°C]	35.0
$\dot{Q}_{\mathrm{cool,Cool-6}}$ [MW_{th}]	7.86
$T_{\mathrm{out,Cool-6}}$ [°C]	28.2
$\dot{Q}_{\mathrm{cool,Cool-7}}$ [MW_{th}]	31.74
$T_{\mathrm{out,Cool-7}}$ [°C]	21.2
$\dot{Q}_{\mathrm{chill,tot}}$ [MW_{th}]	2.93
$\dot{Q}_{\mathrm{chill,Chill-1}}$ [MW_{th}]	2.80
$T_{\mathrm{out,Chill-1}}$ [°C]	13.0
$\dot{Q}_{\mathrm{chill,Chill-2}}$ [MW_{th}]	0
$T_{\mathrm{out,Chill-2}}$ [°C]	-
$\dot{Q}_{\mathrm{chill,Chill-3}}$ [MW_{th}]	0.13
$T_{\mathrm{out,Chill-3}}$ [°C]	15.0
$\dot{W}_{\mathrm{aux,tot}}$ [MW_{el}]	2.23

This project has received funding from the European Union's Horizon2020 Research and Innovation Programme under Grant Agreement No 641185. This work was supported by the Swiss State Secretariat for Education, Research and Innovation (SERI) under contract number 15.0160

$\dot{W}_{\mathrm{aux,Fan-1}}$ [MW$_{el}$]	0.67
$\dot{W}_{\mathrm{aux,Pump-1}}$ [MW$_{el}$]	1.56
$\dot{W}_{\mathrm{CO_2comp,Comp-1}}$ [MW$_{el}$]	2.34

This project has received funding from the European Union's Horizon2020 Research and Innovation Programme under Grant Agreement No 641185. This work was supported by the Swiss State Secretariat for Education, Research and Innovation (SERI) under contract number 15.0160

Table 9.10: Main energy consumers of the CAP applied to the "Optional extent of capture" case defined in CEMCAP. Design at medium air leak, run at medium air leak. Second ½ of the year.

Variable	Value
$\dot{Q}_{\mathrm{heat,tot}}$ [MW$_{\mathrm{th}}$]	58.29
$\dot{Q}_{\mathrm{heat,Reb-1}}$ [MW$_{\mathrm{th}}$]	52.31
$T_{\mathrm{Reb-1}}$ [°C]	147
$\dot{Q}_{\mathrm{heat,Reb-2}}$ [MW$_{\mathrm{th}}$]	4.38
$T_{\mathrm{Reb-2}}$ [°C]	99
$\dot{Q}_{\mathrm{heat,Reb-3}}$ [MW$_{\mathrm{th}}$]	1.60
$T_{\mathrm{Reb-3}}$ [°C]	105
$\dot{Q}_{\mathrm{cool,tot}}$ [MW$_{\mathrm{th}}$]	74.39
$\dot{Q}_{\mathrm{cool,Cond-1}}$ [MW$_{\mathrm{th}}$]	0
$T_{\mathrm{out,Cond-1}}$ [°C]	-
$\dot{Q}_{\mathrm{cool,Cond-2}}$ [MW$_{\mathrm{th}}$]	3.29
$T_{\mathrm{out,Cond-2}}$ [°C]	68.0
$\dot{Q}_{\mathrm{cool,Cool-1}}$ [MW$_{\mathrm{th}}$]	9.32
$T_{\mathrm{out,Cool-1}}$ [°C]	21.2
$\dot{Q}_{\mathrm{cool,Cool-2}}$ [MW$_{\mathrm{th}}$]	1.69
$T_{\mathrm{out,Cool-2}}$ [°C]	21.2
$\dot{Q}_{\mathrm{cool,Cool-3}}$ [MW$_{\mathrm{th}}$]	15.31
$T_{\mathrm{out,Cool-3}}$ [°C]	21.2
$\dot{Q}_{\mathrm{cool,Cool-4}}$ [MW$_{\mathrm{th}}$]	0.39
$T_{\mathrm{out,Cool-4}}$ [°C]	50.0
$\dot{Q}_{\mathrm{cool,Cool-5}}$ [MW$_{\mathrm{th}}$]	0.57
$T_{\mathrm{out,Cool-5}}$ [°C]	35.0
$\dot{Q}_{\mathrm{cool,Cool-6}}$ [MW$_{\mathrm{th}}$]	8.09
$T_{\mathrm{out,Cool-6}}$ [°C]	28.2
$\dot{Q}_{\mathrm{cool,Cool-7}}$ [MW$_{\mathrm{th}}$]	35.72
$T_{\mathrm{out,Cool-7}}$ [°C]	21.2
$\dot{Q}_{\mathrm{chill,tot}}$ [MW$_{\mathrm{th}}$]	5.55
$\dot{Q}_{\mathrm{chill,Chill-1}}$ [MW$_{\mathrm{th}}$]	5.50
$T_{\mathrm{out,Chill-1}}$ [°C]	12.0
$\dot{Q}_{\mathrm{chill,Chill-2}}$ [MW$_{\mathrm{th}}$]	0
$T_{\mathrm{out,Chill-2}}$ [°C]	-
$\dot{Q}_{\mathrm{chill,Chill-3}}$ [MW$_{\mathrm{th}}$]	0.05
$T_{\mathrm{out,Chill-3}}$ [°C]	15.0
$\dot{W}_{\mathrm{aux,tot}}$ [MW$_{\mathrm{el}}$]	2.25

This project has received funding from the European Union's Horizon2020 Research and Innovation Programme under Grant Agreement No 641185. This work was supported by the Swiss State Secretariat for Education, Research and Innovation (SERI) under contract number 15.0160

$\dot{W}_{\mathrm{aux,Fan-1}}$ [MW$_{el}$]	0.85
$\dot{W}_{\mathrm{aux,Pump-1}}$ [MW$_{el}$]	1.39
$\dot{W}_{\mathrm{CO_2comp,Comp-1}}$ [MW$_{el}$]	2.41

This project has received funding from the European Union's Horizon2020 Research and Innovation Programme under Grant Agreement No 641185. This work was supported by the Swiss State Secretariat for Education, Research and Innovation (SERI) under contract number 15.0160

9.4 Steam import

Table 9.11: Specifications of the streams of the CAP applied to the "Steam import" case defined in CEMCAP. Design at medium air leak, run at low air leak. First ½ of the year.

						Composition (mole frac.)												
#	F [kg/s]	T [°C]	P [bar]	N [kmol/s]	H [kJ/s]	H_2O	NH_3	CO_2	NH_4^+	H^+	OH^-	CO_3^{2-}	HCO_3^-	NH_2COO^-	Air	SO_2	$(NH_4)_2SO_4$	H_2SO_4
1	8.84E+01	130.0	1.10	2.90E+00	-3.19E+05	1.10E-01	0.00E+00	2.20E-01	0.00E+00	0.00E+00	0.00E+00	0.00E+00	0.00E+00	0.00E+00	6.70E-01	200 mg/Nm^3	0.00E+00	0.00E+00
2	1.86E+02	48.2	1.01	1.03E+01	-2.93E+06	1.00E+00	0.00E+00	7.94E-05	0.00E+00	8.36E-07	1.88E-11	1.27E-12	8.36E-07	0.00E+00	7.06E-06	0.00E+00	0.00E+00	0.00E+00
3	7.55E-01	34.3	1.01	4.19E-02	-1.19E+04	1.00E+00	0.00E+00	1.44E-05	0.00E+00	3.49E-07	1.85E-11	1.02E-12	3.49E-07	0.00E+00	1.12E-05	0.00E+00	0.00E+00	0.00E+00
4	1.81E+02	21.2	1.01	1.01E+01	-2.88E+06	1.00E+00	0.00E+00	7.94E-05	0.00E+00	7.74E-07	3.22E-12	8.01E-13	7.74E-07	0.00E+00	7.06E-06	0.00E+00	0.00E+00	0.00E+00
5(1)	3.46E-02	20.0	1.10	1.95E-03	-4.54E+02	7.39E-01	2.61E-01	0.00E+00	0.00E+00	0.00E+00	0.00E+00	0.00E+00	0.00E+00	0.00E+00	0.00E+00	0.00E+00	0.00E+00	0.00E+00
6(1)	5.95E-02	20.0	1.01	1.70E-03	-4.54E+02	8.50E-01	0.00E+00	0.00E+00	0.00E+00	0.00E+00	0.00E+00	0.00E+00	0.00E+00	0.00E+00	0.00E+00	0.00E+00	1.50E-01	0.00E+00
7	8.39E+01	22.2	1.01	2.66E+00	-2.69E+05	2.66E-02	0.00E+00	2.41E-01	0.00E+00	0.00E+00	0.00E+00	0.00E+00	0.00E+00	0.00E+00	7.33E-01	0.00E+00	0.00E+00	0.00E+00
8	8.39E+01	29.9	1.10	2.66E+00	-2.68E+05	2.66E-02	0.00E+00	2.41E-01	0.00E+00	0.00E+00	0.00E+00	0.00E+00	0.00E+00	0.00E+00	7.33E-01	0.00E+00	0.00E+00	0.00E+00
9	8.89E+02	24.8	1.05	4.42E+01	-1.29E+07	8.93E-01	4.52E-03	9.40E-05	5.39E-02	4.74E-11	1.22E-08	4.90E-03	1.99E-02	2.42E-02	5.59E-07	0.00E+00	0.00E+00	0.00E+00
10	1.07E+02	12.0	1.40	5.31E+00	-1.56E+06	8.91E-01	3.24E-03	1.83E-04	5.63E-02	2.19E-11	7.68E-09	7.38E-03	1.84E-02	2.31E-02	5.59E-07	0.00E+00	0.00E+00	0.00E+00
11	0.00E+00	na	na	0.00E+00	na	0.00E+00	0.00E+00	0.00E+00	0.00E+00	0.00E+00	0.00E+00	0.00E+00	0.00E+00	0.00E+00	0.00E+00	0.00E+00	0.00E+00	0.00E+00
12	0.00E+00	na	na	0.00E+00	na	0.00E+00	0.00E+00	0.00E+00	0.00E+00	0.00E+00	0.00E+00	0.00E+00	0.00E+00	0.00E+00	0.00E+00	0.00E+00	0.00E+00	0.00E+00
13	7.82E+02	25.1	10.40	3.89E+01	-1.14E+07	8.93E-01	4.55E-03	9.32E-05	5.38E-02	4.82E-11	1.23E-08	4.86E-03	1.99E-02	2.42E-02	5.59E-07	0.00E+00	0.00E+00	0.00E+00
14	7.53E+02	115.7	10.40	3.77E+01	-1.07E+07	8.84E-01	2.64E-02	7.77E-03	4.13E-02	1.70E-09	6.73E-08	4.14E-04	2.63E-02	1.43E-02	5.55E-07	0.00E+00	0.00E+00	0.00E+00
15	2.93E+01	25.1	10.40	1.46E+00	-4.26E+05	8.93E-01	4.55E-03	9.32E-05	5.38E-02	4.82E-11	1.24E-08	4.86E-03	1.99E-02	2.42E-02	5.59E-07	0.00E+00	0.00E+00	0.00E+00
16	7.56E+02	124.5	10.00	3.89E+01	-1.08E+07	8.95E-01	3.69E-02	8.76E-04	3.37E-02	1.66E-09	1.27E-07	3.51E-04	2.11E-02	1.19E-02	1.38E-13	0.00E+00	0.00E+00	0.00E+00
17	7.55E+02	29.9	10.00	3.88E+01	-1.11E+07	9.07E-01	2.04E-02	3.23E-06	3.88E-02	1.29E-11	1.19E-07	4.55E-03	6.31E-03	2.34E-02	1.38E-13	0.00E+00	0.00E+00	0.00E+00
18	7.55E+02	21.2	1.05	3.88E+01	-1.11E+07	9.06E-01	1.94E-02	2.60E-06	4.03E-02	6.61E-12	1.10E-07	5.98E-03	5.36E-03	2.30E-02	1.38E-13	0.00E+00	0.00E+00	0.00E+00
19(1)	1.05E-02	20.0	1.01	5.90E-04	-1.37E+02	7.39E-01	2.61E-01	0.00E+00	0.00E+00	0.00E+00	0.00E+00	0.00E+00	0.00E+00	0.00E+00	0.00E+00	0.00E+00	0.00E+00	0.00E+00
20	2.55E+01	53.5	9.50	5.85E-01	-2.28E+05	1.50E-02	5.58E-04	9.84E-01	0.00E+00	0.00E+00	0.00E+00	0.00E+00	0.00E+00	0.00E+00	3.72E-05	0.00E+00	0.00E+00	0.00E+00
21	8.68E+00	53.0	9.50	4.40E-01	-1.29E+05	9.19E-01	5.28E-04	3.39E-03	3.84E-02	2.71E-09	1.91E-09	2.14E-04	3.56E-02	2.38E-03	1.31E-09	0.00E+00	0.00E+00	0.00E+00

This project has received funding from the European Union's Horizon2020 Research and Innovation Programme under Grant Agreement No 641185. This work was supported by the Swiss State Secretariat for Education, Research and Innovation (SERI) under contract number 15.0160

22	8.57E-02	20.0	1.01	4.76E-03	-1.36E+03	1.00E+00	0.00E+00	0.00E+00	0.00E+00	1.50E-09	1.50E-09	0.00E+00	0.00E+00	0.00E+00	0.00E+00	0.00E+00	0.00E+00	0.00E+00
23	8.77E+00	50.0	9.50	4.44E-01	-1.30E+05	9.20E-01	4.79E-04	3.29E-03	3.81E-02	2.48E-09	1.76E-09	2.24E-04	3.53E-02	2.32E-03	1.29E-09	0.00E+00	0.00E+00	0.00E+00
24	2.54E+01	35.0	9.50	5.79E-01	-2.27E+05	6.36E-03	8.52E-06	9.94E-01	0.00E+00	0.00E+00	0.00E+00	0.00E+00	0.00E+00	0.00E+00	3.76E-05	0.00E+00	0.00E+00	0.00E+00
25	2.53E+01	28.2	110.00	5.76E-01	-2.33E+05	0.00E+00	0.00E+00	1.00E+00	0.00E+00	0.00E+00	0.00E+00	0.00E+00	0.00E+00	0.00E+00	0.00E+00	0.00E+00	0.00E+00	0.00E+00
26	8.97E-02	35.0	9.50	4.72E-03	-1.37E+03	9.55E-01	4.70E-05	5.99E-03	1.96E-02	5.38E-09	7.63E-10	2.82E-05	1.93E-02	1.65E-04	3.03E-09	0.00E+00	0.00E+00	0.00E+00
27	1.09E-01	53.0	9.50	5.52E-03	-1.62E+03	9.19E-01	5.28E-04	3.39E-03	3.84E-02	2.71E-09	1.91E-09	2.14E-04	3.56E-02	2.38E-03	1.31E-09	0.00E+00	0.00E+00	0.00E+00
28	1.23E+00	29.9	10.00	6.34E-02	-1.81E+04	9.07E-01	2.04E-02	3.23E-06	3.88E-02	1.29E-11	1.19E-07	4.55E-03	6.31E-03	2.34E-02	1.38E-13	0.00E+00	0.00E+00	0.00E+00
29	1.43E+00	73.1	9.50	7.36E-02	-2.08E+04	9.09E-01	2.11E-02	4.52E-05	3.56E-02	2.10E-10	1.13E-07	1.32E-03	1.41E-02	1.88E-02	2.92E-10	0.00E+00	0.00E+00	0.00E+00
30	5.68E-01	94.1	1.15	2.82E-02	-6.04E+03	7.13E-01	1.97E-01	8.96E-02	0.00E+00	0.00E+00	0.00E+00	0.00E+00	0.00E+00	0.00E+00	7.64E-10	0.00E+00	0.00E+00	0.00E+00
31	8.63E-01	105.0	1.25	4.79E-02	-1.34E+04	1.00E+00	1.66E-04	2.28E-08	8.32E-06	4.60E-11	5.09E-06	1.19E-07	2.97E-06	1.38E-08	8.76E-28	0.00E+00	0.00E+00	0.00E+00
32	8.63E-01	43.0	1.25	4.79E-02	-1.36E+04	1.00E+00	1.65E-04	4.25E-10	1.01E-05	2.05E-12	5.79E-06	1.19E-06	1.90E-06	4.21E-08	0.00E+00	0.00E+00	0.00E+00	0.00E+00
33	5.81E+01	12.4	1.01	2.05E+00	-3.45E+04	1.32E-02	2.70E-03	3.34E-02	0.00E+00	0.00E+00	0.00E+00	0.00E+00	0.00E+00	0.00E+00	9.51E-01	0.00E+00	0.00E+00	0.00E+00
34	5.80E+01	15.8	1.01	2.05E+00	-3.44E+04	1.78E-02	1.44E-04	3.11E-02	0.00E+00	0.00E+00	0.00E+00	0.00E+00	0.00E+00	0.00E+00	9.51E-01	0.00E+00	0.00E+00	0.00E+00
35	6.17E+01	47.3	1.01	2.25E+00	-8.25E+04	1.08E-01	0.00E+00	2.85E-02	0.00E+00	0.00E+00	0.00E+00	0.00E+00	0.00E+00	0.00E+00	8.64E-01	0.00E+00	0.00E+00	0.00E+00
36[(1)]	1.47E-02	20.0	1.10	1.63E-04	na	1.00E-01	0.00E+00	0.00E+00	0.00E+00	0.00E+00	0.00E+00	0.00E+00	0.00E+00	0.00E+00	0.00E+00	0.00E+00	0.00E+00	9.00E-01
37[(1)]	1.97E-02	20.0	1.01	1.63E-04	na	1.00E-01	0.00E+00	0.00E+00	0.00E+00	0.00E+00	0.00E+00	0.00E+00	0.00E+00	0.00E+00	0.00E+00	0.00E+00	9.00E-01	0.00E+00
38	1.18E+01	12.5	1.04	6.41E-01	-1.85E+05	9.84E-01	4.08E-04	4.77E-05	7.92E-03	6.85E-11	2.34E-08	3.35E-04	6.46E-03	7.82E-04	1.61E-05	0.00E+00	0.00E+00	0.00E+00
39	1.18E-04	1.5	1.20	6.41E-06	-1.85E+00	9.84E-01	3.09E-04	4.94E-05	8.03E-03	3.84E-11	1.48E-08	4.47E-04	6.36E-03	7.71E-04	1.61E-05	0.00E+00	0.00E+00	0.00E+00
40	1.18E+01	90.6	1.40	6.43E-01	-1.81E+05	9.84E-01	3.86E-03	3.04E-03	4.62E-03	5.47E-10	3.53E-07	5.91E-05	3.90E-03	5.99E-04	1.60E-05	0.00E+00	0.00E+00	0.00E+00
41	1.14E+01	98.8	1.01	6.33E-01	-1.77E+05	9.99E-01	9.28E-04	1.28E-07	4.00E-05	3.03E-11	5.92E-06	2.01E-06	2.91E-05	9.01E-07	3.74E-25	0.00E+00	0.00E+00	0.00E+00
42	1.16E+01	15.0	1.01	6.45E-01	-1.85E+05	9.99E-01	8.91E-04	3.21E-10	5.86E-05	3.21E-13	5.15E-06	2.19E-05	7.93E-06	1.76E-06	0.00E+00	0.00E+00	0.00E+00	0.00E+00
43	3.52E-01	68.0	1.01	1.28E-02	-2.78E+03	2.09E-01	4.09E-01	3.81E-01	0.00E+00	0.00E+00	0.00E+00	0.00E+00	0.00E+00	0.00E+00	8.08E-04	0.00E+00	0.00E+00	0.00E+00
44	2.18E-01	20.0	1.01	1.21E-02	-3.46E+03	1.00E+00	0.00E+00	0.00E+00	0.00E+00	1.49E-09	1.49E-09	0.00E+00	0.00E+00	0.00E+00	0.00E+00	0.00E+00	0.00E+00	0.00E+00
45	6.69E-02	31.2	9.50	3.71E-03	-1.06E+03	1.00E+00	0.00E+00	0.00E+00	0.00E+00	0.00E+00	0.00E+00	0.00E+00	0.00E+00	0.00E+00	0.00E+00	0.00E+00	0.00E+00	0.00E+00

(1) *Apparent composition*

This project has received funding from the European Union's Horizon2020 Research and Innovation Programme under Grant Agreement No 641185. This work was supported by the Swiss State Secretariat for Education, Research and Innovation (SERI) under contract number 15.0160

Table 9.12: Specifications of the streams of the CAP applied to the "Steam import" case defined in CEMCAP. Design at medium air leak, run at medium air leak. Second ½ of the year.

						Composition (mole frac.)													
#	F [kg/s]	T [°C]	P [bar]	N [kmol/s]	H [kJ/s]	H_2O	NH_3	CO_2	NH_4^+	H^+	OH^-	CO_3^{2-}	HCO_3^-	NH_2COO^-	Air	SO_2	$(NH_4)_2SO_4$	H_2SO_4
1	1.08E+02	110.0	1.10	3.59E+00	-3.23E+05	9.00E-02	0.00E+00	1.80E-01	0.00E+00	0.00E+00	0.00E+00	0.00E+00	0.00E+00	0.00E+00	7.30E-01	200 mg/Nm^3	0.00E+00	0.00E+00
2	2.24E+02	42.9	1.01	1.24E+01	-3.54E+06	1.00E+00	0.00E+00	7.24E-05	0.00E+00	7.97E-07	1.43E-11	1.18E-12	7.97E-07	0.00E+00	8.13E-06	0.00E+00	0.00E+00	0.00E+00
3	6.28E-01	31.2	1.01	3.49E-02	-9.95E+03	1.00E+00	0.00E+00	1.19E-05	0.00E+00	3.14E-07	1.66E-11	9.66E-13	3.14E-07	0.00E+00	1.18E-05	0.00E+00	0.00E+00	0.00E+00
4	2.20E+02	21.2	1.01	1.22E+01	-3.49E+06	1.00E+00	0.00E+00	7.25E-05	0.00E+00	7.39E-07	3.37E-12	8.00E-13	7.39E-07	0.00E+00	8.13E-06	0.00E+00	0.00E+00	0.00E+00
5[(1)]	4.07E-02	20.0	1.10	2.29E-03	-5.33E+02	7.39E-01	2.61E-01	0.00E+00	0.00E+00	0.00E+00	0.00E+00	0.00E+00	0.00E+00	0.00E+00	0.00E+00	0.00E+00	0.00E+00	0.00E+00
6[(1)]	7.00E-02	20.0	1.01	1.99E-03	-5.93E+02	8.50E-01	0.00E+00	0.00E+00	0.00E+00	0.00E+00	0.00E+00	0.00E+00	0.00E+00	0.00E+00	0.00E+00	0.00E+00	1.50E-01	0.00E+00
7	1.04E+02	21.8	1.01	3.36E+00	-2.76E+05	2.61E-02	0.00E+00	1.93E-01	0.00E+00	0.00E+00	0.00E+00	0.00E+00	0.00E+00	0.00E+00	7.81E-01	0.00E+00	0.00E+00	0.00E+00
8	1.04E+02	29.7	1.10	3.36E+00	-2.75E+05	2.61E-02	0.00E+00	1.93E-01	0.00E+00	0.00E+00	0.00E+00	0.00E+00	0.00E+00	0.00E+00	7.81E-01	0.00E+00	0.00E+00	0.00E+00
9	8.61E+02	26.0	1.05	4.24E+01	-1.24E+07	8.78E-01	6.54E-03	5.73E-05	6.05E-02	3.55E-11	1.37E-08	6.05E-03	1.80E-02	3.05E-02	3.31E-07	0.00E+00	0.00E+00	0.00E+00
10	1.55E+02	9.0	1.40	7.63E+00	-2.24E+06	8.76E-01	4.29E-03	1.52E-04	6.52E-02	1.14E-11	7.43E-09	1.09E-02	1.55E-02	2.80E-02	3.31E-07	0.00E+00	0.00E+00	0.00E+00
11	0.00E+00	na	na	0.00E+00	na	0.00E+00	0.00E+00	0.00E+00	0.00E+00	0.00E+00	0.00E+00	0.00E+00	0.00E+00	0.00E+00	0.00E+00	0.00E+00	0.00E+00	0.00E+00
12	0.00E+00	na	na	0.00E+00	na	0.00E+00	0.00E+00	0.00E+00	0.00E+00	0.00E+00	0.00E+00	0.00E+00	0.00E+00	0.00E+00	0.00E+00	0.00E+00	0.00E+00	0.00E+00
13	7.06E+02	26.3	10.40	3.48E+01	-1.01E+07	8.78E-01	6.58E-03	5.68E-05	6.05E-02	3.61E-11	1.38E-08	5.99E-03	1.80E-02	3.05E-02	3.31E-07	0.00E+00	0.00E+00	0.00E+00
14	6.71E+02	117.0	10.40	3.33E+01	-9.37E+06	8.67E-01	3.24E-02	7.79E-03	4.68E-02	1.65E-09	5.73E-08	4.87E-04	2.83E-02	1.76E-02	3.29E-07	0.00E+00	0.00E+00	0.00E+00
15	3.53E+01	26.3	10.40	1.74E+00	-5.07E+05	8.78E-01	6.58E-03	5.68E-05	6.05E-02	3.61E-11	1.38E-08	5.99E-03	1.80E-02	3.05E-02	3.31E-07	0.00E+00	0.00E+00	0.00E+00
16	6.80E+02	126.1	10.00	3.48E+01	-9.59E+06	8.79E-01	4.58E-02	7.66E-04	3.74E-02	1.62E-09	1.16E-07	4.17E-04	2.23E-02	1.43E-02	1.50E-13	0.00E+00	0.00E+00	0.00E+00
17	6.78E+02	31.4	10.00	3.46E+01	-9.82E+06	8.92E-01	2.79E-02	2.18E-06	4.27E-02	1.13E-11	1.08E-07	4.94E-03	5.85E-03	2.70E-02	1.50E-13	0.00E+00	0.00E+00	0.00E+00
18	6.79E+02	21.2	1.05	3.46E+01	-9.84E+06	8.91E-01	2.68E-02	1.67E-06	4.45E-02	5.03E-12	1.00E-07	6.75E-03	4.80E-03	2.62E-02	1.50E-13	0.00E+00	0.00E+00	0.00E+00
19[(1)]	3.09E-02	20.0	1.01	1.74E-03	-4.05E+02	7.39E-01	2.61E-01	0.00E+00	0.00E+00	0.00E+00	0.00E+00	0.00E+00	0.00E+00	0.00E+00	0.00E+00	0.00E+00	0.00E+00	0.00E+00
20	2.58E+01	52.0	9.50	5.91E-01	-2.31E+05	1.36E-02	5.89E-04	9.86E-01	0.00E+00	0.00E+00	0.00E+00	0.00E+00	0.00E+00	0.00E+00	1.95E-05	0.00E+00	0.00E+00	0.00E+00
21	8.76E+00	51.6	9.50	4.43E-01	-1.30E+05	9.19E-01	4.76E-04	3.58E-03	3.84E-02	2.76E-09	1.70E-09	2.07E-04	3.58E-02	2.23E-03	7.06E-10	0.00E+00	0.00E+00	0.00E+00
22	1.09E-01	20.0	1.01	6.03E-03	-1.73E+03	1.00E+00	0.00E+00	0.00E+00	0.00E+00	1.50E-09	1.50E-09	0.00E+00	0.00E+00	0.00E+00	0.00E+00	0.00E+00	0.00E+00	0.00E+00

This project has received funding from the European Union's Horizon2020 Research and Innovation Programme under Grant Agreement No 641185. This work was supported by the Swiss State Secretariat for Education, Research and Innovation (SERI) under contract number 15.0160

23	8.87E+00	50.0	9.50	4.49E-01	-1.32E+05	9.20E-01	4.51E-04	3.50E-03	3.80E-02	2.63E-09	1.66E-09	2.10E-04	3.54E-02	2.18E-03	6.96E-10	0.00E+00	0.00E+00	0.00E+00
24	2.57E+01	35.0	9.50	5.86E-01	-2.30E+05	6.37E-03	8.24E-06	9.94E-01	0.00E+00	0.00E+00	0.00E+00	0.00E+00	0.00E+00	0.00E+00	1.96E-05	0.00E+00	0.00E+00	0.00E+00
25	2.56E+01	28.2	110.00	5.82E-01	-2.35E+05	0.00E+00	0.00E+00	1.00E+00	0.00E+00	0.00E+00	0.00E+00	0.00E+00	0.00E+00	0.00E+00	0.00E+00	0.00E+00	0.00E+00	0.00E+00
26	8.64E-02	35.0	9.50	4.55E-03	-1.32E+03	9.56E-01	4.55E-05	5.95E-03	1.91E-02	5.46E-09	7.70E-10	2.69E-05	1.89E-02	1.56E-04	1.60E-09	0.00E+00	0.00E+00	0.00E+00
27	1.22E-01	51.6	9.50	6.20E-03	-1.82E+03	9.19E-01	4.76E-04	3.58E-03	3.84E-02	2.76E-09	1.70E-09	2.07E-04	3.58E-02	2.23E-03	7.06E-10	0.00E+00	0.00E+00	0.00E+00
28	1.86E+00	31.4	10.00	9.48E-02	-2.69E+04	8.92E-01	2.79E-02	2.18E-06	4.27E-02	1.13E-11	1.08E-07	4.94E-03	5.85E-03	2.70E-02	1.50E-13	0.00E+00	0.00E+00	0.00E+00
29	2.07E+00	76.5	9.50	1.06E-01	-2.97E+04	8.94E-01	2.97E-02	3.40E-05	3.89E-02	1.99E-10	1.08E-07	1.47E-03	1.37E-02	2.23E-02	1.10E-10	0.00E+00	0.00E+00	0.00E+00
30	8.68E-01	93.2	1.15	4.30E-02	-9.03E+03	6.85E-01	2.23E-01	9.20E-02	0.00E+00	0.00E+00	0.00E+00	0.00E+00	0.00E+00	0.00E+00	2.71E-10	0.00E+00	0.00E+00	0.00E+00
31	1.20E+00	105.0	1.25	6.65E-02	-1.86E+04	1.00E+00	1.74E-04	2.38E-08	8.24E-06	4.42E-11	4.80E-06	1.29E-07	3.17E-06	1.56E-08	1.00E-30	0.00E+00	0.00E+00	0.00E+00
32	1.20E+00	36.7	1.25	6.65E-02	-1.89E+04	1.00E+00	1.71E-04	2.73E-10	1.06E-05	1.38E-12	5.74E-06	1.51E-06	1.78E-06	4.75E-08	0.00E+00	0.00E+00	0.00E+00	0.00E+00
33	7.74E+01	9.3	1.01	2.73E+00	-3.73E+04	1.07E-02	3.46E-03	2.65E-02	0.00E+00	0.00E+00	0.00E+00	0.00E+00	0.00E+00	0.00E+00	9.59E-01	0.00E+00	0.00E+00	0.00E+00
34	7.71E+01	14.1	1.01	2.73E+00	-3.69E+04	1.60E-02	1.82E-04	2.36E-02	0.00E+00	0.00E+00	0.00E+00	0.00E+00	0.00E+00	0.00E+00	9.60E-01	0.00E+00	0.00E+00	0.00E+00
35	8.08E+01	42.4	1.01	2.93E+00	-8.33E+04	8.33E-02	0.00E+00	2.23E-02	0.00E+00	0.00E+00	0.00E+00	0.00E+00	0.00E+00	0.00E+00	8.94E-01	0.00E+00	0.00E+00	0.00E+00
36[(1)]	2.49E-02	20.0	1.10	2.77E-04	na	1.00E-01	0.00E+00	0.00E+00	0.00E+00	0.00E+00	0.00E+00	0.00E+00	0.00E+00	0.00E+00	0.00E+00	0.00E+00	0.00E+00	9.00E-01
37[(1)]	3.34E-02	20.0	1.01	2.77E-04	na	1.00E-01	0.00E+00	0.00E+00	0.00E+00	0.00E+00	0.00E+00	0.00E+00	0.00E+00	0.00E+00	0.00E+00	0.00E+00	9.00E-01	0.00E+00
38	1.57E+01	9.6	1.04	8.54E-01	-2.47E+05	9.81E-01	5.21E-04	4.89E-05	9.67E-03	5.07E-11	2.31E-08	5.34E-04	7.36E-03	1.24E-03	1.60E-05	0.00E+00	0.00E+00	0.00E+00
39	1.57E-04	1.5	1.20	8.54E-06	-2.47E+00	9.81E-01	4.21E-04	5.43E-05	9.79E-03	3.30E-11	1.62E-08	6.59E-04	7.25E-03	1.23E-03	1.60E-05	0.00E+00	0.00E+00	0.00E+00
40	1.57E+01	89.6	1.40	8.57E-01	-2.41E+05	9.80E-01	4.79E-03	3.54E-03	5.70E-03	5.14E-10	3.51E-07	8.27E-05	4.63E-03	9.04E-04	1.59E-05	0.00E+00	0.00E+00	0.00E+00
41	1.51E+01	98.8	1.01	8.41E-01	-2.35E+05	9.99E-01	9.26E-04	1.29E-07	3.99E-05	3.03E-11	5.91E-06	2.00E-06	2.91E-05	8.99E-07	2.96E-25	0.00E+00	0.00E+00	0.00E+00
42	1.55E+01	12.8	1.01	8.60E-01	-2.46E+05	9.99E-01	8.85E-04	2.63E-10	5.89E-05	2.75E-13	5.00E-06	2.24E-05	7.33E-06	1.69E-06	0.00E+00	0.00E+00	0.00E+00	0.00E+00
43	5.77E-01	68.0	1.01	2.12E-02	-4.52E+03	2.08E-01	4.22E-01	3.69E-01	0.00E+00	0.00E+00	0.00E+00	0.00E+00	0.00E+00	0.00E+00	6.43E-04	0.00E+00	0.00E+00	0.00E+00
44	3.43E-01	20.0	1.01	1.91E-02	-5.45E+03	1.00E+00	0.00E+00	0.00E+00	0.00E+00	1.49E-09	1.49E-09	0.00E+00	0.00E+00	0.00E+00	0.00E+00	0.00E+00	0.00E+00	0.00E+00
45	6.75E-02	31.1	9.50	3.75E-03	-1.07E+03	1.00E+00	0.00E+00	0.00E+00	0.00E+00	0.00E+00	0.00E+00	0.00E+00	0.00E+00	0.00E+00	0.00E+00	0.00E+00	0.00E+00	0.00E+00

(1) *Apparent composition*

This project has received funding from the European Union's Horizon2020 Research and Innovation Programme under Grant Agreement No 641185. This work was supported by the Swiss State Secretariat for Education, Research and Innovation (SERI) under contract number 15.0160

Table 9.13: Main energy consumers of the CAP applied to the "Steam import" case defined in CEMCAP. Design at medium air leak, run at low air leak. First ½ of the year.

Variable	Value
$\dot{Q}_{\mathrm{heat,tot}}$ [MW_{th}]	61.88
$\dot{Q}_{\mathrm{heat,Reb-1}}$ [MW_{th}]	57.30
$T_{\mathrm{Reb-1}}$ [°C]	124
$\dot{Q}_{\mathrm{heat,Reb-2}}$ [MW_{th}]	3.21
$T_{\mathrm{Reb-2}}$ [°C]	99
$\dot{Q}_{\mathrm{heat,Reb-3}}$ [MW_{th}]	1.37
$T_{\mathrm{Reb-3}}$ [°C]	105
$\dot{Q}_{\mathrm{cool,tot}}$ [MW_{th}]	80.67
$\dot{Q}_{\mathrm{cool,Cond-1}}$ [MW_{th}]	0
$T_{\mathrm{out,Cond-1}}$ [°C]	-
$\dot{Q}_{\mathrm{cool,Cond-2}}$ [MW_{th}]	2.42
$T_{\mathrm{out,Cond-2}}$ [°C]	68.0
$\dot{Q}_{\mathrm{cool,Cool-1}}$ [MW_{th}]	9.71
$T_{\mathrm{out,Cool-1}}$ [°C]	21.2
$\dot{Q}_{\mathrm{cool,Cool-2}}$ [MW_{th}]	1.54
$T_{\mathrm{out,Cool-2}}$ [°C]	21.2
$\dot{Q}_{\mathrm{cool,Cool-3}}$ [MW_{th}]	25.85
$T_{\mathrm{out,Cool-3}}$ [°C]	21.2
$\dot{Q}_{\mathrm{cool,Cool-4}}$ [MW_{th}]	0.09
$T_{\mathrm{out,Cool-4}}$ [°C]	50.0
$\dot{Q}_{\mathrm{cool,Cool-5}}$ [MW_{th}]	0.58
$T_{\mathrm{out,Cool-5}}$ [°C]	35.0
$\dot{Q}_{\mathrm{cool,Cool-6}}$ [MW_{th}]	10.02
$T_{\mathrm{out,Cool-6}}$ [°C]	28.2
$\dot{Q}_{\mathrm{cool,Cool-7}}$ [MW_{th}]	30.45
$T_{\mathrm{out,Cool-7}}$ [°C]	21.2
$\dot{Q}_{\mathrm{chill,tot}}$ [MW_{th}]	4.07
$\dot{Q}_{\mathrm{chill,Chill-1}}$ [MW_{th}]	4.04
$T_{\mathrm{out,Chill-1}}$ [°C]	12.0
$\dot{Q}_{\mathrm{chill,Chill-2}}$ [MW_{th}]	0
$T_{\mathrm{out,Chill-2}}$ [°C]	-
$\dot{Q}_{\mathrm{chill,Chill-3}}$ [MW_{th}]	0.03
$T_{\mathrm{out,Chill-3}}$ [°C]	15.0
$\dot{W}_{\mathrm{aux,tot}}$ [MW_{el}]	1.64

This project has received funding from the European Union's Horizon2020 Research and Innovation Programme under Grant Agreement No 641185. This work was supported by the Swiss State Secretariat for Education, Research and Innovation (SERI) under contract number 15.0160

$\dot{W}_{\mathrm{aux,Fan-1}}$ [MW$_{el}$]	0.67
$\dot{W}_{\mathrm{aux,Pump-1}}$ [MW$_{el}$]	0.96
$\dot{W}_{\mathrm{CO_2comp,Comp-1}}$ [MW$_{el}$]	3.97

This project has received funding from the European Union's Horizon2020 Research and Innovation Programme under Grant Agreement No 641185. This work was supported by the Swiss State Secretariat for Education, Research and Innovation (SERI) under contract number 15.0160

Table 9.14: Main energy consumers of the CAP applied to the "Steam import" case defined in CEMCAP. Design at medium air leak, run at medium air leak. Second ½ of the year.

Variable	Value
$\dot{Q}_{\mathrm{heat,tot}}$ [MW_{th}]	67.22
$\dot{Q}_{\mathrm{heat,Reb-1}}$ [MW_{th}]	60.50
$T_{\mathrm{Reb-1}}$ [°C]	126
$\dot{Q}_{\mathrm{heat,Reb-2}}$ [MW_{th}]	4.67
$T_{\mathrm{Reb-2}}$ [°C]	99
$\dot{Q}_{\mathrm{heat,Reb-3}}$ [MW_{th}]	2.05
$T_{\mathrm{Reb-3}}$ [°C]	105
$\dot{Q}_{\mathrm{cool,tot}}$ [MW_{th}]	82.25
$\dot{Q}_{\mathrm{cool,Cond-1}}$ [MW_{th}]	0
$T_{\mathrm{out,Cond-1}}$ [°C]	-
$\dot{Q}_{\mathrm{cool,Cond-2}}$ [MW_{th}]	3.41
$T_{\mathrm{out,Cond-2}}$ [°C]	68.0
$\dot{Q}_{\mathrm{cool,Cool-1}}$ [MW_{th}]	9.02
$T_{\mathrm{out,Cool-1}}$ [°C]	21.2
$\dot{Q}_{\mathrm{cool,Cool-2}}$ [MW_{th}]	3.00
$T_{\mathrm{out,Cool-2}}$ [°C]	21.2
$\dot{Q}_{\mathrm{cool,Cool-3}}$ [MW_{th}]	26.82
$T_{\mathrm{out,Cool-3}}$ [°C]	21.2
$\dot{Q}_{\mathrm{cool,Cool-4}}$ [MW_{th}]	0.04
$T_{\mathrm{out,Cool-4}}$ [°C]	50.0
$\dot{Q}_{\mathrm{cool,Cool-5}}$ [MW_{th}]	0.57
$T_{\mathrm{out,Cool-5}}$ [°C]	35.0
$\dot{Q}_{\mathrm{cool,Cool-6}}$ [MW_{th}]	10.14
$T_{\mathrm{out,Cool-6}}$ [°C]	28.2
$\dot{Q}_{\mathrm{cool,Cool-7}}$ [MW_{th}]	29.25
$T_{\mathrm{out,Cool-7}}$ [°C]	21.2
$\dot{Q}_{\mathrm{chill,tot}}$ [MW_{th}]	7.98
$\dot{Q}_{\mathrm{chill,Chill-1}}$ [MW_{th}]	7.98
$T_{\mathrm{out,Chill-1}}$ [°C]	9.0
$\dot{Q}_{\mathrm{chill,Chill-2}}$ [MW_{th}]	0
$T_{\mathrm{out,Chill-2}}$ [°C]	-
$\dot{Q}_{\mathrm{chill,Chill-3}}$ [MW_{th}]	0
$T_{\mathrm{out,Chill-3}}$ [°C]	-
$\dot{W}_{\mathrm{aux,tot}}$ [MW_{el}]	1.74

This project has received funding from the European Union's Horizon2020 Research and Innovation Programme under Grant Agreement No 641185. This work was supported by the Swiss State Secretariat for Education, Research and Innovation (SERI) under contract number 15.0160

$\dot{W}_{\mathrm{aux,Fan-1}}$ [MW_{el}]	0.85
$\dot{W}_{\mathrm{aux,Pump-1}}$ [MW_{el}]	0.88
$\dot{W}_{\mathrm{CO_2comp,Comp-1}}$ [MW_{el}]	4.02

This project has received funding from the European Union's Horizon2020 Research and Innovation Programme under Grant Agreement No 641185. This work was supported by the Swiss State Secretariat for Education, Research and Innovation (SERI) under contract number 15.0160